

## Integrated biostratigraphy of Upper Cretaceous deposits from an exceptional continental vertebrate-bearing marine section (Transylvanian Basin, Romania) provides new constraints on the advent of ‘dwarf dinosaur’ faunas in Eastern Europe

R. Bălc<sup>a,b,c</sup>, R. Bindiu-Haitonic<sup>d,\*</sup>, S.-A. Kövecsi<sup>d</sup>, M. Vremir<sup>e,†</sup>, M. Ducea<sup>f,g</sup>, Z. Csiki-Sava<sup>c,g</sup>, D. Țabără<sup>h</sup>, Ș. Vasile<sup>c,g</sup>

<sup>a</sup> Babeș-Bolyai University, Faculty of Environmental Science and Engineering, 30 Fântânele Street, Cluj-Napoca 400294, Romania

<sup>b</sup> Interdisciplinary Research Institute on Bio-Nano Sciences, Babeș-Bolyai University, 42 Treboniu Laurian Street, Cluj-Napoca 400271, Romania

<sup>c</sup> Center for Risk Studies, Space Modeling and Dynamics of Terrestrial and Coastal Systems, University of Bucharest, 1 Nicolae Bălcescu Ave., Bucharest 010041, Romania

<sup>d</sup> Babeș-Bolyai University, Department of Geology and Research Centre for Integrated Geological Studies, 1 Mihail Kogălniceanu Street, Cluj-Napoca 400084, Romania

<sup>e</sup> Department of Natural Sciences, Transylvanian Museum Society, 2-4 Napoca Street, Cluj-Napoca 400009, Romania

<sup>f</sup> Department of Geosciences, University of Arizona, Tucson, AZ 85721, USA

<sup>g</sup> University of Bucharest, Department of Geology, Mineralogy and Paleontology, 1 Nicolae Bălcescu Ave., Bucharest 010041, Romania

<sup>h</sup> “Al. I. Cuza” University of Iași, Department of Geology, 20A Carol I Blv., Iași 700505, Romania

### ARTICLE INFO

#### Keywords:

Micropalaeontology  
Marine sediments  
Palaeoenvironmental reconstruction  
Detrital zircon  
Campanian  
Hațeg Island

### ABSTRACT

The present paper outlines the results of a detailed study of calcareous nannofossils and small foraminifera made on Campanian marine deposits from the southwestern part of the Transylvanian Basin, Romania, part of the marine-to-continental transitional Petrești succession that yielded the oldest temporally well-constrained continental vertebrate remains in this area. These results are integrated with new and previously published palynostratigraphic information as well as with novel detrital zircon geochronometry data. All three groups of fossils (calcareous nannofossils, small foraminifera, and palynomorphs) convergently indicate an early to middle Late Campanian age for the marine part of the Petrești section. Based on detrital zircon analyses, the most likely maximum depositional age of the studied deposits is  $76 \pm 1.7$  Ma, thus confirming the age supported by microfossil assemblages. Palaeoenvironmental interpretation of the fossil assemblages recovered from the marine part of the Petrești section suggests that despite their flysch-like facies, these beds were deposited in a continental shelf setting, under suboxic conditions and frequent fluctuations in nutrient supply to the seafloor, but quite stable environmental conditions within the water column. The synthesis of all currently available biostratigraphic and geochronologic data from the Petrești succession suggests a middle-late Late Campanian start for the expansion of the emergent land areas that made up the latest Cretaceous Hațeg Island, earlier than previously accepted dates (Maastrichtian) for this event. Furthermore, it documents the establishment of a diversified continental vertebrate faunal assemblage by the second half of the Late Campanian on these emergent lands while also providing further evidence for a later, post-Campanian arrival of certain iconic Hațeg Island dinosaur groups such as titanosaurs and hadrosauroids. Finally, our data show that kogaionid multituberculate mammals were already members of the earliest known Hațeg Island faunas, extending the fossil record of this group from the Maastrichtian into the later part of the middle Late Campanian.

\* Corresponding author.

E-mail addresses: [ramona.balc@ubbcluj.ro](mailto:ramona.balc@ubbcluj.ro) (R. Bălc), [raluca.bindiu@ubbcluj.ro](mailto:raluca.bindiu@ubbcluj.ro), [raluca.haitonic@ubbcluj.ro](mailto:raluca.haitonic@ubbcluj.ro) (R. Bindiu-Haitonic), [szabolcs.kovecsi@ubbcluj.ro](mailto:szabolcs.kovecsi@ubbcluj.ro) (S.-A. Kövecsi), [ducea@arizona.edu](mailto:ducea@arizona.edu) (M. Ducea), [zoltan.csiki@g.unibuc.ro](mailto:zoltan.csiki@g.unibuc.ro) (Z. Csiki-Sava), [dan.tabara@yahoo.com](mailto:dan.tabara@yahoo.com) (D. Țabără), [yokozuna\\_uz@yahoo.com](mailto:yokozuna_uz@yahoo.com) (Ș. Vasile).

† Deceased.

<https://doi.org/10.1016/j.marmicro.2023.102328>

Received 22 February 2023; Received in revised form 22 December 2023; Accepted 30 December 2023

Available online 6 January 2024

0377-8398/© 2024 Elsevier B.V. All rights reserved.

1. Introduction

Upper Cretaceous marine and continental deposits outcrop in different areas in Romania (e.g., Apuseni Mountains, Eastern and Southern Carpathians; Fig. 1), in part within a channel artificially created slightly more than a decade ago (e.g., Codrea et al., 20100; Vremir, 2010; Csiki-Sava et al., 2012). This local succession exposes the upper part of the marine Bozeş Formation, which is apparently conformably covered by way of a transitional, brackish sequence that corresponds to the uppermost Bozeş Formation, by the vertebrate-bearing red deposits of the uppermost Cretaceous continental Sebeş Formation (Vremir, 2010; Csiki-Sava et al., 2012; Vremir et al., 2014, 2015a; Țabără et al., 2022) (Fig. 2).

As such, the Petrești succession appears to document the final, terminal Cretaceous events of the Late Cretaceous synrift evolutionary stage of the Transylvanian Basin (Krézsek and Bally, 2006), characterized by the withdrawal of the sea that covered this area for the most part of the late Late Cretaceous and the subsequent emergence of the insular

landmass of the so-called ‘Hațeg Island’, part of the Late Cretaceous European Archipelago (e.g., Benton et al., 2010; Vremir et al., 2014; Csiki-Sava et al., 2015). Most importantly, the Petrești succession also yielded fossils of continental vertebrates such as anuran and albanerpetontid amphibians, dortokid pleurodiran turtles, diverse crocodyliforms, azhdarchid pterosaurs, rhabdodontid and nodosaurid dinosaurs, as well as multituberculate mammals (e.g., Vremir, 2010; Csiki-Sava et al., 2012, 2021, 2022; Brusatte et al., 2013; Vremir et al., 2015a, 2015b; Vasile et al., 2021, 2022), members of the fauna with dwarf dinosaurs that inhabited the ‘Hațeg Island’ (e.g., Nopcsa, 1923; Weishampel et al., 1991; Benton et al., 2010; Csiki-Sava et al., 2015). These vertebrate remains, identified inclusively within the uppermost marine, as well as the transitional, beds of the Bozeş Formation (Vremir et al., 2014, 2015b; Csiki-Sava et al., 2021; Csiki-Sava et al., 2022; Vasile et al., 2021, 2022), represent the best evidence currently available for the inception as well as for the early taxic composition and evolutionary history of this unique island fauna.

As such, the Petrești section contains a unique combination of sedimentary and palaeontological records that allows deciphering the marine-to-continental transition that took place in the western Transylvanian area as a consequence of latest Cretaceous ‘Second Getide’ mountain-building processes (e.g., Săndulescu, 1984). These processes

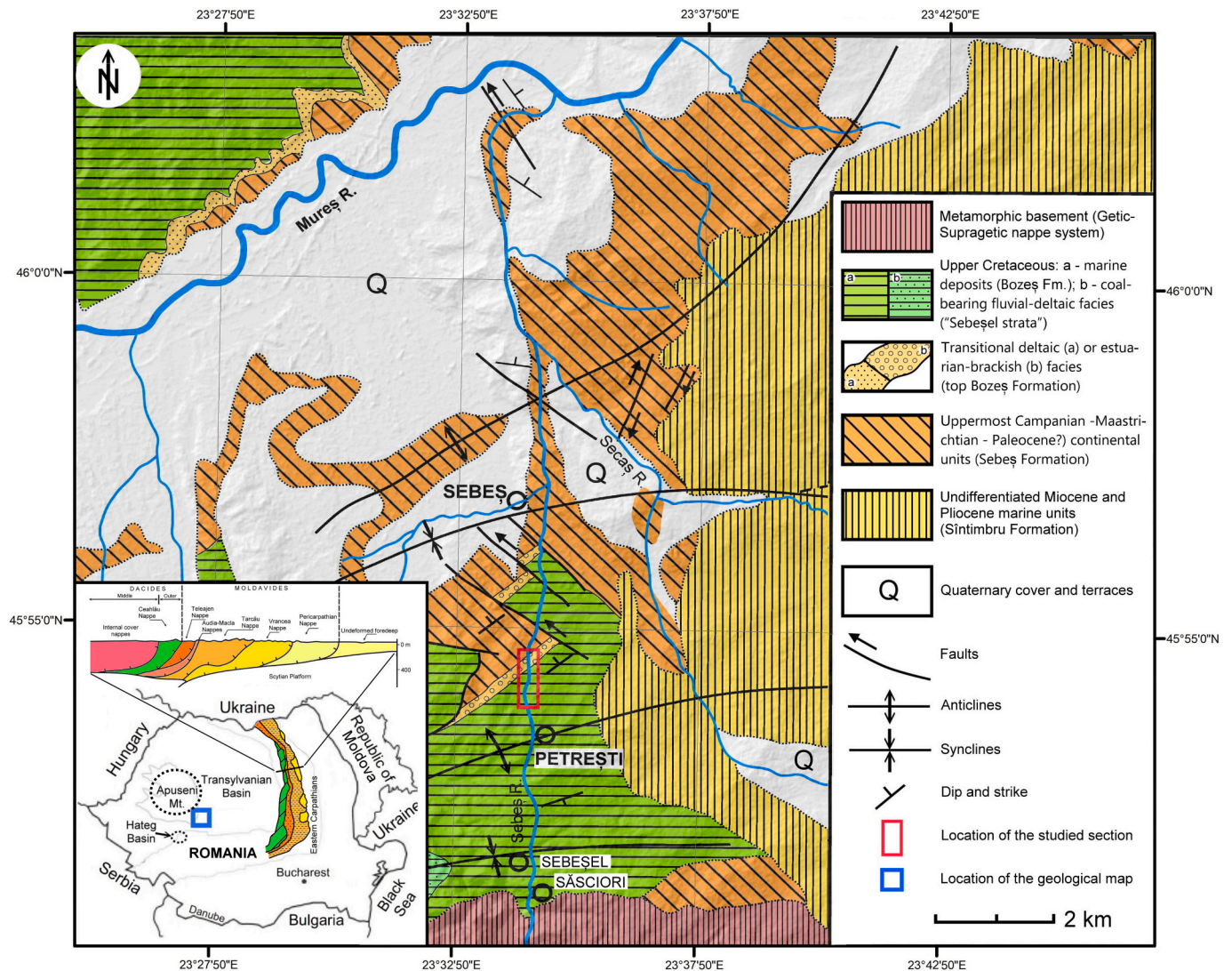
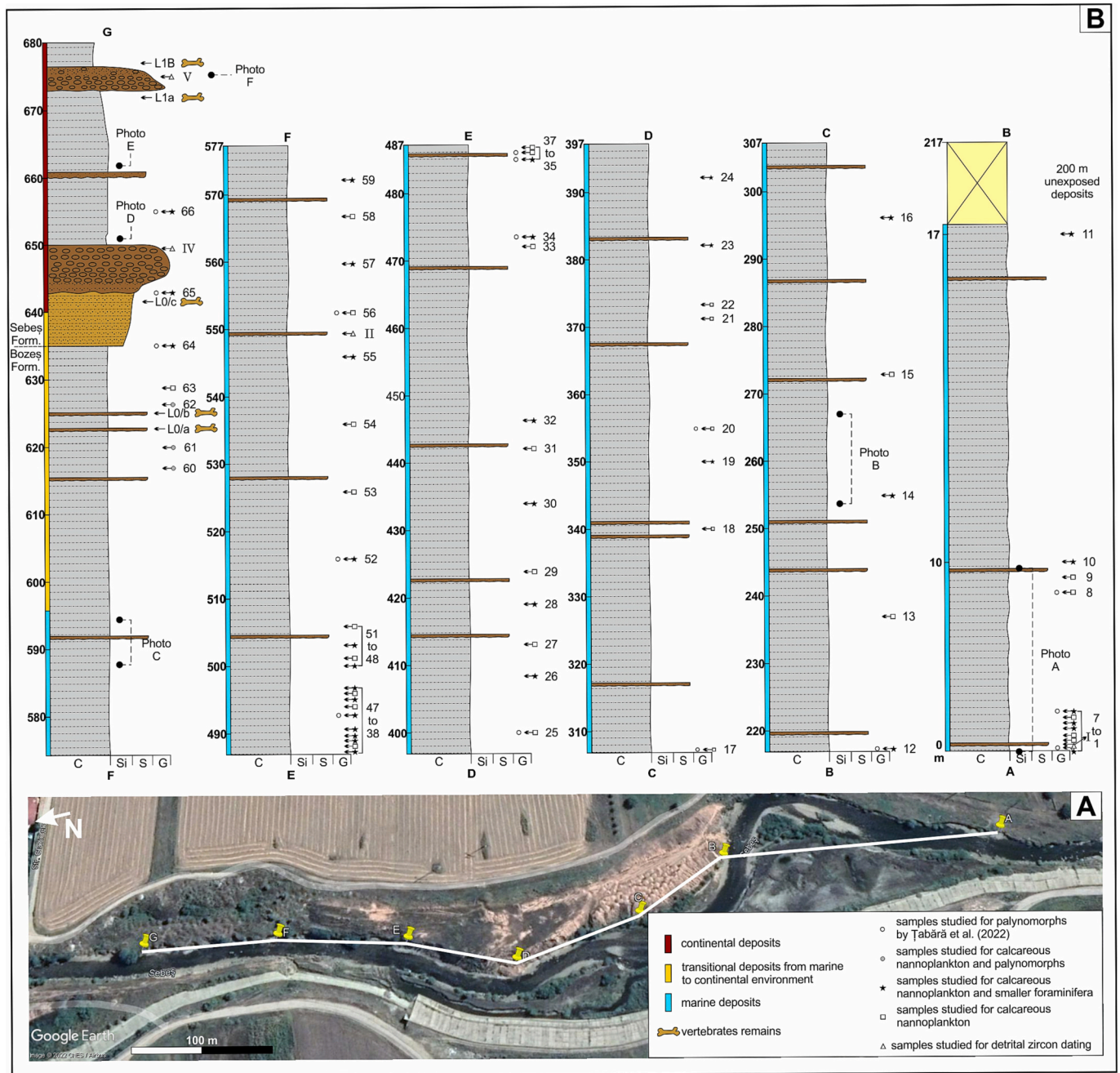


Fig. 1. Geological map of Sebeş-Petrești area (boxed area in inset map, left), overlaid on topographic surface, re-drawn and simplified from Vremir et al. (2013, 2014). Inset map also highlights other Carpathian areas discussed in the text (e.g., Hațeg Basin); simplified cross section of the Eastern Carpathians according to Ștefănescu and Polonic (1988).



**Fig. 2.** Lithological log of the studied section with information related to the sampling points and the position of the section on Google Earth map. Blue color indicates deposits belonging to the marine Bozeş Formation, yellow color marks the transition from marine to continental beds, and red color designates the continental part of the Sebeş Formation. (For interpretation of the references to color in this figure legend, the reader is referred to the web version of this article.)

concluded the Late Cretaceous synrift stage of the basin evolution and also initiated the advent of the dwarfed dinosaurian assemblages of the ‘Hațeg Island’.

In order to fully understand the tempo and patterns of these major end-Cretaceous palaeogeographic and biotic changes, however, it is critical to establish their precise temporal framework and palaeoenvironmental context, as documented by the Petrești section, in the finest possible details. Thus, this study aims to contribute to a better understanding of these terminal Cretaceous events that led up to the emergence of the dwarf dinosaur fauna-bearing Hațeg Island, through: i) detailed analyses of the calcareous nannofossils, foraminifera and palynomorph content of the marine deposits from the Petrești area (representing the Bozeş Formation), and their thorough statistical

interpretation in order to reconstruct the palaeoecological conditions that prevailed during the accumulation of the marine and the overlying transitional beds; and ii) development of better time constraints for these events by comprehensive correlation of the biostratigraphic information provided by the calcareous nannofossil assemblages with those provided by foraminifera and palynomorphs from the same succession, using an integrated biostratigraphic approach, further backed up by the first detrital zircon U-Pb geochronometry data available for this area.

## 2. Geological setting

The Transylvanian Basin is a major sedimentary area in the

southeastern part of the Carpathian orogenic system, filled in by sedimentary deposits ranging from the Upper Cretaceous to the Pliocene (e.g., [Huisman et al., 1997](#)). Its evolution can be divided into four stages represented by distinct tectonostratigraphic megasequences: a Late Cretaceous synrift stage; a Paleogene sag stage; an early Miocene flexural stage; and a middle to late Miocene-Pliocene back-arc basin stage ([Kr zsek and Bally, 2006](#)). The Upper Cretaceous deposits consist of conglomerates, sandstones, marls, and rudist limestones, deposited in continental, shallow-marine, and deep-marine settings ([Paraschiv, 1979](#); [de Broucker et al., 1998](#)), overlying a basement that was strongly tectonized before and during the Early Cretaceous ([Ciulavu and Bertotti, 1994](#)). These sediments reach their maximum thickness in the western part of the basin, where they consist mainly of coarse-grained sandstones and conglomerates ([Ciulavu and Bertotti, 1994](#)). In the southwestern part of the Transylvanian Basin, the bulk of the Upper Cretaceous deposits belong to the Bozeş Formation ([Ghiţulescu and Socolescu, 1941](#)), which is a turbidite-type marine unit with a maximum thickness of 3000 m.

The Bozeş Formation, the main marine lithostratigraphic unit exposed in the Petreşti section ([Fig. 1](#)), is characterized by the presence of turbidite-type sequences consisting of two different types of sedimentary material: the first type is made up of greywacke sandstones and mudstones alternating with grey marls, and the second one, of microconglomerates, sandstones, and grey marls ([Silye and Bălc, 2011](#); [Bălc et al., 2012](#)). The origin of the Bozeş Formation sedimentary material was tracked back to two major sources: i) a low- to medium-grade metamorphic source, suggested by the large amount of garnet, epidote, and staurolite, and ii) an older sedimentary source pointed out by the ultra-stable mineral group of zircon, tourmaline, and rutile ([Pojar et al., 2014](#)). The depositional setting of this formation was reconstructed as located on a convergent continental margin, in connection with a volcanic arc developed atop a thin continental crust ([Zaharia et al., 2016](#)).

As discussed above, in the Petreşti section (also cited previously as Petreştii de Jos, e.g., [Codrea et al., 2010](#), or as Petreşti-Arini, e.g., [Csiki-Sava et al., 2012](#)), the studied uppermost Cretaceous deposits crop out as a seemingly continuous, >750 m thick succession of marine-to-terrestrial beds accumulated in the southwestern marginal areas of the Transylvanian Basin towards the end of the Late Cretaceous synrift stage of the basin evolution. In the lower (i.e., upstream, given the general dip of the deposits towards the basin interior) part of the local succession, the shallowing-upward marine deposits that belong to the upper part of the Bozeş Formation consist of an alternation between the dominant dark grey-coloured claystone/marlstone deposits and intercalated beds of lighter grey, fine sandstones (Electronic Supplement - [Fig. 1A-C](#)) amounting to >600 m in stratigraphic thickness ([Fig. 2](#)).

Although initially the age of the marine beds of the upper Bozeş Formation was suggested to extend into the early Maastrichtian, based on a preliminary assessment of the calcareous nannofossil assemblages and incomplete ammonite specimens they yielded ([Csiki-Sava et al., 2012](#)), it was later revised as being restricted to the early-mid Late Campanian ([Vremir et al., 2014](#); [Țabără et al., 2022](#)). Towards the top of the probably fully marine section of the Bozeş Formation, which contain ammonite coil fragments and solitary corals, small charred plant remains also appear, suggesting evolution towards a shallower, nearshore environment ([Vremir et al., 2014, 2015a](#)). These nearshore deposits also yielded the oldest vertebrate fossils on record from the Petreşti succession, represented by remains of rhabdodontid ornithomimid dinosaurs (*Zalmoxes* sp.) and indeterminate azhdarchid pterosaurs ([Vremir et al., 2014](#)). These are the oldest known members of the latest Cretaceous Haţeg Island ecosystem ([Vremir et al., 2014](#); [Csiki-Sava et al., 2016](#)).

In the upper (i.e., downstream) part of the Petreşti section, a transition towards more brackish environments was observed, represented by the uppermost Bozeş Formation beds that are slightly coarser-grained, more sandy, and yield a mainly brackish mollusk fauna ([Vremir et al., 2014](#); [Țabără et al., 2022](#); [Fig. 2](#)). These grey-coloured

uppermost, brackish Bozeş deposits grade into the similarly grey-coloured beds of the basalmost Sebeş Formation that were interpreted to represent estuarine and channel deposits overlain by wetland-lacustrine ones, as they lack the brackish mollusk fauna of the underlying strata ([Vremir et al., 2014](#)). A mixed microvertebrate-macrovertebrate bonebed was reported to occur within the basal 5 m of this grey continental unit ([Vremir et al., 2015a, 2015b](#); [Vasile et al., 2021](#), [Vasile et al., 2022](#); [Fig. 2 – L0/c](#)). It yielded a diverse vertebrate fauna composed of different aquatic, semi-aquatic, and purely terrestrial taxa, including dinosaurs and multituberculate mammals; all of the taxa recovered from the bonebed are typical for the Haţeg Island faunal assemblages synthesized by [Csiki-Sava et al. \(2015\)](#).

Towards the top of the local succession, the remainder of the outcropping basal part of the continental Sebeş Formation is characterized by the dominance of fine-grained, red-coloured deposits of fluvial (mainly floodplain) origin (Electronic Supplement - [Fig. 1D-F](#)). Vertebrate remains were discovered at several different levels from these red sandy-silty mudstone beds, including those of dortokid turtles, rhabdodontid ornithomimid dinosaurs, and kogaionid multituberculates, all typical members of the faunas that inhabited the Haţeg Island ([Csiki-Sava et al., 2012](#); [Vremir et al., 2014, 2015a](#)).

### 3. Materials and methods

The main focus of the present study, the uppermost Cretaceous marine succession of the Bozeş Formation cropping out at Petreşti, was sampled thoroughly for calcareous nannofossils and foraminifera analyses; a small number of samples also originate from the uppermost transitional beds of the Bozeş Formation, as well as from the basalmost, mainly grey-coloured beds of the overlying continental Sebeş Formation ([Fig. 2](#)). The majority of the samples used in this study were collected during a systematic sampling campaign in 2017, covering mostly the lower, fully marine part of the Bozeş Formation from the local outcropping section. The 2017 sampling was aimed at extending and completing the previous, stratigraphically less extensive calcareous nannofossil-oriented sampling reported by [Csiki-Sava et al. \(2012\)](#) and [Vremir et al. \(2014\)](#); for more details on the 2017 sampling see [Țabără et al. \(2022\)](#), who studied part of these samples regarding their palynological content. Subsequently, seven samples covering the brackish-estuarine beds of the Bozeş-Sebeş formational transition were also collected in the summer of 2021, amounting to a total of 66 micropalaeontological samples used in this study. Furthermore, in addition to the 18 samples from the 2017 fieldwork previously studied palynologically by [Țabără et al. \(2022\)](#), three of the samples collected in 2021 from the uppermost, transitional part of the Bozeş Formation section were also analyzed for their palynomorph content in order to better constrain the age of these deposits and to achieve a more precise correlation with the calcareous nannofossil and foraminiferal data derived from the same samples. Finally, four samples were collected for detrital zircon U-Pb geochronometry investigations from the coarser-grained, silty-sandy levels interbedded within the mainly silty-shaly deposits that were preferentially sampled for their micropalaeontological and palynological content ([Fig. 2](#)).

In assessing the chronostratigraphy/age of the Petreşti section deposits, we have adopted the two-fold subdivision of the Campanian Stage, with short Lower and relatively long Upper substages, proposed by [Gradstein et al. \(2020\)](#) for the European Upper Cretaceous; nevertheless, whenever relevant, we will also mention corresponding chronostratigraphic subdivisions of the tri-partite Campanian stratigraphic scheme developed for the Western Interior Seaway, with three more or less equally long substages (Lower, Middle, and Upper Campanian, sensu WIS). Furthermore, in order to constrain more precisely the stratigraphic position of the different bioevents discussed, for sake of convenience, we use the informal terms 'lower', 'middle', and 'upper' to roughly designate quasi-equal subdivisions of the lengthy (about 9 Myr long) European Upper Campanian, and the terms 'lower' and 'upper' to

refer to corresponding parts of the much shorter (<3 My) European Lower Campanian.

All of the 66 samples were analyzed for calcareous nannofossils content, and all of them provided useful data for biostratigraphical and palaeoecological interpretations. The samples were prepared following the smear slides standard technique (Bown and Young, 1998), and were examined under a light microscope (Axiolab A) in cross and polarized light at 1000× magnification. A quantitative study was conducted, counting at least 300 specimens per sample; however, one sample yielded only nine specimens, while in seven other samples only 100 specimens could be counted due to the low abundance of the calcareous nannofossils (Electronic Supplement – Table 1). The specimens were photographed using an AxioCam ERCc5s digital microscopy camera at the Department of Environmental Science, Babeş-Bolyai University (Cluj-Napoca, Romania).

The calcareous nannofossil zonation schemes of Burnett (1998) and Perch-Nielsen (1985) were used to identify the biozones and assess the age of the studied sediments.

Statistical methods based on the most abundant calcareous nannofossil species were applied using the PAST version 3.26b software; Multivariate Hierarchical Clustering (MHC) by Ward's Method and Principal Component Analysis (Hammer and Harper, 2006) were chosen to analyze the assemblages and assess variations in palaeo-environmental conditions. We used the arcsine square root transformation –  $ASIN(\sqrt{Data/100})$  – on the relative abundance (percentages of counts) of the resulting raw dataset before running the multivariate data analysis (Kallanxhi et al., 2018; Bindu-Haitonic et al., 2021; Chan et al., 2022). The species selected for statistical analysis (representing >2% in most of the samples) are *Cribrosphaerella ehrenbergii*, *Eiffellithus eximius*, *Micula staurophora*, *Prediscosphaera cretacea*, *Retecapsa crenulata*, *Tranolithus orionatus*, and *Watznaueria barnesiae*. In addition, taxa that showed an increase in relative abundance at certain intervals (e.g. *Russellia* spp.) were also added to the statistical analyses.

The Temperature Index (TI) values were calculated for every sample by using the warm- vs. cool/cold-water calcareous nannofossil taxa. The TI calculation was done using the following formula (Watkins and Self-Trail, 2005):

$$TI = \frac{\%warm\ taxa}{(\%warm\ taxa + \%cold\ taxa)} \times 100$$

where:

warm taxa – *Watznaueria barnesiae*, *Ceratolithoides* sp.;

cold taxa – *Ahmuelerella octoradiata*, *Arkhangelskiella cymbiformis*, *Eiffellithus turrisseiffellii*, *Micula staurophora*, *Prediscosphaera cretacea*, *Gartnerago segmentatum*, *Kamptnerius magnificus*, *Prediscosphaera stoveri*.

The Nannoplankton Nutrient Index (NI) was calculated according to the formula used by Bottini et al. (2015), as follows:

$$NI = \frac{(Bc + Di + Ze)}{(Bc + Di + Ze + Wb)} \times 100$$

Where:

Bc – *Biscutum constans*,

Di – *Discorhabdus ignotus*,

Ze – *Zeugrhabdotus erectus*, and.

Wb – *Watznaueria barnesiae*.

Of the total of 66 samples, 34 were also investigated for planktonic and smaller benthic foraminifera (see Fig. 2). One hundred and fifty grams of each sample were prepared following the standard micropalaeontological methods described in Armstrong and Brasier (2005): drying, soaking in water, boiling and washing on a 63 µm mesh sieved with tap water, followed by drying. Where it was necessary, the residues were treated with 3% hydrogen peroxide, washed again using a 63 µm sieve, and then dried. The dried samples were weighted before and after processing. In the case of the samples with high foraminifera abundance, between 200 and 300 foraminifera specimens were picked, whereas in

the case of those with low foraminifera abundance, all the specimens present on 10 picking trays were picked out and identified under an Optika SZM-1 stereomicroscope (Electronic Supplement – Table 2). The samples with <50 individuals were considered quasi-sterile and were excluded from further analysis. In the case of agglutinated tubular forms, since these individuals are often represented by fragments, we considered two fragments as one individual during counting. The age-diagnostic and representative specimens were examined and photographed using an EmCrafts CUBE II table top scanning electron microscope (SEM) available at the Department of Geology, Babeş-Bolyai University (Cluj-Napoca, Romania).

The biozonation schemes proposed by Petrizzo et al. (2011), Coccioni and Premoli Silva (2015), Peryt and Dubicka (2015), Dubicka and Peryt (2016), and Peryt et al. (2022) were employed to constrain the age of the studied deposits.

We have calculated several different palaeoecological proxies using the retrieved smaller foraminifera assemblages, such as relative abundance (the number of smaller foraminifera specimens/1 g of sediment), rarefaction diversity index (calculated using the PAST software, Hammer et al., 2001) for the total foraminifera, benthic foraminifera, and planktonic foraminifera assemblages, respectively (Hurlbert, 1971; Hammer and Harper, 2006), planktonic/benthic percentages, epifaunal/inafaunal percentages, benthic foraminifera oxygen index–BFOI (Kranter et al., 2022), main calcareous benthic foraminifera genera percentages, main planktonic foraminifera family percentages, as well as morphogroups of calcareous benthic foraminifera (Koutsoukos and Hart, 1990; Cetean et al., 2011) and agglutinated foraminifera (Kaminski and Gradstein, 2005; Cetean et al., 2011; Setoyama et al., 2011a, 2011b, 2013, 2017; Bindu Haitonic, 2018; Józsa et al., 2023). For the foraminifera relative abundance (foraminifera/g), the planktonic foraminifera relative abundance (planktonic foraminifera/g), and the calcareous benthic foraminifera relative abundance (calcareous benthic foraminifera/g) calculations, the mass of dry sediment was taken into account (see ES\_Table2). The diversity index was computed by applying a rarefaction method to the dataset containing the raw foraminifera counts. In order to meaningfully compare two samples with different total number of individuals, the studied samples should be reduced to a common value; for total foraminifera assemblages, this common value was established at 100, while in the case of the benthic foraminifera and planktonic foraminifera assemblages, it had values of 50, and 20, respectively. These specific values were chosen accordingly to the sizes of the samples (concerning the number of collected foraminifera), and the rarefaction method assumes diversity calculation through standardization and rarefaction to the sample with the smallest number of individuals. For the calculation of the BFOI, the samples with a content of <100 calcareous benthic individuals were excluded from the interpretations. The study of Kranter et al. (2022) brings important updates for the BFOI calculation: (i) agglutinated forms are considered in the calculations together with suboxic indicators (S) if the oxalic indicators (O) appear in percentages >10% (Eq. 3 -  $BFOI = 100 * (O / (O + D + S/2))$ ); (ii) oxalic indicators must be accounted for even if they are present in low percentages (Eq. 4 -  $BFOI = 50 * (S / (S + D) - 1) + O$ ); and (iii) if disoxic indicators (D) are present in higher percentages than the oxalic ones, these should also be considered in calculations (Eq. 5 -  $BFOI = (100 * (O / (O + D + S/2)) + 50 * (S / (S + D) - 1) + O) / 2$ ).

The palynological investigations were carried out using an amount of 50 g from each sample, prepared using the standard palynological techniques (Batten, 1999). The samples were treated with 37% HCl to dissolve the carbonates, followed by a 48% HF treatment to remove the silicate minerals. After every chemical treatment, the samples were washed with water to a neutral pH. The organic residue was separated from the denser particles using  $ZnCl_2$  with a density of 2.0 g/cm<sup>3</sup>. The microscopic slides were prepared using glycerine jelly as a mounting medium. The palynomorphs were examined using transmitted light microscopy under 10× and 40× objectives, using a Leica DM1000 microscope equipped with a Leica DFC420 digital camera, available at the

Department of Geology, “Al. I. Cuza” University of Iași, Romania. Out of the three new samples analyzed from the uppermost part of the Bozeș Formation and reported here (samples 60–62), only two proved to be productive, with most of the palynomorphs being recovered from sample 61.

We performed U-Pb detrital zircon geochronology on coarser-grained siliciclastic samples. Three kilograms of bulk sample from each sampling location were crushed and then sieved in order to separate the fraction smaller than 300  $\mu\text{m}$ . Heavy mineral mass fraction <300  $\mu\text{m}$  was separated with a high-density liquid (diiodomethane with a density of 3.3  $\text{g}/\text{cm}^3$  density), followed by a further magnetic

separation using a Frantz Magnetic Barrier Separator. The separated zircons were mounted in epoxy resin alongside other zircon specimens of known age. U-Pb isotopic analyses were performed on polished individual grains using laser ablation at the Arizona LaserChron Center, on an Element2 high-resolution single collector inductively coupled plasma-mass spectrometer (LA-ICP-MS) equipped with a Teledyne G2 193 nm Excimer laser with a beam diameter of 30  $\mu\text{m}$  (Gehrels et al., 2008). The random selection of 100 crystals ensured an analyzed sample representative of the entire zircon population (Gehrels, 2014). Every five crystals of unknown age were bracketed by a known standard; our primary standards for this study were the Sri Lanka and R33 zircons,

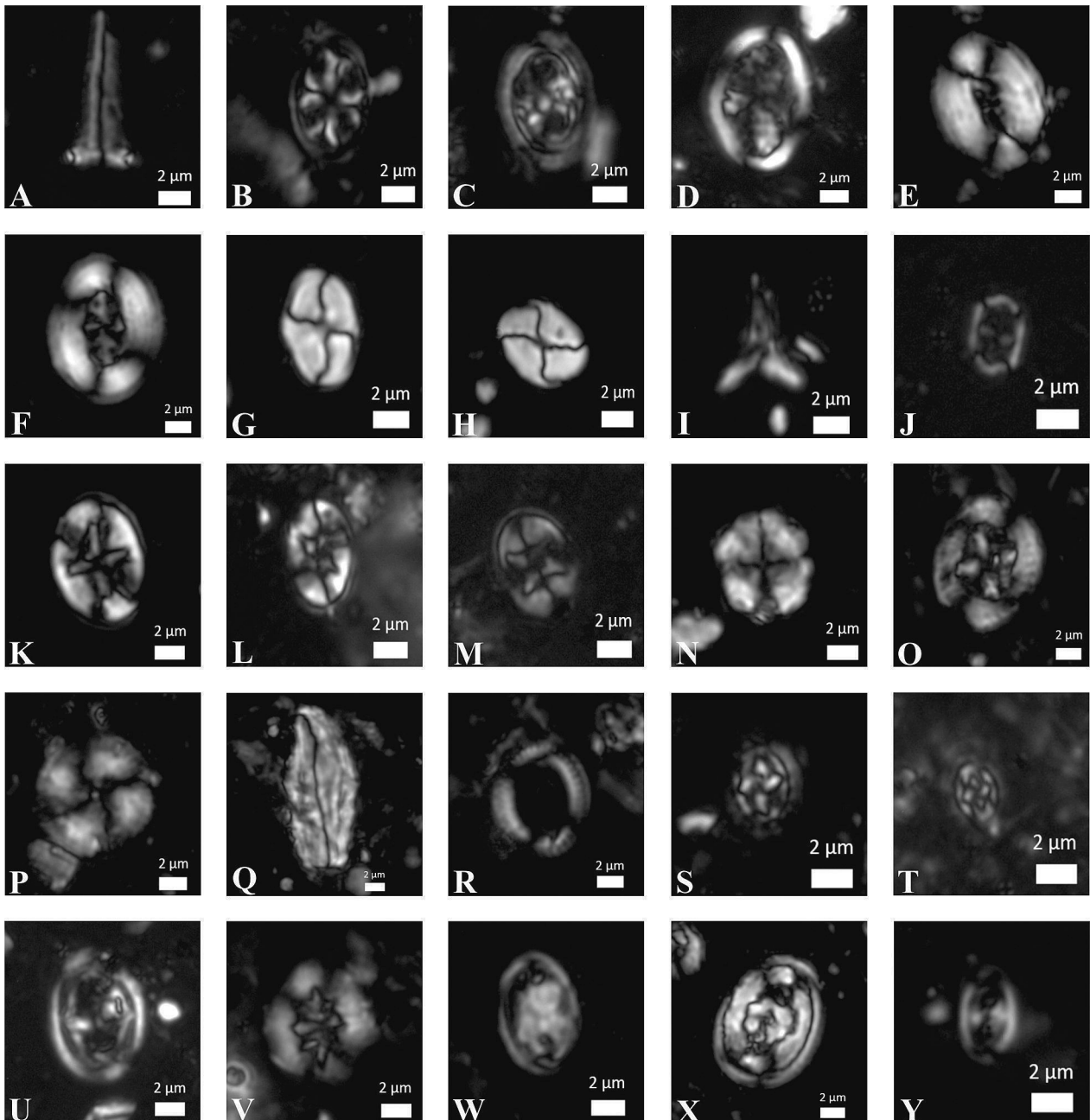


**Fig. 3.** Selected calcareous nannofossil species identified in the marine deposits of the Petrești section. A. *Acuturris scotus* (sample 25); B. *Ahmuellerella octoradiata* (sample 19); C. *Amphizygus brooksii* (sample 38); D. *Arkhangelskiella cymbiformis* (sample 20); E. *Broinsonia parca constricta* (sample 8); F. *Broinsonia parca parca* (sample 9); G. *Calculites obscurus* (sample 35); H. *Calculites ovalis* (sample 4); I. *Ceratolithoides aculeus* (sample 34); J. *Corollithion signum* (sample 3); K. *Eiffellithus eximius* (sample 4); L. *Eiffellithus gorkae* (sample 19); M. *Eiffellithus turriseiffelii* (sample 3); N. *Eproolithus floralis* (sample 13); O. *Grantarhabdus coronadventis* (sample 19); P. *Haqius circumradiatus* (sample 8); Q. *Lucianorhabdus windii* (sample 8); R. *Manivitella pemmatoidea* (sample 57); S. *Prediscosphaera spinosa* (sample 34); T. *Prediscosphaera stoveri* (sample 17); U. *Reinhardtites anthophorus* (sample 17); V. *Retecapsa angustiforata* (sample 23); W. *Tranolithus orionatus* (sample 9); X. *Zeugrhabdotus embergeri* (sample 35); Y. *Zeugrhabdotus erectus* (sample 19).

which have ages similar to most of our unknowns. Ages that are <90% concordant (discordance between <sup>206</sup>Pb/<sup>238</sup>U and <sup>207</sup>Pb/<sup>235</sup>U ages) were discarded from further analysis. For ages <1.4 Ga, the 6/8 age was reported and used, whereas for ages older than 1.4 Ga, we used the 5/7 age. For the purpose of this paper, the results were plotted on probability density function graphs using the kernel density estimation (KDE) in the DensityPlotter software (<https://www.ucl.ac.uk/~ucfbpve/densityplotter/>). Maximum depositional ages of the samples (only one of these, the most relevant one for the aims of the research being reported here) were calculated by the ISOPLOT-R package (Vermeesch, 2018).

#### 4. Results

##### 4.1. Calcareous nannofossils preservation and abundance

In the studied samples, calcareous nannofossils (Fig. 3) appear in a moderate to good state of preservation and are abundant in most of them, with only eight out of the 66 analyzed samples containing specimen-poor assemblages. A total of 133 species (Electronic Supplement – Appendix A and Table 1) were identified in the 66 samples. Of these, *Watznaueria barnesiae* is the dominant species in the assemblage, exceeding 50% in three samples and having the lowest recorded abundance of 25.70%. In terms of abundance, this species is followed by *Prediscosphaera cretacea* (up to 13.40%), *Tranolithus orionatus* (up to 11.11%), *Eiffellithus eximius* (up to 9.52%), *Cribrosphaerella ehrenbergii* (up to 8.84%), *Retecapsa crenulata* (up to 8.82%), and *Micula staurophora* (up to 8.67%). All of the above-mentioned species show abundance fluctuations along the studied section, with more than one peak of abundance registered for each (Fig. 4).

Other distinctive features of the calcareous nannofossil assemblages observed in the studied samples are related to: i) the absence or rarity of the Tethyan species; ii) the presence of certain dissolution-sensitive taxa (e.g., *Biscutum constans*, *Discorhabdus ignotus*); and iii) the presence of taxa such as *Russellia laswellii* and *Russellia bukryi* that show higher values of abundance (up to 11.46% and 7.43%, respectively) in the lower part of the section, with their abundance slowly decreasing upwards (Fig. 4).

Overall nannofossils abundance displays relatively low-level fluctuations, with an average count of 0.95 specimens per one field of view. The highest values (up to 3.33 nannofossils/field of view) are recorded in the lower part of the studied section.

The calculated calcareous nannofossils Species Richness is moderate (mean 48) and varies from 5 to 63 species per sample. The Shannon diversity index (H) is moderate/high (mean 7.8), with individual values ranging from 2.4 to 9.0. Sample Evenness (E) varies from 2.31 to as high as 135.6 (Fig. 5).

The TI values recorded in the Petrești section vary from 57.2 to 86.6. The highest values of TI occur in the uppermost part of the section, with TI of 70 or above found in 24 samples. The lower and middle parts of the section are characterized by more widely alternating TI values, but their average still remains around 73.5. These values indicate the predominance of warm-water taxa in the entire studied section. The NI values vary from 0 (in ten samples) to 17.6, with a mean value of 5.40. A continuous fluctuation of the NI was identified throughout the section, but overall, conditions of suppressed fertility can be reconstructed for the latest Cretaceous marine basin near Petrești, with occasional very minor increases in organic nutrient content as evidenced by NI values above 10 recorded in only ten samples (15% of the total), mainly grouped in the lower part of the studied section (Fig. 5).

Based on Pearson's correlation matrix (Table 1) the highest positive correlation was found between: i) *Discorhabdus ignotus* and *Zeugrhabdus* spp., *Russellia* spp., *Micula staurophora*, and *Prediscosphaera cretacea*; ii) *Watznaueria barnesiae* and *Tranolithus orionatus* and *Eprolithus floralis*; and iii) *Biscutum constans* and *Eprolithus floralis*. On the other hand, the highest negative correlation was identified between *Watznaueria barnesiae* and *Biscutum constans*, *Prediscosphaera cretacea* and

**Table 1** Pearson's correlation matrix of selected calcareous nannofossil taxa from the Petrești section.

	<i>Watznaueria barnesiae</i>	<i>Biscutum constans</i>	<i>Prediscosphaera cretacea</i>	<i>Tranolithus orionatus</i>	<i>Micula staurophora</i>	<i>Eiffellithus eximius</i>	<i>Cribrosphaerella ehrenbergii</i>	<i>Retecapsa crenulata</i>	<i>Russellia</i> spp.	<i>Discorhabdus ignotus</i>	<i>Eprolithus floralis</i>	<i>Zeugrhabdus</i> spp.	<i>Staurolithes</i> spp.
<i>Watznaueria barnesiae</i>													
<i>Biscutum constans</i>	<b>-0.558</b>												
<i>Prediscosphaera cretacea</i>	<b>-0.500</b>	0.123											
<i>Tranolithus orionatus</i>	-0.002	-0.186	0.101										
<i>Micula staurophora</i>	-0.184	0.183	0.086	<b>-0.316</b>									
<i>Eiffellithus eximius</i>	0.212	<b>-0.199</b>	<b>-0.455</b>	-0.292	-0.178								
<i>Cribrosphaerella ehrenbergii</i>	<b>-0.379</b>	0.168	0.127	-0.327	0.135	-0.050							
<i>Retecapsa crenulata</i>	0.364	<b>-0.219</b>	-0.139	-0.028	-0.152	0.309	<b>-0.229</b>						
<i>Russellia</i> spp.	<b>-0.558</b>	<b>0.467</b>	0.111	-0.164	0.157	<b>-0.211</b>	0.100	<b>-0.442</b>					
<i>Discorhabdus ignotus</i>	-0.165	0.364	0.026	-0.196	0.009	<b>-0.216</b>	0.196	<b>-0.217</b>	0.024				
<i>Eprolithus floralis</i>	0.020	0.001	-0.122	-0.055	0.145	0.228	<b>-0.274</b>	0.060	-0.123	-0.121			
<i>Zeugrhabdus</i> spp.	-0.134	-0.055	-0.058	-0.075	-0.054	0.226	0.197	0.011	<b>-0.207</b>	-0.031	0.154		
<i>Staurolithes</i> spp.	<b>-0.514</b>	<b>0.327</b>	0.284	<b>-0.228</b>	0.183	<b>-0.248</b>	<b>0.461</b>	<b>-0.369</b>	<b>0.307</b>	0.294	-0.203	0.064	

Significant coefficients (p < 0.01) are in bold.

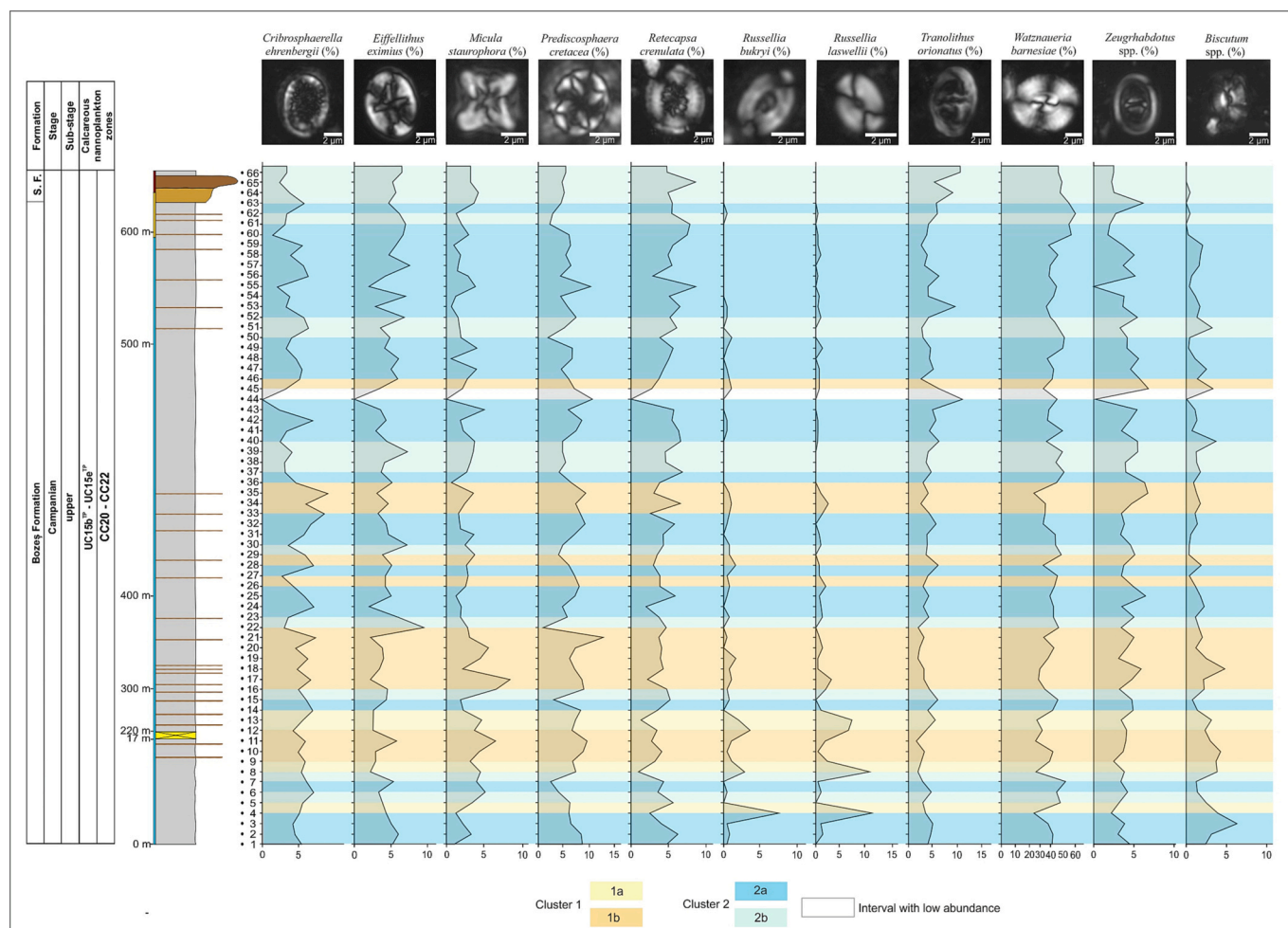


**Fig. 4.** Abundance patterns of the dominant and subdominant calcareous nannofossil species plotted along the sampling interval together with the distribution of the main identified clusters. *Zeughrabdodus diplogrammus* and *Biscutum constans* are illustrated for *Zeughrabdodus* spp. and *Biscutum* spp. groups. Lithological column - not to scale.

*Russelia* spp. Other, less significant positive and negative correlations are also shown in Table 1.

We have employed two different statistical analyses based on the most abundant calcareous nannofossil species – Multivariate Hierarchical Clustering (MHC; Electronic Supplement - Fig. 2) and Principal Component Analysis (PCA; Fig. 6) – to more properly investigate their distribution patterns along the studied section as well as the fluctuations in the palaeoecological conditions under which the marine deposits from the Petrești section were formed. The MHC separated two main clusters and four sub-clusters among the studied samples, with two sub-clusters within each main cluster, as follows:

- **Cluster 1** contains 19 samples characterized by the lowest values of abundance for *Watznaueria barnesiae*, and it is further divided into two sub-clusters. In **sub-cluster 1a**, including 15 samples, *Watznaueria barnesiae* was registered with a relative abundance varying between 25.61% and 42.39%; remarkably, these values, albeit still rather high, are lower than those registered in most of the other samples (excepting those from sub-cluster 1b). **Sub-cluster 1b** grouped only four samples characterized by the highest observed abundance values for *Russelia laswellii* and *R. bukryi* (up to 11.46% and 7.43%, respectively) correlated with the lowest abundance recorded for *Watznaueria barnesiae* (between 25.70% and 32.49%).
- **Sub-cluster 2a of Cluster 2** contains 31 samples without any distinctive features. In these, *Watznaueria barnesiae* still remains the dominant species within each individual assemblage, albeit with

moderate values for its relative abundance. **Sub-cluster 2b** groups 15 samples showing the highest amounts of *Watznaueria barnesiae* (over 43%). The remaining taxa all registered fluctuations in their abundance in these samples.

According to the Principal Component Analysis, the first two principal components are relevant (Fig. 6), and together, these explain around 65% of the variability present in the relative abundance of the main calcareous nannofossil taxa. Principal Component 1 explains 51.27% of the observed variance, and negatively correlates the samples with a significant participation of *Russelia laswellii* and *R. bukryi* (>0.4 correlation loadings) with those with *Watznaueria barnesiae* (less than –0.60 correlation loadings). Principal Component 2 accounts for 13.84% of the observed variance and separates the samples with *Watznaueria barnesiae* and *Russelia laswellii* (>0.5 correlation loadings) from those with *Prediscosphaera cretacea* (less than –0.50 correlation loadings).

#### 4.2. Smaller foraminifera: Preservation, abundance, diversity, BFOI, main groups and morphogroups

The foraminifera assemblages (Fig. 7) are generally characterized by moderate to poor preservation of the specimens. For a better understanding of the sequence of the paleoecological conditions, we consider as the basal part of the sedimentary sequence the interval between 0 and 410 m (the interval of samples 1–26), the middle part between 410 and

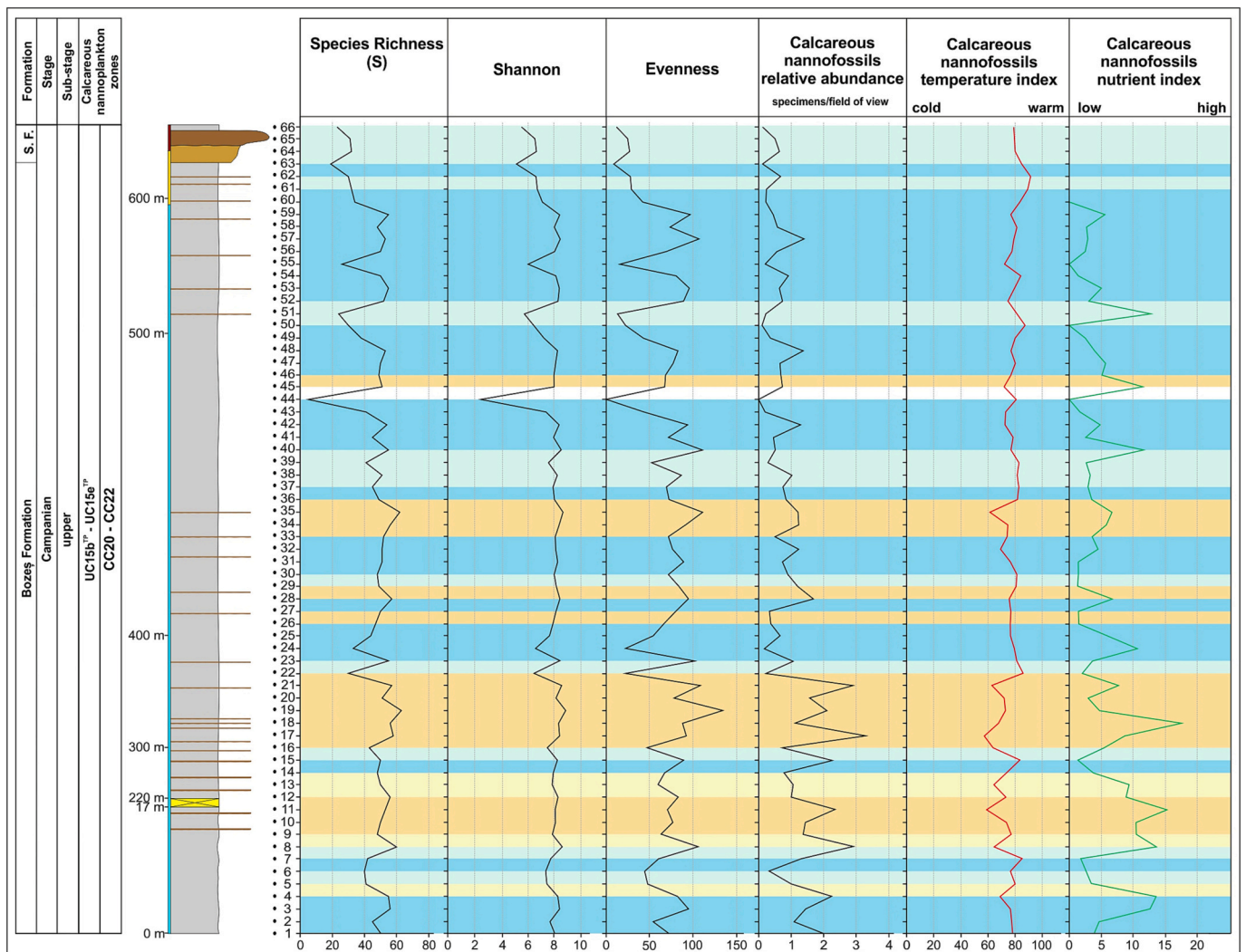


**Fig. 5.** Species Richness, Shannon Diversity Index, Evenness, vertical distribution of relative calcareous nannofossils abundance, calcareous nannofossils temperature index, and calcareous nannofossils nutrient index data from the Petrești section (SW Transylvanian Basin). For color coding of the different clusters, see text and Fig. 4. Lithological column - not to scale.

488 m (samples 26–38) and the upper part the interval between 488 and 680 m (samples 39–66). The values of foraminifera relative abundance per 1 g of sample (see Materials and Methods chapter) shows important variations along the sampled section, as samples/intervals rich in foraminifera alternate with sterile/quasi-sterile ones. The highest relative abundance values have been recorded in samples 38 and 26 (221 and 200 specimens/g), compared to the minimum values recorded in samples 23 and 41 as well as in the upper part of the section (2 and 3 specimens/g) (Fig. 8). The maximum relative abundance is recorded in samples 12 and 26 (39 and 25 specimens/g) for planktonic foraminifera, respectively in samples 38 and 28 (197 and 196 specimens/g) for benthic foraminifera; meanwhile, the minimum values of the relative abundance were noticed in samples 7 and 16 as well as in the upper part of the section (1 individual/1 g) for planktonic foraminifera, respectively in samples 23 and 41, as well as in the upper part of the section (1 individual/1 g) for benthic foraminifera.

From the total of 130 identified foraminifera species, 40 (30.7%) are agglutinated benthic, 63 (48.4%), calcareous benthic, and only 27 (20.7%) are planktonic (Electronic Supplement – Appendix B and Table 2). The percentage abundance of the planktonic forms registers an increase from the base to the middle/top part of the section (from a minimum of 6.45% in sample 16 to a maximum of 80% in sample 47), while the benthic forms display a minimum participation of 20% in

sample 47 and a maximum of 93.55% in sample 16 (Fig. 8). The relative percentages calculated according to the mode of life show that the epifaunal taxa (such as species of *Ammosphaeroidina*, *Epistomina*, *Gyroldinoides*) dominate in the basal and middle parts of the sampled section (with a maximum abundance of 79.35% recorded in sample 7). These epifaunal taxa are, however, surpassed in abundance by the infaunal forms (different species of *Bolivinoidea*, *Praebulimina*, *Pseudovigenerina*) in the middle/upper part of the section, with a maximum presence value of 78.26% for the latter registered in sample 41 (Fig. 9).

Analysis of the relative abundance distribution of the main calcareous benthic foraminifera genera highlights first of all the particular (albeit not very high) percentage values recorded for the genus *Bolivinoidea*, which was identified only in samples 11 and 12 (with a maximum of 1.20% in sample 11) (Fig. 9). The genus *Epistomina* shows fluctuating values throughout the succession, with both the maximum values (12.12%, sample 5) and the lowest ones (0.47% in sample 12) recorded in the basal part. Meanwhile, in the stratigraphic interval placed between samples 32 and 41, this genus was not identified. The infaunal taxa *Praebulimina* and *Pseudovigenerina* increase in percentage starting with the middle part of the succession, although it is interesting to note that their relative abundance values are somewhat negatively correlated, i.e., high percentage values of *Praebulimina* (such as in samples 38 to 47, with an average of 38.82%) correspond to low values for the genus

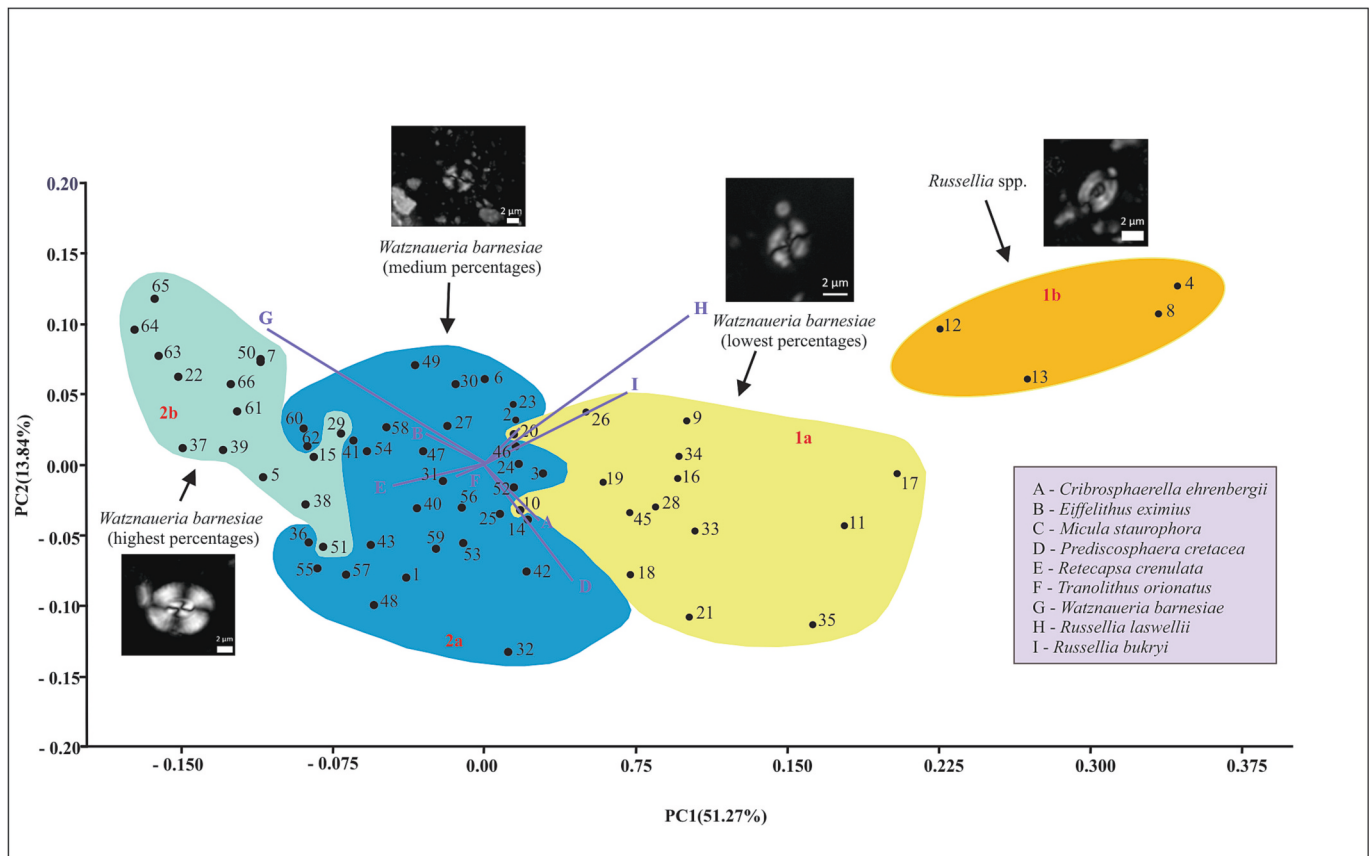


Fig. 6. Principal Component Analysis carried out using selected calcareous nannofossil taxa, and the distribution of the identified clusters and sub-clusters within the first two principal components.

*Pseudouvierina* (Fig. 9) and vice versa. The highest percentages of *Pseudouvierina* were recorded in the middle part of the succession (samples 26 and 28: 31.69%, respectively 25.95%). The highest percentage values of the different planktonic foraminifera families, calculated from the total count of planktonic foraminifera, are registered by the Hedbergellidae, Globotruncanidae, and Heterohelicidae (with an average of 23.05%, 13.14%, and 24.54%, respectively), followed in order of decreasing abundance by the Globigerinelloididae (average 17.66%) and Rugoglobigerinidae (average 10.89%) (Fig. 9).

The resulting values of the benthic foraminifera oxygen index (BFOI) to the sea floor range from  $-40$  (sample 16) to 13.5 (sample 30; Fig. 8). The calcareous benthic foraminifera were divided into two main morphogroups: Ch-A and Ch-B (Electronic Supplement - Fig. 3), according to the classification proposed by Koutsoukos and Hart (1990). Morphogroup Ch-A was separated based on the presence of low to high trochospiral and planispiral morphotypes, and it records maximum values of up to 75% in the base of the succession (sample 4). The Ch-B morphogroup shows maximum abundance values of 80% in the middle part of the succession (sample 41) (Electronic Supplement - Fig. 3) due to the large number of foraminiferal individuals characterized by elongate tests generally corresponding to/pointing at an infaunal deposit-feeding strategy. Separation of the agglutinated foraminifera into morphogroups (Electronic Supplement - Fig. 3) revealed the presence of all important categories in the studied samples except for morphotype M3b (*Ammolagena clavata*). The different agglutinated foraminifera morphogroups display different abundance values across the studied samples. The most abundant morphotypes are the M3c type (*Ammosphaeroidina* spp., *Cystammina* spp., *Paratrochamminoides* spp.) with a maximum abundance of 37.8% (sample 30), the M4a type (*Haplophragmoides* spp.) reaching 100% in sample 43, and the M4b type (*Ammobaculites* spp., *Karrerulina* spp., *Reophax* spp.) with a maximum

abundance value of 42.86% in sample 41 (Electronic Supplement - Fig. 3).

#### 4.3. Palynofloral assemblage

In our previous palynological investigation of the Petrești section (Țabără et al., 2022), we noted the absence of continental and/or marine palynomorphs at the top of the Bozeș Formation, an absence that was due to a combination between poor preservation of palynomorphs in this part of the section and a much sparser sampling, corrected by our renewed sampling of 2021, focused on that particular segment of the local succession. In order to mitigate this sampling shortcoming, we conducted palynological analyses of three new samples collected from this stratigraphical interval (Fig. 2), which allowed us to outline a palynological assemblage (Fig. 10) represented mainly by pollen and spores (Fig. 10B–P), besides a minor fraction of dinoflagellates (Fig. 10A). Two of the three analyzed samples (i.e., samples 60 and 61) were productive. Overall, this newly identified palynomorph assemblage shows a composition largely similar to that previously reported from the Bozeș Formation (see Țabără et al., 2022), although a number of primitive angiosperm pollen taxa assigned to the Normapollis group, e.g., *Longanulipollis fornicatus*, *Pseudopapilopollis* cf. *praesubhercynicus*, *Trudopollis rusticus*, *Trudopollis granulosus*, and *Trudopollis lativerrucatus*, represent new occurrences reported from this section.

Gymnosperm pollen represents the most abundant taxonomic group in the newly identified assemblage and includes typical Mesozoic representatives of Araucariaceae (i.e., *Araucariacites australis*). Among angiosperms, the pollen of Juglandaceae (*Subtriporopollenites constans*) and Myricaceae also occur in high abundance. Fern spores such as *Deltoidospora*, *Laevigatosporites*, *Polypodiaceosporites*, and *Triplanosporites* are the most common pteridophytes represented.

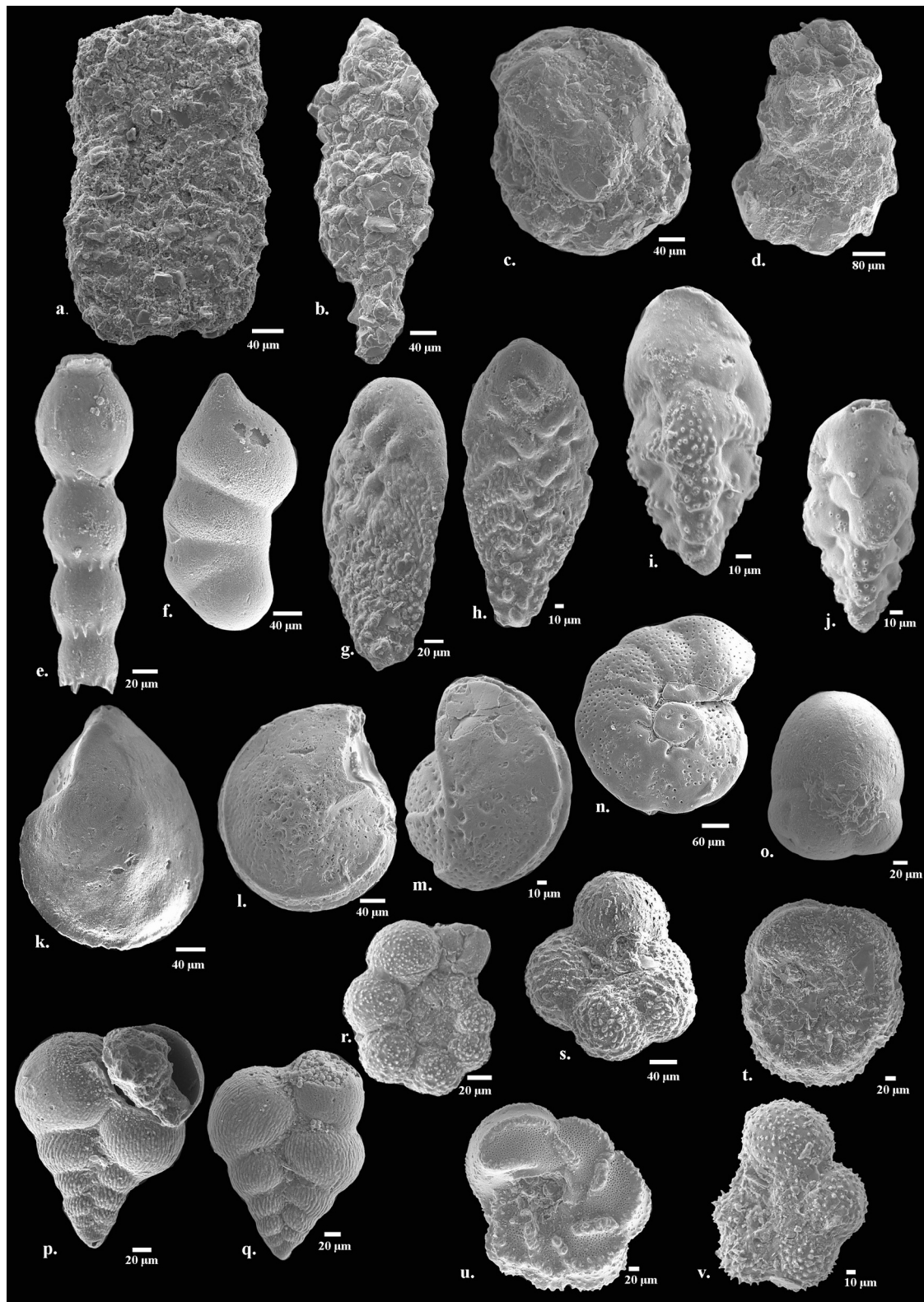


Fig. 7. Selected elements of the latest Cretaceous foraminifera assemblages from the Petrești section, southwestern Transylvanian Basin. a. *Bathysiphon* sp. (sample 1); b. *Reophax subfusiformis* (sample 7); c. *Haplophragmoides horridus* (sample 4); d. *Ammobaculites subcretaceus* (sample 19); e. *Stilostomella* sp. (sample 19); f. *Astacolus linearis* (sample 12); g. *Bolivinoidea* sp. (sample 11); h. *Bolivinoidea laevigatus* (sample 11); i-j. *Pseudovigierina rudita* (samples 26 and 28); k. *Lenticulina* sp. (sample 10); l. *Epistomina* sp. 1 (sample 10); m. *Epistomina* sp. 2 (sample 26); n. *Brotzenella monterelensis* (sample 7); o. *Quadrimorphina varsoviensis* (sample 19); p. *Planoheterohelix globulosa* (sample 32); q. *Planoheterohelix* sp. (sample 42); r. *Muricohedbergella* sp. (sample 30); s. *Rugoglobigerina rugosa* (sample 12); t. *Contusotruncana plummerae* (sample 11); u. *Globotruncana linneiana* (sample 10); v. *Globotruncanella minuta* (sample 10).

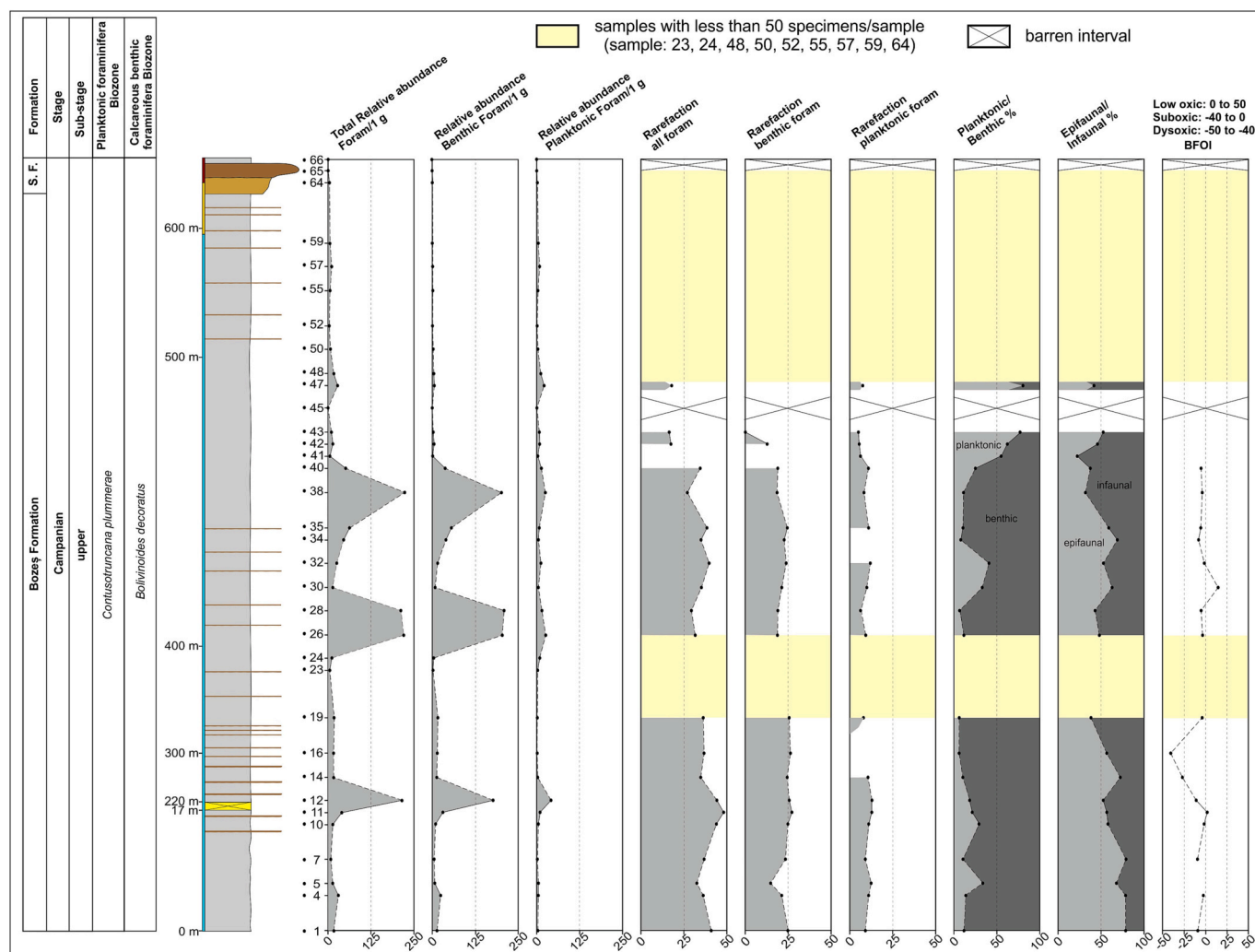


Fig. 8. Plots of relative abundance, diversity indices (rarefaction), percentages of planktonic, benthic, epifaunal and infaunal foraminifera, and benthic foraminifera oxygen index of the latest Cretaceous foraminifera assemblages from the Petrești section (for abbreviations, see Materials and Methods). Lithological column - not to scale.

#### 4.4. Detrital zircon geochronology

Out of the four sandstone samples collected and submitted to detrital zircon U-Pb geochronometry analyses (Fig. 2), the results of one are currently available and bear relevance to the dating of the Petrești succession. Sample IV, reported here, is located in the upper marine-to-continental transitional part of the local succession (Fig. 2), and yielded 110 zircon grains that were analyzed for geochronology (raw measurement data are presented in the Electronic Supplement – Table 3, and in Fig. 11A). Remarkably, the great majority of these zircons (77, representing 70%) have Late Cretaceous ages, indicating that this sample is primarily a siliciclastic-volcaniclastic rock derived from the erosion of the nearby volcanic arc stretching across the Apuseni Mountains and western Southern Carpathians (northwest and west to the Petrești area) — a volcanic arc that formed in response to the closure of the Neo-Tethys and is locally known as the banatitic arc (Berza et al., 1998; Gallhofer et al., 2015). Individual ages within the dominant Late Cretaceous component of the analyzed sample range from 76 to 82 Ma (with associated errors; Fig. 11B) and yield a mean calculated maximum depositional age (MDA) of about 80 Ma (Electronic Supplement – Fig. 4, but see below, Discussions).

The remainder of the zircons from the sample fall into the Neoproterozoic to Silurian age range with minor Variscan metamorphic grains, a spectrum that is common in the nearby Dacian basement

(Balintoni et al., 2014; Stoica et al., 2016). They are complemented here (and elsewhere, where the Dacian basement supplies detritic material) by a few Proterozoic grains typically older than 2 Ga.

## 5. Discussion

### 5.1. Biostratigraphy and biochronology

As noted in the Materials and Methods section, our chronostratigraphical/biochronological discussions will employ the bipartite division of the Campanian as presented in Gradstein et al. (2020), with further informal refining of this scheme through the usage of the terms lower, middle (only for the Upper Campanian) and upper to designate roughly equal subintervals of the two stages.

There are a number of calcareous nanofossil biozonation schemes developed/proposed for the Campanian, including the cosmopolitan biozonation schemes of Sissingh (1977 – CC Biozones), Perch-Nielsen (1985 – CC Biozones), and Bralower et al. (1995 – NC Biozones), respectively, an array of regional schemes proposed for northwestern Europe such as those of Burnett (1991 – Germany), Crux (1982 – England), Mortimer (1987 – Southern Norwegian and Danish North Sea – NK Biozones), Bergen and Sikora (1999 – Norwegian North Sea, KN Biozones), and Burnett (1998 – UC Biozones – for Boreal, Austral, and Tethyan-intermediate sites).

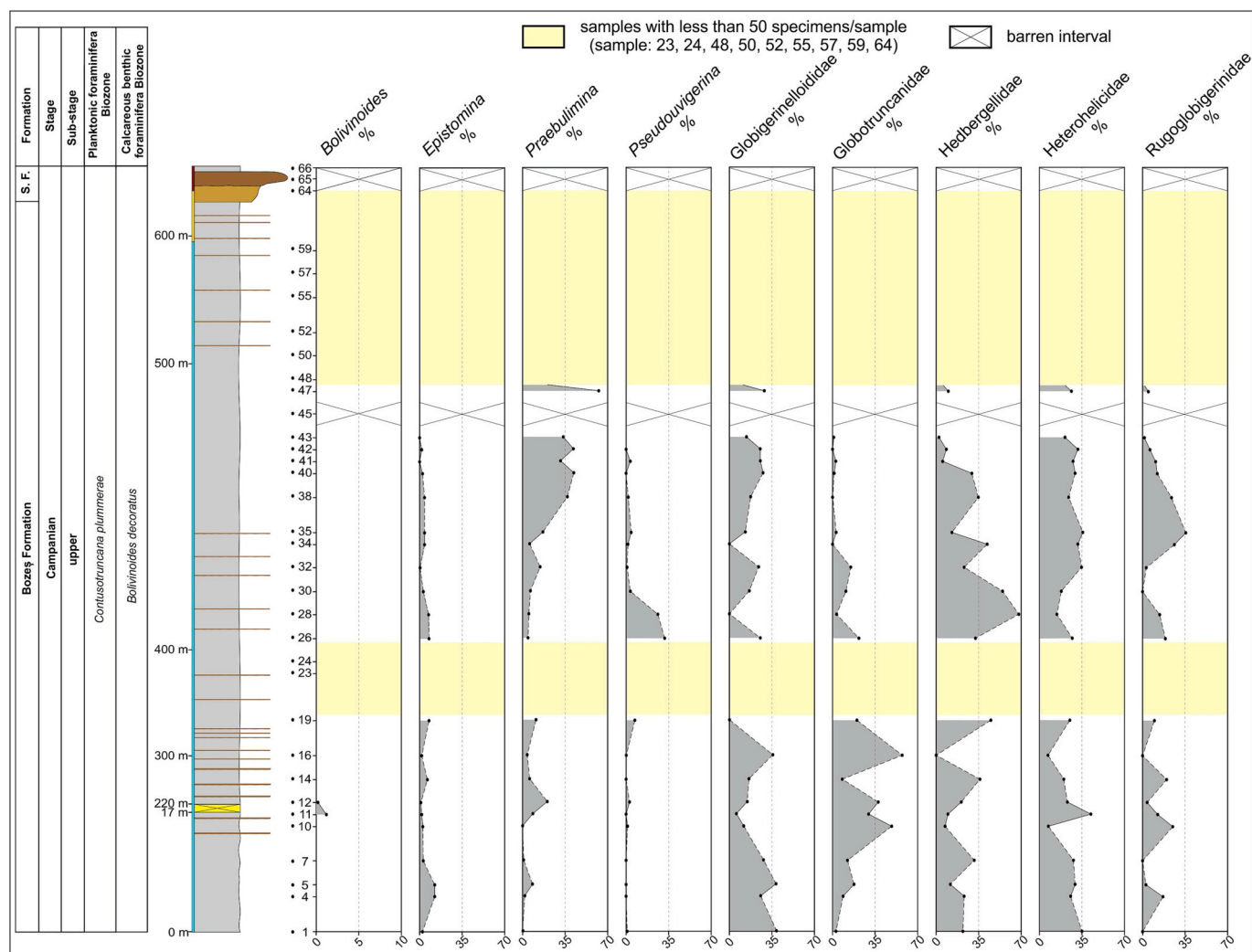


Fig. 9. Percentages of the main calcareous benthic foraminifera genera and of the main planktonic foraminifera families in the uppermost Cretaceous succession from Petrești, Southwestern Transylvanian Basin. Lithological column - not to scale.

All of the above-mentioned biozonation schemes employed certain important marker bioevents to define the boundaries between the different biozones. But since the relevant marker species are not continuously present in our study section, and thus no clear bioevent could be emphasized, we will briefly present the identified marker species and their occurrence patterns in the investigated material. The presence of *Calculites obscurus* was identified in 35 samples, with a higher abundance in the lower part of the section and a decrease in abundance upwards. The following taxa were identified in low numbers: *Broinsonia parca parca* (in 23 samples), *Marthasterites furcatus* (in 10 samples), and *Ceratolithoides aculeus* (in five samples). In addition, the presence of *Eiffelithus eximius* and *Reinhardtites anthophorus* was reported continuously or quasi-continuously, in the uppermost part of the section.

Accordingly, it can be concluded that the age of studied marine section is definitely not younger than the middle Late Campanian, and even the basalmost, grey-coloured beds of the overlying and dominantly continental Sebeș Formation may still fall within the middle Upper Campanian (Fig. 12).

Indeed, based on the co-occurrence of *Ceratolithoides aculeus*, *Eiffelithus eximius*, and *Reinhardtites anthophorus*, the marine deposits of the Bozeș Formation from the Petrești section can be assigned to the Tethyan-Intermediate Province Zones UC15<sub>b</sub> to UC15<sub>e</sub> (Burnett, 1998)/CC20–CC22 Biozones (Perch-Nielsen, 1985), corresponding to the late

Early Campanian to late Late Campanian. The first occurrence datum (FO) of *C. aculeus* is marked at the base of the UC15<sub>b</sub> subzone (about 79 Ma)/CC20 Zone (Perch-Nielsen, 1985), corresponding to the middle of the early Late Campanian based on Gradstein et al. (2020) (= early Middle Campanian in the tripartite scheme). In addition, the presence of *E. eximius* and *R. anthophorus*, both having their last occurrence datum (LO) in the later part of the middle Late Campanian (within the UC15<sub>e</sub> subzone of Burnett, 1998, at about 75.93–80.97 Ma and 75.93–76.82 Ma, respectively), restricts the age of these deposits as no younger than the late Late Campanian, including here the uppermost Bozeș beds yielding calcareous nannofossil assemblages (upper part of the transitional deposits – sample 64), and even the two samples collected from the basalmost beds of the continental Sebeș Formation. It is worth emphasizing here that the reported (albeit unexpected) presence of marine calcareous nannofossils within these deposits can be attributed, probably, to sporadic intrusions of marine waters into this marginal continental setting, reconstructed as an estuarine-coastal plain palaeoenvironment (Vremir et al., 2014).

In our study, the composition of planktonic foraminiferal assemblages shows similarities to those described from the Central European Basin (Peryt et al., 2022) and their low diversity, as well as the significant participation of *Planoheterohelix globulosa*, *P. planata*, *Hedbergella globulosa*, *Globigerinelloides asper*, *G. bolli*, *Contusotruncana plummerae*, *Globotruncana arca*, *G. ventricosa*, and *C. plummerae* (identified in

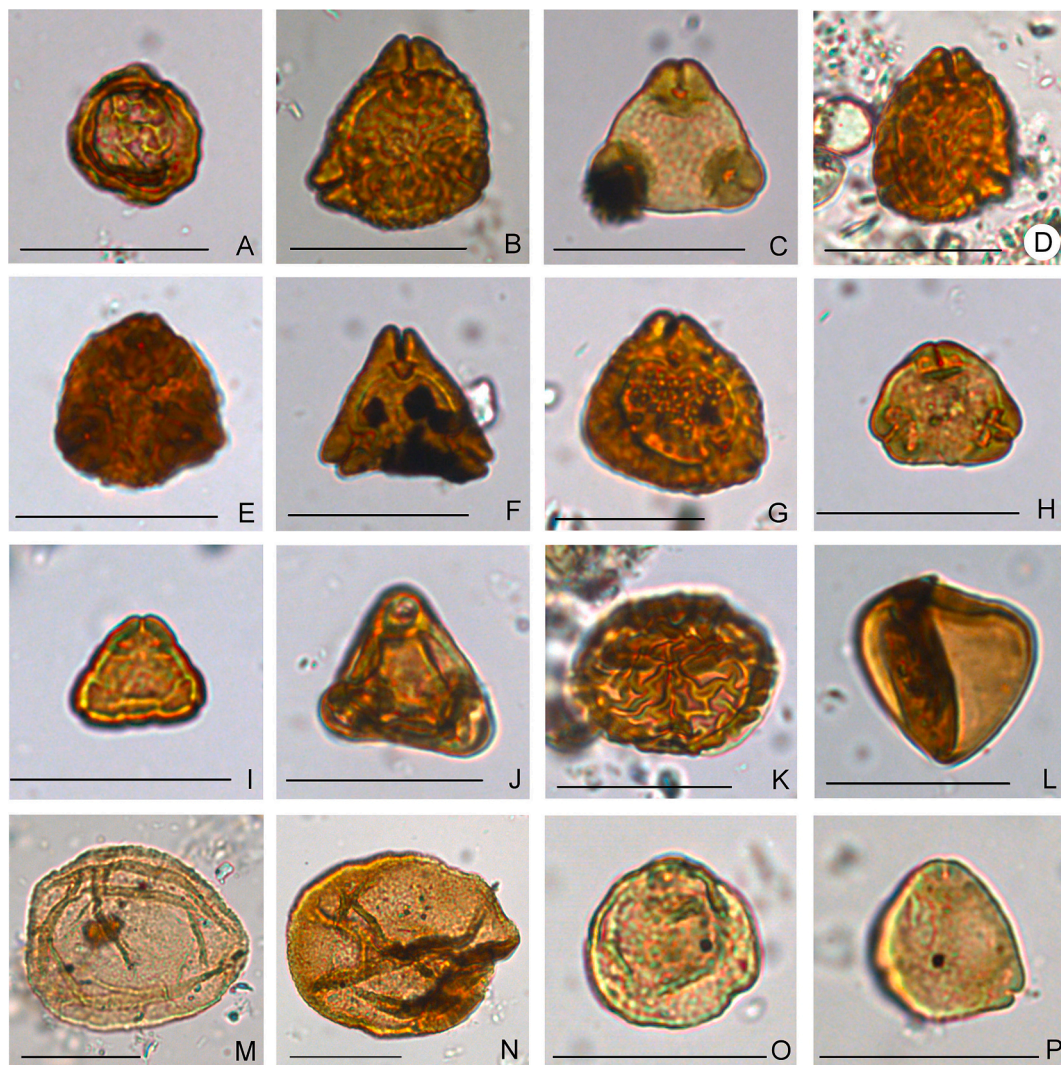


**Fig. 10.** Selected palynomorphs (dinoflagellate cyst, angiosperm and gymnosperm pollen, and cryptogam spores) identified in the uppermost part of the Bozeş Formation (scale bar: 30 µm). A. *Samlandia* cf. *vermicularia*, isolated operculum (sample 61); B. *Trudopollis rusticus* (61); C. *Trudopollis granulatus* (61); D. *Trudopollis lativerrucatus* (60); E. *Oculopollis praedicatus* (61); F. *Longanulipollis fornicatus* (61); G. *Krutzschipollis crassis* (61); H. *Pseudopapilipollis* cf. *praesubhercynicus* (61); I. *Suemegipollis triangularis* (61); J. *Interporopollenites proporus* (61); K. *Camarozonosporites insignis* (61); L. *Triplanosporites microsinosuosus* (61); M. *Araucariacites australis* (60); N. *Araucariacites australis* (61); O. *Subtriporopollenites constans* (61); P. *Myricipites* sp. (61).

samples 1–12), is characteristic of the *Contusotruncana plummerae* Interval Zone of the Upper Campanian in the Bottacione section and in Central European basins (Petruzzo et al., 2011; Coccioni and Premoli Silva, 2015; Peryt et al., 2022). There are recommendations stating that *G. ventricosa* (present in samples 1–12) should be used with caution in biozones for tropical and subtropical areas, and correlated with marker species such as *C. plummerae*, as it has its FO at the base of the *Contusotruncana plummerae* Zone in the Central European Basin (Peryt et al., 2022), whereas in the more southerly Italy it appears in the upper part of the *Contusotruncana plummerae* Zone (Petruzzo et al., 2011).

On the other hand, the species that define the upper part of the *C. plummerae* Zone (*Rugoglobigerina pennyi* and *Radotruncana calcarata*) were not identified in our samples; thus, in order to develop a better constrained biostratigraphic framework, we additionally used the data provided by calcareous benthic foraminifera as well. The main biostratigraphic markers of the calcareous benthic foraminifera group are *Bolivinooides decoratus*, *B. granulatus*, *B. laevigatus*, and *Brotzenella monterelensis* (all of these identified in the basal part of the section, in samples 1–12). From these, *B. monterelensis* was identified in Romania with a relatively long stratigraphic range, more precisely in Lower to Upper Campanian chalk deposits from Southern Dobrogea (Neagu,

1992) and in upper Santonian–Upper Campanian clayey deposits from the Ceahlău Nappe of External Dacides (Cetean et al., 2011). Setoyama et al. (2017) reported *B. monterelensis* from Lower to middle Campanian deep marine deposits in the Labrador Sea; Podobina (1995) and Alekseev and Kopaevich (1997) identified the same species in Upper Campanian deposits from Crimea and Siberia; and Robaszynski et al. (2005) reported it from Upper Campanian chalk deposits of the Paris Basin. Gawor-Biedowa (1992) described the biozone with *B. monterelensis* as being characteristic of the upper part of the Lower Campanian from Poland. Subsequently, Peryt and Dubicka (2015) and Dubicka and Peryt (2016) attributed *B. decoratus* species to the uppermost Lower Campanian–middle Upper Campanian, *B. granulatus* species to the upper Lower Campanian to lower Upper Campanian, *B. laevigatus* species to the upper Lower Campanian to middle Upper Campanian, and *Brotzenella monterelensis* to the middle Campanian to middle Upper Campanian in the Upper Cretaceous deposits of Poland and Ukraine.

Meanwhile, based on a wide assembly of samples originating from different sites, including boreholes recovered by the Deep Sea Drilling Project/Ocean Drilling Program, and from museum and university collections with worldwide coverage (e.g., Ehrenberg, Cushman, Petters, and McGugan collections), Georgescu (2018) proposes a middle

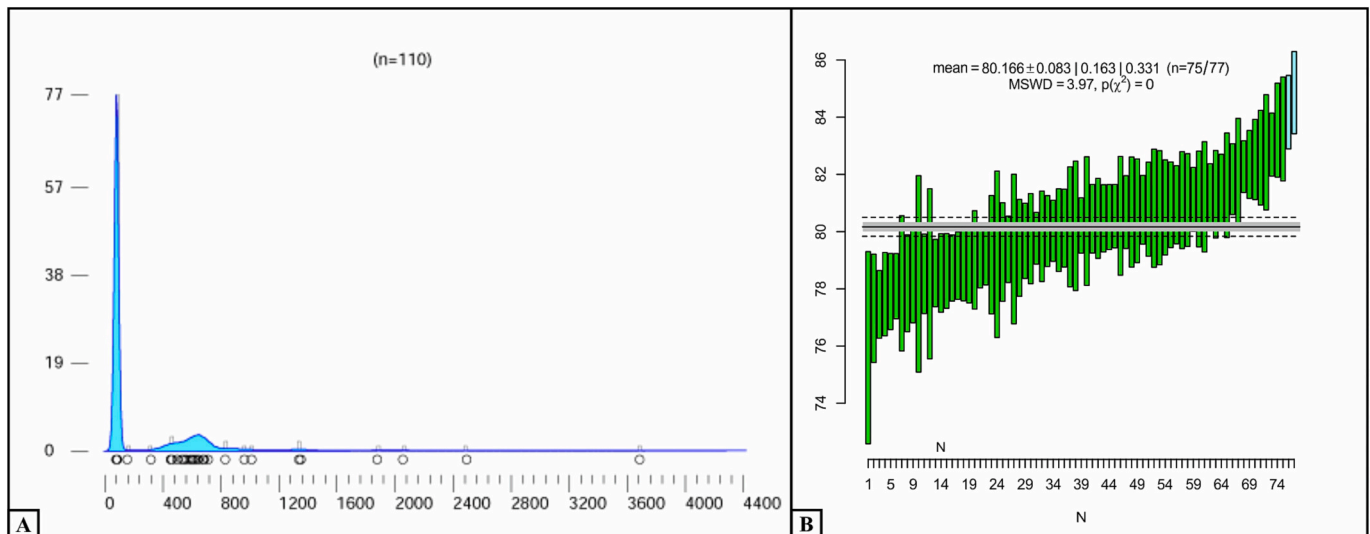


**Fig. 11.** (A) KDE plot of the  $^{206}\text{Pb}/^{238}\text{U}$  age spectrum of the detrital zircon population of sample IV from the uppermost Cretaceous transitional beds of Petrești section (see Fig. 2), southwestern Transylvanian Basin, showing two major peaks, a prominent Late Cretaceous (Campanian, see text and Fig. 11B) one representing a pene-contemporaneous volcanic arc signal, and an Ediacaran-Ordovician one, typical for the nearby metamorphic basement. Graphed using Density Plotter (Vermeesch, 2018); small open circles at the bottom of x axis show ages of individual samples. (B) Distribution of  $^{206}\text{Pb}/^{238}\text{U}$  ages and individual errors of the detrital zircons forming the Late Cretaceous peak (77 ages), with their weighted mean (80.16 Ma - Campanian) and errors (95% confidence intervals) drawn as horizontal lines.

Campanian to lower Maastrichtian stratigraphic range for *B. decoratus*, a Campanian–Maastrichtian range for *B. granulatus*, and an uppermost Lower Campanian–lower Maastrichtian range for *B. laevigatus*. Jaff (2021), Jaff et al. (2014), and Jaff and Lawa (2019) defined the *Bolivinoidea decoratus*, *Bolivinoidea laevigatus*, and *Brotzenella monterelensis* – *Brotzenella stephensoni* biozones characteristic to Upper Campanian deposits from Iraq. In our local biozonation scheme, we will rely mainly on the existing data from the Carpathian and peri-Carpathian areas as well as from the Bottacione section. Accordingly, considering together the somewhat poorly constrained biostratigraphic data based on planktonic and calcareous benthic foraminifera, we tentatively suggest a middle Late Campanian age for the basal and middle parts of the studied deposits. However, for the upper part of the section (samples 48–66; 495 m to 680 m) where the samples are quasi-sterile, barren in foraminifera, the (bio)stratigraphic assessments must rely primarily on calcareous nanofossil assemblages, palynological data, and detrital zircon results.

Preliminary palynostratigraphic results from the Petrești succession have been presented recently by Țabără et al. (2022); according to these previous results, the age for the largest part of the marine Bozeș Formation beds at Petrești can be constrained to the middle to later parts of the Campanian. Subsequently obtained new data from the transitional part of the succession (samples 60–62 in Fig. 2), not suitably covered by the earlier 2017 sampling reported by Țabără et al. (2022) now contribute further time constraints for the palynostratigraphy of the Petrești succession. Similarly to the local palynological assemblages reported by Țabără et al. (2022), those recovered from the new samples are represented mainly by pollen and spores of continental origin. Dinoflagellate cysts that belong to the marine phytoplankton still have rare occurrences in these newly identified assemblages, again replicating the pattern found previously by Țabără et al. (2022). Nevertheless, an isolated operculum assigned to the dinoflagellate *Samlandia* cf. *vermicularia* (Fig. 10A) was identified in sample 61. According to Slimani et al. (2021), the first occurrence of *Samlandia vermicularia* characterizes the base of *Samlandia mayi* Zone of Slimani (2001) of the Upper Campanian in the Netherlands, Belgium, and Poland. The last occurrence of *S. vermicularia* is reported from the lower part of the *Florentinia mayi*–*Samlandia mayi* dinocyst Subzone in Poland (Niechwedowicz and Walaszczyk, 2022), corresponding to the lower Maastrichtian, and thus the presence of this dinoflagellate restricts the geological age of the

palynological assemblage derived from the top of the Bozeș Formation to the Late Campanian–early Maastrichtian time interval.

Besides the dinocyst *Samlandia* cf. *vermicularia*, certain pollen taxa representing early angiosperms of the Normapolles group identified in samples 60 and 61 are also useful to date Upper Cretaceous deposits. Three such taxa (i.e., *Krutzschippollis crassis*, *Trudopollis rusticus*, and *T. granulatus*), described mainly from Turonian–Campanian deposits of Hungary, Bulgaria, and France (Góczán, 1964; Góczán and Siegl-Farkas, 1989; Góczán and Siegl-Farkas, 1990; Antonescu and Odin, 2001; Polette and Batten, 2017; Pavlishina et al., 2019), occur exclusively in sample 61. Other taxa identified recently in the uppermost part of the Bozeș Formation, i.e., *Oculopollis praedicatus*, *Longanulipollis fornicatus*, and *Trudopollis lativerrucatus*, are typical for the upper Upper Cretaceous, mainly the Santonian–Maastrichtian. Of these, the latter two taxa – *L. fornicatus* and *T. lativerrucatus* – are mentioned here for the first time from Upper Cretaceous deposits in Romania.

An interesting occurrence in the newly recovered palynological assemblage from the Petrești section is that of *Pseudopapillopollis* cf. *praesubhercynicus*, previously considered a biostratigraphic marker for the Maastrichtian in Hungary (Góczán, 1964; Góczán and Siegl-Farkas, 1990) and for the upper Maastrichtian in Romania (Antonescu, 1973; Antonescu et al., 1983), respectively. Later, however, this same taxon was reinterpreted as a marker species for the uppermost lower Campanian to the lowermost Maastrichtian interval in Romania (Ion et al., 1998). Other occurrences of this taxon have been reported from Campanian deposits from France (Tercis les Bains section; Antonescu and Odin, 2001) and Hungary (Siegl-Farkas and Haas, 2002). Taxa such as *Camarozonosporites insignis*, *Interporopollenites proporus*, *Suemegipollis triangularis*, and *Triplanosporites microsinosus* are also present in sample 61; these have also been previously identified in the lower–middle part of the Bozeș Formation from the Petrești section (Țabără et al., 2022), as well as from Campanian–lower Maastrichtian deposits of the Hațeg Basin (Țabără and Slimani, 2019; Botfalvai et al., 2021).

In summary, the occurrence of key taxa such as the marine dinoflagellate *Samlandia* cf. *vermicularia* in association with continental palynomorphs of the Normapolles group such as *Krutzschippollis crassis*, *Pseudopapillopollis* cf. *praesubhercynicus*, *Trudopollis rusticus*, and *T. granulatus* is considered to be broadly age-diagnostic. This assemblage brackets the age of the deposits from the uppermost Bozeș Formation at

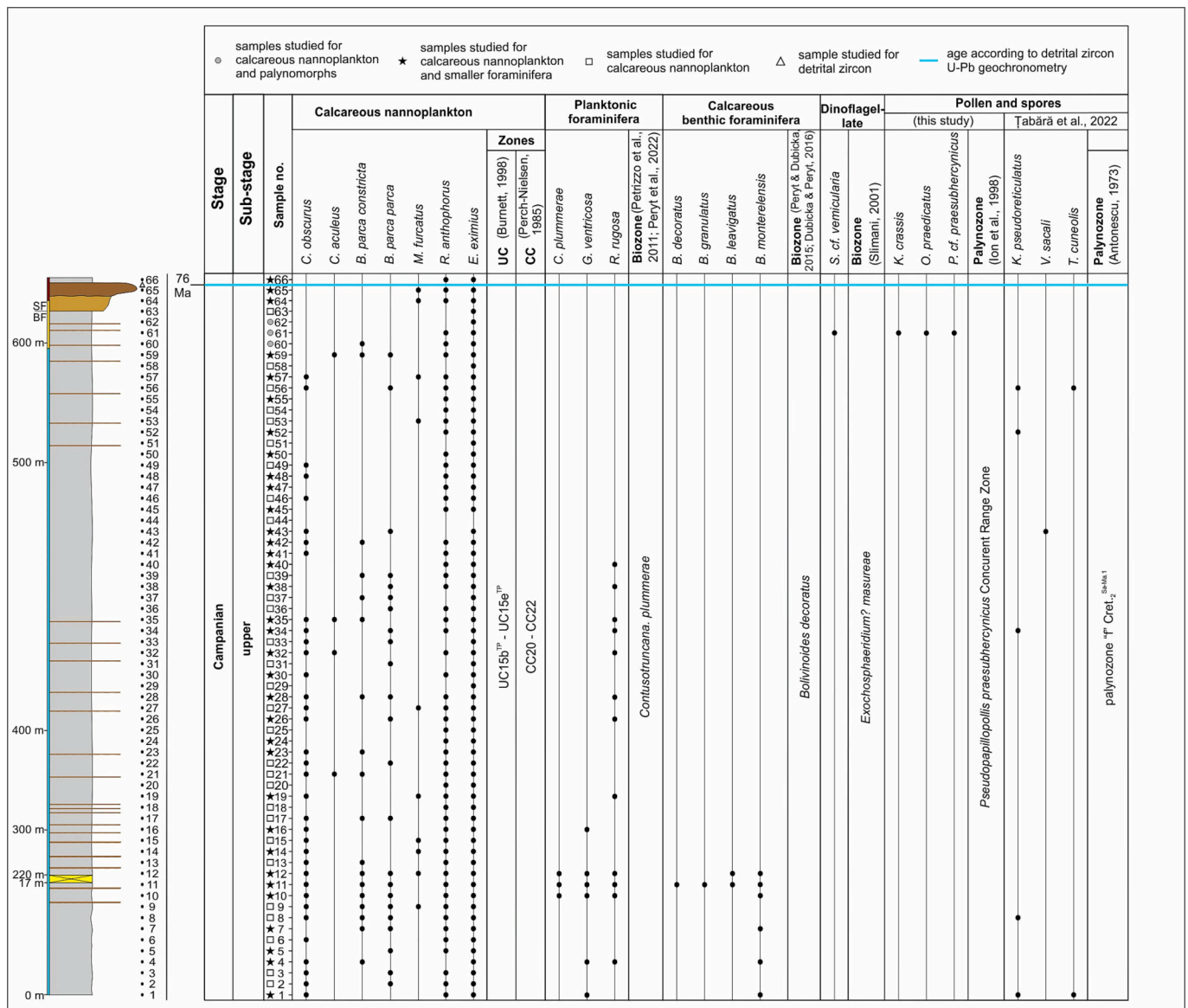


Fig. 12. Distribution of the stratigraphically significant microfossils, completed with results of detrital zircon U-Pb geochronometry for the Petrești succession, southwestern Transylvanian Basin. Lithological column - not to scale.

Petrești (i.e., the topmost 12 m of the Bozeș Formation succession, right below the estuarine basal beds of the Sebeș Formation) to between the Late Campanian and the earliest Maastrichtian.

To summarize the previously discussed biostratigraphic information, the uppermost Cretaceous deposits from the Petrești section belong to three distinctive lithological entities whose ages/chronostratigraphic positions are constrained as follows (Fig. 12):

- The main body of the Bozeș Formation, corresponding to the largest part of the locally exposed section (meters 0 to about 595 in the measured stratigraphic log, Fig. 2): a lower Upper Campanian to middle Upper Campanian marine unit with a lithology typical for a turbiditic facies, represented by an alternation of sandstones and mudstones/shales. The microfossil assemblages of this entity include calcareous nannofossil assemblages typical for UC15<sub>b</sub> to UC15<sub>e</sub> biozones (late Early to late Late Campanian) and small foraminifera ones characteristic for a Late Campanian age. Our new results are consistent with those of the study of Tabără et al. (2022) which reported a palynomorph assemblage documenting the presence of the middle and upper parts of the Campanian within this part of the local

succession. Macroinvertebrates such as corals, inocerams, and oysters were found to be common in this unit, alongside with rare ammonite coil fragments (Vremir et al., 2014).

- A transitional succession marking the passage from marine to continental deposits (between 595 and 640 m in the local log; Fig. 2), interpreted to represent a near-shore to estuarine, brackish environment with generally coarser sediments (dark grey marly siltstones and mudstones) containing calcareous nannofossils and palynomorphs but entirely devoid of foraminifera. The calcareous nannofossil assemblages are similar to those described from the underlying marine beds (and their presence is probably due to episodic intrusions of normal marine waters into these brackish coastal-estuarine settings), and the identified palynomorphs are suggestive of a Late Campanian–early Maastrichtian age. The Bozeș-Sebeș formational contact was drawn on lithological grounds within this transitional succession by Vremir et al. (2014), and this lithostratigraphic interpretation is followed here as well (Fig. 2). The contact is located at the base of the first thicker and coarser-grained bed of silty-sandy marls covered by a thick, prominent sandy-conglomerate bed interpreted as a channel deposit. The

stratigraphically lowest occurrences of isolated dinosaur and pterosaur fossils described from the uppermost part of the Bozeş Formation as the oldest known members of the Haţeg Island palaeoecosystem originate from the lower, brackish marine part of this transitional succession (Vremir et al., 2014; see Fig. 2 - L0/a, L0/b). Meanwhile, the lowest-lying rich continental vertebrate accumulation reported preliminarily by Vremir et al. (2015b; see also Vasile, 2021, 2022) is located slightly higher within the basalmost Sebeş Formation, right above the formational contact and below the thick channel deposit marking the onset of typical continental sedimentation (Fig. 2 - L0/c).

- The basal part of the continental Sebeş Formation (from about 640 m upwards in the local log), characterized by alternating floodplain and channel deposits, represented by dominantly reddish, sometimes green-mottled mudstones, sandstones, and rare microconglomerates, with vertebrate fossils discovered from several different levels (Csiki-Sava et al., 2012; Brusatte et al., 2013; Vremir et al., 2014, 2015a; Fig. 2 - L1a, L1b). Although reliable and precise age constraints (even palynomorphs) are currently unavailable for these beds, they are regarded as (probably earliest to early) Maastrichtian in age based on their vertebrate fossil content, largely similar to that of other Maastrichtian vertebrate-bearing units of the southwestern Transylvanian area (e.g., Csiki-Sava et al., 2016).

Most notably, the preliminary results of an entirely new dating approach for this section, that is, detrital zircon U-Pb geochronometry, are largely congruent with these integrated biostratigraphy conclusions. The sample reported here (Petreşti IV) was collected from the thick and coarse sandstone-conglomerate bed from the basalmost Sebeş Formation (Fig. 2 - between 645 and 650 m) directly overlying the dark grey silty mudstones that host the stratigraphically lowest-lying multitaxic continental vertebrate fossil accumulation recorded in the Petreşti succession (Vremir et al., 2015b; Vasile et al., 2021, 2022). As noted above (see Results and Electronic Supplement - Fig. 4), the maximum depositional age (MDA; Vermeesch, 2021) of this sample - remarkably enriched in latest Cretaceous-age 'banatitic' zircons - was estimated to be about 80 Ma, largely similar with the average pooled age of these zircons (Fig. 11B). Lack of plateaus of different ages in the banatitic zircon U-Pb age spectrum (Fig. 11B) is indeed broadly consistent with the entire population being the result of one eruption, thus being of the same (= calculated mean) age.

Nevertheless, this statistical average calculated using the approach advocated by Vermeesch (2021) may well be different from the actual MDA of the deposit, depending on whether some of these zircons are instead inherited grains from a longer-lived magma chamber (antecrysts) or, alternatively, whether they originate from (and thus reflect the age of) several, temporally closely spaced volcanic events fitting into the recorded age range (about 76 to about 82 Ma). Our detrital zircon data cannot resolve this; furthermore, there is no knowledge of a nearby volcanic center(s) that would represent the immediate source(s) of these grains. However, as the typical banatitic volcanic centers regionally are known to have been stratovolcanoes, we speculate that the youngest recorded zircon grain age of  $76 \pm 1.7$  Ma approximates better the actual maximum age of this sedimentary unit. Given the dominance of young igneous grains in this sample, identifying the source rock as a siliciclastic-volcanic deposit resulted from the erosion of volcanic apparatuses from the nearby banatitic volcanic arc, it is likely that the actual age of sedimentation was not much younger than the age of the volcanic source itself since stratovolcanoes are ephemeral features, on average relatively short-lived and rapidly removed by subsequent erosion (e.g., Ducea et al., 2015). Accordingly, these preliminary U-Pb geochronometric results seem to constrain the age of the uppermost brackish marine - basalmost continental deposits as not much younger than  $76 \pm 1.7$  Ma (that is, falling within the late middle to early late Late Campanian), in good accordance with the calcareous nannofossil biostratigraphy and palynostratigraphy data reported in the present

study. Meanwhile, the remainder of the analyzed detrital zircon sample comprises mainly Neoproterozoic to Silurian age zircons, with a very small amount of Variscan and Palaeoproterozoic grains. Altogether, the age spectrum yielded by the pre-Late Cretaceous zircon grains is a signature feature of the nearby Getic-Supragetic basement terranes that are found immediately to the south of the study area and which are considered to have been an actively uplifting and eroding source area during the deposition of the uppermost Cretaceous beds across the entire southwestern Transylvanian area (e.g., Willingshofer et al., 2001; Csiki-Sava et al., 2016).

## 5.2. Palaeoenvironmental interpretations

### 5.2.1. Palaeotemperature

A significant global palaeoclimatic change that took place during the Late Cretaceous was identified by several studies (Huber et al., 1995; Friedrich et al., 2012; Linnert et al., 2014), from one of the warmest climates known to have existed during the Late Cenomanian to early Turonian towards a significant cooling from the late Turonian onward until the end of the Cretaceous. This cooling trend was accelerated at the beginning of the Campanian (Friedrich et al., 2012; Linnert et al., 2014; Bindu et al., 2013) and extended into the Maastrichtian (Huber and Watkins, 1992; Huber et al., 1995; Lees, 2002; Thibault and Gardin, 2007; Sheldon et al., 2010; Friedrich et al., 2012; Linnert et al., 2014).

However, such a global cooling pattern is not confirmed by the calcareous nannofossil assemblages from the Petreşti section due to the high abundance of *Watznaueria barnesiae* (a marker for sub-cluster 2b), a species considered to be a warm-water taxon (Doeven, 1983; Gardin, 2002; Sheldon et al., 2010; Tantawy, 2003) and one that was typical for low-latitude Tethyan sites, according to Wolfgring et al. (2021). From the planktonic foraminifera assemblages identified at Petreşti, globotruncanids (amounting up to 57% in some samples) are considered to indicate a warm and oligotrophic subsurface mixed layer (Li and Keller, 1998; Petrizzo, 2002; Abramovich et al., 2003, 2010; Saïdi and Zaghib-Turki, 2016), whereas rugoglobigerinids (up to 35%) are characteristic of warm-temperate stratified waters (Lommerzheim, 1991; Hradecká, 2002; Falzoni et al., 2014). The terrestrial palynomorphs recovered from the top of the Bozeş Formation (sampling interval 60–61; Fig. 2) comprise pollen of ancestral Juglandaceae (e.g., *Subtriporopollenites constans*), taxa that preferred the relatively warmer and dryer conditions of the lowlands or hilly areas (Friis et al., 2011; Daly and Jolley, 2015). Neither is this cooling trend evidenced by the Campanian–Maastrichtian continental vegetation from western Romania, characterized by elements of subtropical to warm-temperate forests (Van Isterbeek et al., 2005; Ţabără and Slimani, 2019; Botfalvai et al., 2021; Ţabără et al., 2022).

Nevertheless, even if the microfossil assemblages suggest generally warm conditions, certain thermally tolerant cold-water taxa were also identified in few samples along the studied section. These include examples of calcareous nannofossils (*Ahmuelerella octoradiata*, *Gartnerago segmentatum*, *Kamptnerius magnificus*, *Prediscosphaera stoveri* - Wind, 1979; Watkins et al., 1996; Burnett, 1998; Svábénická, 2001; Linnert et al., 2011), foraminifera (e.g., *Hedbergella*, *Globigerinelloides*, *Heterohelix* - Caron, 1985; Lommerzheim, 1991; Hradecká, 2002; Petrizzo, 2002; Rostami and Balmaki, 2018), and palynomorphs (elements of the Normapolles flora; Ţabără et al., 2022).

Considered together, however, these marine and continental microorganisms convergently point to overall warm surface water conditions during the largest part of the Late Campanian, the depositional time of the marine sediments from Petreşti.

### 5.2.2. Nutrient input

According to our nannoplankton investigations, the surface waters at Petreşti were dominated by *Watznaueria barnesiae*, a taxon reported from oligotrophic (Erba et al., 1992; Herrle et al., 2003; Thibault and Gardin, 2007; Chan et al., 2022) and low fertility (Roth, 1989; Roth and

Krumbach, 1986; Premoli Silva et al., 1989; Watkins, 1989; Erba, 1992) environments. There are studies, however, that interpreted similar abundance patterns of *Watznaueria barnesiae* as resulting from a combination between poor preservation and an oligotrophic depositional environment (Erba, 1992; Roth and Bowdler, 1981; Alves et al., 2018). Due to the currently existing uncertainties regarding the specific contributions of the different factors that control the abundance of *Watznaueria barnesiae*, it is difficult to decide whether its abundance recorded at Petrești is the result of a relatively warmer and oligotrophic environment or that of dissolution processes in action. The existence of oligotrophic conditions is, nevertheless, supported independently by the presence of globotruncanids (Li and Keller, 1998; Petrizzo, 2002; Abramovich et al., 2003, 2010; Saïdi and Zaghbib-Turki, 2016). Subsequently, heterohelicids (generally seen as indicators for increased surface water productivity - Keller et al., 2001; Pardo and Keller, 2008) register relatively high values of relative abundance at some intervals. This pattern positively correlates with values of the nutrient index calculated for calcareous nannofossils, and probably indicates the occurrence of short eutrophic episodes.

At or near the sea floor, the benthic foraminifera assemblages suggest meso-eutrophic conditions. Occurrence of mesotrophic conditions are indicated in samples 1–11, 14–19, 30–35, and 40–47, through low total relative abundance and low benthic foraminifera relative abundance values correlated with high percentages of calcareous benthic epifaunal forms (Ch-A morphogroup: *Gyroidinoides* spp., *Cibicidoides* spp., *Epistomina* sp., *Lenticulina* spp.), tubular agglutinated taxa (M1 morphogroup: *Bathysiphon* sp., *Rhizammina* sp.), and rounded agglutinated forms (M2a morphogroup: *Saccamina* spp.). Of these taxa, *Gyroidinoides* is typical for meso- to eutrophic environments with low oxygen content at the sea floor and moderate food availability (Erbachen et al., 1998; Friedrich et al., 2005; Gebhardt et al., 2013; Wendler et al., 2013; Kranner et al., 2022), the species of *Cibicidoides* are characteristic for more oligotrophic environments with increased bottom current activity (Thomas et al., 2000; Sgarrella et al., 2012; Arreguín-Rodríguez et al., 2016; Russo et al., 2022), *Epistomina* is considered opportunistic (Reolid et al., 2012; Wendler et al., 2013) and indicates shallow-water clayey/shaly facies (Williamson and Stam, 1988), and erect epifaunal tubular agglutinated forms belonging to M1 morphogroup characterize mesotrophic environments with moderate oxygenation and low content of organic matter flux (Kaminski and Gradstein, 2005; Cetean et al., 2011; Bindu et al., 2013, 2016; Setoyama et al., 2017; Bindu-Haitonic et al., 2017, 2019; Bindu Haitonic, 2018). Meanwhile, in samples 12, 26 to 28, and 35 to 40, intervals with high relative foraminifera abundances (total and benthic indices, both) are positively correlated with high percentages of infaunal forms (Ch-B calcareous benthic morphogroup: *Bolivinoidea* spp., *Praebulimina* spp., *Pseudouvierina* spp.) and of *Haplophragmoides* spp. (M4a agglutinated foraminifera morphotype); this pattern suggests more eutrophic environments with high productivity and low oxygenation to the seafloor (Nagy et al., 1988; Murray, 1991; Nagy and Basov, 1998; van der Zwaan et al., 1999; Alegret et al., 2003; Kaminski and Gradstein, 2005; Murray, 2006; Schweizer, 2006; Setoyama et al., 2017).

### 5.2.3. Oxygenation

At the seafloor, the dissolved oxygen content is best expressed by the benthic foraminifera oxygen index (BFOI) that was first described and applied by Kaiho (1991, 1994), subsequently used in numerous studies (e.g., Bernhard and Bowser, 1999; Kaminski, 2012; Singh et al., 2015; Hoogakker et al., 2015; Rathburn et al., 2018; Ilieș et al., 2020; Bindu-Haitonic et al., 2021; Kranner et al., 2022). Employing the newly developed equations of Kranner et al. (2022) for the Petrești samples with a microfossil content of over 100 benthic forms, the resulting BFOI values (see Fig. 8) place the original depositional environments mainly into the suboxic category (except for the intervals corresponding to samples 11 and 30 where the conditions were low-oxic). These suboxic conditions (probably caused by a high flux of organic matter to the

seafloor) may also be indicated by high values of relative abundance of benthic foraminifera (Fig. 8), as suggested by certain previous studies (e.g. Setoyama and Kanungo, 2020). Extreme suboxic conditions are recorded in samples 14 and 16 (BFOI values of –28 and –40, respectively), concordantly indicated by the important occurrence of *Haplophragmoides* spp. that display values up to 20.5% of the total benthics in these samples, as this genus with disoxic affinities is a shallow infaunal taxon that thrives in eutrophic environments with low-oxygen conditions (Ortiz, 1995; Kuhnt et al., 1996; Kaminski et al., 1999; Alegret et al., 2003; Kaminski and Gradstein, 2005). For other samples, suboxic conditions are suggested by the presence of *Bolivina*, *Bolivinoidea*, *Praebulimina*, and *Pseudouvierina*, genera known as disoxic indicators (Kaiho, 1991, 1994; Murray, 1991, 2006; van der Zwaan et al., 1999; Schweizer, 2006; Kranner et al., 2022). Slightly more oxygenated intervals corresponding to samples 11 and 30 (BFOI: 1.84 and 13.5) are pointed out by the percentage increases of the different epifaunal *Cibicidoides*, *Hoeglundina*, and *Brotzenella* species known to be oxic indicators (e.g., Murray, 1991, 2006; Kender et al., 2008; Kranner et al., 2022).

The presence of generalized low-oxygen conditions at the seafloor during the deposition of the Petrești marine succession is independently supported by the lithological characteristics of these mainly dark-coloured shaly-clayey deposits (Electronic Supplement – Fig. 3A-B), since such muddy substrates are characteristic of low bottom-water oxygen concentrations (Hayward et al., 1999). Accordingly, the BFOI values, oxygenation preferences of certain species, and the lithofacial features consistently characterize the marine depositional environments represented in the Bozeș Formation deposits at Petrești as being dominantly suboxic, in good accordance with the results of the geochemical analyses carried out by Țabără et al. (2022) on selected samples from the same section, although with two short-lived low-oxic intervals.

### 5.2.4. Palaeobathymetry

All three groups of microfossils provided interesting palaeobathymetric information, informing in detail about the depth(s) of the depositional environment(s). Among these indicators, the foraminiferal assemblages represent one of the most intensely employed tools in palaeodepth reconstructions, by using either percentage participation of planktonic and benthic foraminifera, benthic species diversity, bathymetric preferences of certain benthic or planktonic species, or a combination of the above-mentioned methods (Phleger and Parker, 1951; Murray, 1973, 1976, 1991; Hayward and Buzas, 1979; Hayward, 1986; Leckie, 1987; Hayward, 2004; Székely et al., 2016). Surveying the above-mentioned characteristics (Fig. 8) suggests that the depositional setting represented by the basal 490 m of the Petrești section (corresponding to sampling interval 1 to 38 Fig. 2) was shallower than that represented by the overlying 10 m succession (corresponding to samples 38 to 48). For the final part of the studied section, unfortunately, no palaeobathymetry-informative foraminifera data was available due to their low abundance or even complete absence. We assess that the activity of higher-energy currents (as documented by the presence of intercalated conglomeratic levels) caused unfavorable environments for the development of foraminifera communities, thus justifying the sterility of these uppermost samples.

The stratigraphic interval between samples 1–38 is characterized by the highest values of indices such as total relative abundance of foraminifera as well as relative abundance and diversity of benthic foraminifera, doubled by low percentages of planktonic foraminifera (Fig. 8). The benthic foraminifera assemblages here are dominated by epifaunal forms (*Cibicidoides* spp., *Epistomina* spp., *Gyroidinoides* spp., *Trochamminoides* spp.). Starting with sample 38, values of these indices (i.e., total relative abundance and abundance of benthic foraminifera) begin to decrease, while in the calcareous benthic foraminifera group, epifaunal foraminifera are outnumbered by infaunal ones (represented by species of *Praebulimina* and *Pseudouvierina*). Planktonic foraminifera (even if they occur in small numbers) register percentages of up to 80%, being

characterized by a decrease in the percentage of hedbergellinids (considered shallow marine environment indicators - Eicher, 1969; Eicher and Worstell, 1970; Sliter, 1972; Leckie, 1987) and globotruncanids up-section. In general, an abundance and diversity increase of the planktonic forms is associated with greater depths, shifting from shallow-water zones to bathyal areas lying above calcite compensation depths (Buzas and Gibson, 1969; Gibson, 1989; Hayward et al., 1999; Iliş et al., 2020). The agglutinated taxa *Haplophragmoides* spp. (M4a morphotype) also register very high percentage values in this interval (ES Fig. 3). Since *Haplophragmoides* have been reported both from shallow areas (Nagy et al., 2000; Murray, 2006; Jain and Farouk, 2017) and from bathyal ones (e.g. Kaminski and Gradstein, 2005), the simple presence of these agglutinated taxa in itself cannot represent a reliable bathymetric classification criterion for our study area, and it should be interpreted in conjunction with the relatively high values of abundance registered by planktonic foraminifera.

This trend of increasing water depth is also confirmed by the abundance pattern (Fig. 4) of the species of the calcareous nannofossil *Russellia* (the taxa that defines sub-cluster 1b) that are generally regarded as marginal marine or nearshore forms associated with shallow-water deposits (Gardin, 2002) as well as by the presence and abundance patterns of the opaque phytoclasts in the palynomorph assemblages (discussed by Țabără et al., 2022).

Towards the top of the marine succession (covered by samples 48–66), the palynological analyses reported here (see also Țabără et al., 2022) and the lithological-palaeontological features (the presence of coarser, conglomeratic levels, and that of the brackish mollusks and vertebrate remains) both indicate a transition towards more continental depositional settings. This environmental shift is witnessed by the deposits forming the topmost part of the Bozeş Formation and the basal part of the Sebeş Formation, and most likely is represented by a coastal to estuarine environment (Vremir et al., 2014).

### 5.2.5. Terrestrial palaeoenvironments

The largest part of the palynomorphs recovered from the Petreşti succession is represented by different terrestrial taxa that suggest a diversified vegetation existing on the nearby emerged land areas, typical both to lowlands, as well as to well-drained and higher-altitude habitats. The occurrence of hygrophytic fern spores such as *Deltoidospora*, *Laevigatosporites* and *Polypodiaceosporites*, together with various Myricaceae pollen, suggests plant communities growing in lowland fluvial or coastal plain environments (Abbink et al., 2004). Meanwhile, the taxon *Subtripropollenites constans* (well represented in sample 61; Fig. 2) is often associated with *Araucariacites australis* (related to the Araucariaceae conifers), another taxon that also shows a high frequency in the studied palynological assemblage. According to Bowman et al. (2014) and Michels et al. (2018), the *Araucaria* forests were characteristic to well-drained and higher-altitude habitats, requiring cooler temperate conditions, since pollen types similar to *Araucariacites australis* is produced today by *Araucaria araucana*, a modern species growing in cool temperate conditions of the southern hemisphere, with a coldest month mean temperature of 7–8 °C and a warmest month mean temperature of 17–19 °C (Bowman et al., 2014).

Taken together, the palynological assemblage identified in the upper part of the Bozeş Formation consists of representatives of palaeofloras that inhabited both lowland habitats (e.g., Juglandaceae, Myricaceae, ferns) as well as higher-altitude areas (*Araucaria*). Furthermore, the high frequency of *Araucaria* pollen in the middle-upper Upper Campanian deposits from the Petreşti area, as well as its good state of preservation, may be indicative of the presence of high-elevation areas near/close to the shoreline.

## 6. Brief overview of the Campanian marine deposits from Romania, and comparisons with the Petreşti section

The Campanian marine deposits of Romania were studied in some

detail only in a few areas outside the Petreşti region, including the Apuseni Mountains, the Haţeg Basin, and the Eastern Carpathians (see inset map in Fig. 1). In order to emphasize similarities/differences between the different areas containing Campanian deposits, to improve regional correlations, and to outline the importance of the Petreşti section as a continuous marine-to-continental sequence, we will briefly synthesize the data available from those other areas and compare them with the newly acquired data from the Petreşti section. After summarizing the available information regarding the depositional settings of the Campanian deposits from Romania, combined with their current age assessments (as supported by biozones using the main fossil groups also discussed in our study), the following general overview emerges:

- The deepest Campanian marine deposits were identified in: i) the southern part of the Apuseni Mountains (Metaliferi Mts., Bozeş Formation) (Fig. 13A – light grey color), where calcareous nannofossil assemblages indicate the presence of CC17 to CC19 biozones (Bălc et al., 2007), as well as within the Upper Gosau Subgroup (Fig. 13A – blue color) for which, however, no calcareous nannofossil and foraminifera data are currently available; ii) the southeastern part of the Haţeg Basin (Fig. 13B – yellow color), excepting the thin, infralittoral succession of the Strei Formation, where the calcareous nannofossil assemblages indicate the presence of the Campanian biozones up to the basal part of CC22 biozone (Melinte-Dobrinescu, 2010); iii) the northwestern part of the Haţeg Basin (Fig. 13B – dark grey color), where the calcareous nannofossil assemblages indicate the presence of CC16 up to basal part of CC22 biozones (Grigorescu and Melinte, 2001; Melinte-Dobrinescu, 2010); and iv) the Eastern Carpathians (including the largest part of the Tarcău Nappe that roughly corresponds to the central areas of the Carpathian Flysch Basin; Fig. 13C – brown, green and blue colors), where calcareous nannofossils indicate the presence of CC21 to CC23 biozones, and the foraminifera content points to the presence of the *Globotruncana ventricosa* and the *Caudammina gigantea* biozones (Bindiu et al., 2013).
- Somewhat shallower environments that mark the transition from deep to shallow marine deposition were reported from the Eastern Carpathians (Vrancea Nappe; Fig. 13C3), in areas that once bordered the Carpathian Flysch Basin towards the more easterly cratonic region found in a lower-plate position; here, a Campanian age was attributed based on the presence of *Globotruncana ventricosa* (Guerrera et al., 2012).
- Definitely shallow-marine Campanian deposits are present in: i) the Northern Apuseni Mountains (Fig. 13A – blue color), where their Campanian age was based on corals and rudists (Săsăran and Săsăran, 2003); and ii) the inner Eastern Carpathians (Ceahlău Nappe) (Fig. 13C1) where calcareous nannofossil assemblages indicate the presence of CC18 to CC23 biozones, and the planktonic foraminifera belong to the *Globotruncanella elevata*, *Globotruncana ventricosa*, *Radotruncana calcarata*, and *Globotruncanella havanensis* zones (Cetean et al., 2011).

In conclusion, our brief review shows that several different areas within the circum-Transylvanian region of the Carpathians host Campanian deposits that are largely contemporaneous with those cropping out in the Petreşti section, allowing a regional contextualisation of our new biostratigraphic, geochronologic, and palaeoenvironmental data. To begin with, the overview shows that, all these deposits are exclusively of marine origin, documenting the widespread development of marine areas in and around the Transylvanian region during the Campanian. Moreover, it is also noteworthy that in the majority of the documented cases, these deposits were formed at even deeper water depths compared to the depositional palaeoenvironments reconstructed here for the Petreşti beds. And, most significantly, whereas in these other areas deeper-water sedimentation appears to have continued up to the end of the Campanian (or locally, such as in the Eastern Carpathians,

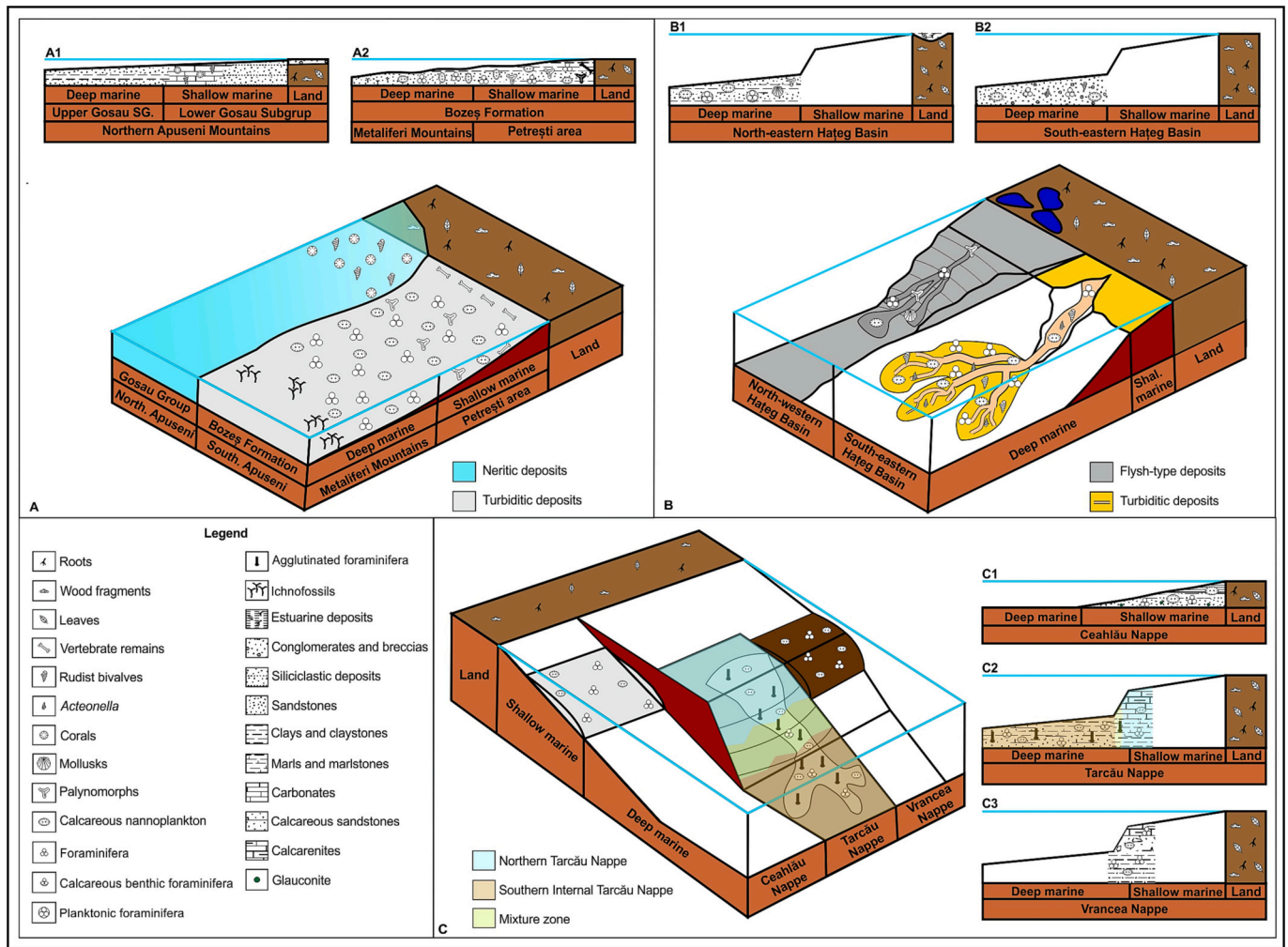


**Fig. 13.** Assessed depositional setting of the Campanian deposits from Romania and the distribution of the main identified fossil groups in: A) Apuseni Mountains; B) Hațeg Basin; C) Eastern Carpathians.

uninterrupted into the Maastrichtian as well), at Petrești the depositional environments were already shifting towards brackish nearshore, shallow neritic ones well before the end of the Campanian, which suggests that this region was among the first Transylvanian sectors that underwent continentalisation as part of the latest Cretaceous ‘Hațeg Island’.

Remarkably, this pattern of diachronous environmental evolution also holds when comparing the Campanian deposits from the Petrești area (and the southwestern Transylvanian Basin) with those from the nearby Hațeg Basin, otherwise known for its well-developed Maastrichtian continental formations with rich and iconic vertebrate faunas (e.g., Nopcsa, 1923; Grigorescu, 2010; Csiki-Sava et al., 2016). This shows that the intermountain Hațeg Basin developed within the Southern Carpathians was probably still largely covered by marine waters when withdrawal of sea was already well underway at the northern foothills of the Southern Carpathians. It is also worth noting that even within the Bozeș Formation itself, sediments suggesting a deeper depositional setting are documented in the northwestern parts of the unit’s sedimentation area (in the Southern Apuseni Mountains) in stark contrast with the shallower settings identified by our research in the southeastern parts (i.e., near Petrești), which supports the proximity of these latter areas to contemporaneous emergent lands presaging the Hațeg Island. Finally, it must be emphasized that from all the above-mentioned areas with known Campanian sedimentation, currently the most complete and continuous record of the transition from marine to

continental palaeoenvironments near the end of the Cretaceous is offered by the Petrești section, which further underscores its importance for regional correlations and palaeogeographic reconstructions.

**7. Implications of the newly reported age constraints from the uppermost Cretaceous Petrești section for the advent of the dwarf dinosaur faunas of the ‘Hațeg Island’**

Continental vertebrate remains have been reported to occur at several superposed levels of the Petrești succession, both in the transitional uppermost Bozeș Formation and in the basal Sebeș Formation (Csiki-Sava et al., 2012, 2022; Vremir et al., 2014, 2015a). Since this succession also records a more or less continuous transition from the marine beds of the Bozeș Formation to the basal beds of the overlying continental Sebeș Formation (Fig. 2), it allows for tracking the timing, tempo, and pattern of the transition from the widespread marine settings that characterized the Transylvanian region for most of the later Late Cretaceous to extensive continental deposition towards the end of the Cretaceous (e.g., Vremir et al., 2014; Csiki-Sava et al., 2016). As such, it represents a trove of crucial information regarding both the emergence of the latest Cretaceous ‘Hațeg Island’ as well as the evolution of its continental vertebrate faunas.

These dwarf dinosaur-bearing faunas from the Transylvanian area rank among the most diverse and important latest Cretaceous continental vertebrate assemblages in Europe and are definitively the most

important ones from eastern and southeastern Europe (e.g., Csiki-Sava et al., 2015). However, whereas other important Central European localities (coming from Hungary and Austria) are Santonian–Early Campanian in age and those from western Europe (mainly from southern France and Spain) cover the entire Early Campanian to latest Maastrichtian time interval (e.g., Csiki-Sava et al., 2015), the Hațeg Island faunas were usually regarded as restricted to the Maastrichtian (e.g., Grigorescu, 2010; Benton et al., 2010). Accordingly, the Transylvanian faunas were supposed to cover a significantly shorter time interval than the western, Ibero-Armorican faunas, and to represent a different, much later time slate than the geographically proximate Central European ones.

The Petrești succession demonstrates, however, that the earliest occurrences of Transylvanian vertebrate remains are actually hosted by middle-upper Upper Campanian beds of the Bozeș Formation (Vremir et al., 2014; Fig. 2). Our renewed and more detailed sampling of the Petrești section, whose results are reported here (see also Țabără et al., 2022), together with more recently identified vertebrate occurrences from this succession (Vremir et al., 2015b; Vasile et al., 2022), now allows a significantly improved temporal assessment of the Petrești beds and their vertebrate record, with implications for the emergence of the Hațeg Island faunas.

One important result of our integrated biostratigraphy data is that the largest part of the transitional sequence from Petrești (i.e., the uppermost, brackish marine beds of the Bozeș Formation and the more continental-influenced, grey-coloured estuarine-coastal basalmost beds of the Sebeș Formation) still falls within the calcareous nannofossils biozone CC22, that is, within the middle Upper Campanian to lower part of upper Upper Campanian interval. This stratigraphic position is also supported convergently by less compelling palynostratigraphic and foraminifera biostratigraphic data and, most importantly, by the first available radiometric age data (obtained through detrital zircon U-Pb geochronometry). Together, these independent lines of evidence provide solid corroborative support for the start of deposition of the basalmost continental beds of the Sebeș Formation in the Petrești area during the middle to later part of the Late Campanian, sometimes shortly after about 76 My. Our new age constraint has two important implications, one concerning the process of continentalization and expansion of the latest Cretaceous Hațeg Island, and another regarding the compositional evolution of the vertebrate fauna that inhabited this emergent land.

As already discussed by Vremir et al. (2014) and Csiki-Sava et al. (2015), emergent land areas were continuously present in the wider Transylvanian area from the beginning of the Late Cretaceous, although these are very difficult to localize or specifically circumscribe. They were most probably relatively small-sized, geographically isolated from each other, and confined to parts of the Carpathian Orogen uplifted during previous mountain-building events (see, e.g., Săndulescu, 1984); these areas became enlarged and confluent with each other only towards the end of the Cretaceous, forming the ‘Hațeg Island’ or the Transylvanian Landmass (e.g., Benton et al., 2010). It was often assumed that the widespread emergence leading to the Hațeg Island took place near the Campanian–Maastrichtian boundary or even during the early Maastrichtian (e.g., Grigorescu, 2010; Melinte-Dobrinescu, 2010). Now, however, our new data, document a generally shallow water depositional depth and the probable proximity of emergent land in the Petrești area already during most of the Late Campanian. Furthermore, they also record the withdrawal of marine waters from this area and the partial emergence of the Hațeg Island - as indicated by partly continental sedimentation - already within the upper part of biozone CC22, that is, in the later part of the middle Late Campanian (see Fig. 2), significantly earlier than was considered previously.

Besides earlier reports of (mostly isolated) vertebrate remains scattered throughout the upper, transitional to continental parts of the Petrești succession (e.g., Csiki-Sava et al., 2012; Brusatte et al., 2013; Vremir et al., 2014), the recent discovery of a vertebrate remain-rich

fossil locality within the basalmost grey beds of the Sebeș Formation (level L0/c, Fig. 2; Vremir et al., 2015a, 2015b) represents the most compelling image yet available of the earliest Hațeg Island faunal assemblages. This taxon-rich L0/c assemblage is made up of lepisosteid fish, anurans, albanerpetontids, lizards, diverse crocodyliforms, different herbivorous dinosaurs (rhabdodontids, nodosaurids), as well as kogaionid multituberculates (e.g., Vasile et al., 2022). Most significantly, two of the uppermost calcareous nannofossil samples reported here (64, 65) bracket the fossiliferous level itself, whereas our detrital zircon U-Pb data derive from the coarse channel-fill lying directly atop the fossiliferous bed; both of these data sources convergently point to a later middle Late Campanian age for the L0/c bonebed. This definitively places the emergence of the oldest known well-diversified Hațeg Island faunal assemblage into the middle Late Campanian, pencontemporaneously with the emergence of the island itself. Accordingly, this early Transylvanian fauna actually overlaps in time with important Late Campanian western European faunas from southern France and Spain. Furthermore, although it still remains significantly younger than the geographically more closely positioned Austrian and, especially, Hungarian faunal assemblages, its discovery reduces the previously assessed large temporal gap separating these Central European faunas from the Transylvanian ones.

Remarkably, however, despite its younger age, the composition of this early, middle Late Campanian Hațeg Island fauna is more reminiscent of the older, Santonian–Early Campanian Central European ones (as well as of the earliest well-known Early Campanian faunal assemblages known from southern France; see Csiki-Sava et al., 2015) due to the presence of rhabdodontid and nodosaurid dinosaurs, combined with the conspicuous absence of hadrosauroids and titanosaurs, whereas titanosaurs are already well represented in the Late Campanian faunas of western Europe. Since hadrosauroids and titanosaurs are known to co-occur with rhabdodontids in the earliest Maastrichtian assemblages of the Hațeg Basin (e.g., Botfalvai et al., 2021), their introduction into the Hațeg Island faunas was definitively a later development. Most probably, the arrival of hadrosauroids and titanosaurs took place sometimes after the Campanian–Maastrichtian boundary, as these taxa are still undocumented in the red basal beds of the Sebeș Formation at Petrești, assessed previously to represent the lowermost Maastrichtian (Vremir et al., 2014), but which may be as old as the latest Campanian according to our new age data. Such regional faunal differences between eastern and western Europe suggest decoupled and diachronous faunal evolution across the different European landmasses in the latest Cretaceous.

A second remarkable occurrence at locality L0/c is that of the kogaionid multituberculates (e.g., Csiki-Sava et al., 2022). These European endemic cimolodontan multituberculates were until recently known to have a fossil record extending from the Maastrichtian to the Paleocene (e.g., Kielan-Jaworowska et al., 2004). The presence of kogaionids in the upper, more continentally influenced part of the transitional series from Petrești, now confidently dated as middle Late Campanian in age, amounts to the oldest known fossil occurrence of the clade globally, extending their known fossil record into the later part of the Campanian. It also shows that kogaionids already colonized the Transylvanian landmass during the middle Late Campanian, if not earlier, and that they were members of the Hațeg Island faunas since their early inception stages.

## 8. Conclusions

We have conducted multidisciplinary stratigraphic analyses of a 600+ thick Upper Cretaceous succession cropping out at Petrești, on the southwestern rim of the Transylvanian Basin (western Romania) near its contact with the Southern Carpathians. This succession was known to record quasi-continuous transition between the flyschoid marine deposits of the Upper Cretaceous Bozeș Formation and the overlying continental red beds of the uppermost Cretaceous Sebeș Formation, a result of orogeny-driven sea withdrawal and land emergence

documented to occur in several parts of the western Transylvanian region. These events led to the formation of a major landmass of the Late Cretaceous European Archipelago, the Hațeg Island, home of a peculiar and markedly endemic continental vertebrate fauna with dwarf dinosaurs.

In order to better constrain the timing and palaeoenvironmental context of these end-Cretaceous events as recorded in the Petrești section, we employed detailed lithological logging combined with fine-scale survey of calcareous nannofossil, foraminifera, and palynomorph assemblages, as well as detrital zircon U-Pb geochronometry, and correlated the results of these studies with the local distribution of continental vertebrate fossils. Our integrated approach showed that the age of the Bozeș Formation deposits at Petrești, including its uppermost, transitional brackish succession, as well as that of the overlying basal-most estuarine-coastal beds of Sebeș Formation, can be adequately constrained using calcareous nannoplankton biostratigraphy (especially by the presence of *Ceratolithoides aculeus*, combined with that of *Eiffelolithus eximius* and *Reinhardtites anthophorus*), foraminifera biostratigraphy (presence of *Bolivinoidea* spp. and *Brotzenella monterelensis*), palinostratigraphy (primarily the occurrence of the marine dinoflagellate *Samlandia* cf. *vermicularia*, associated with continental palynomorphs), backed up by maximum depositional ages derived from detrital zircon U-Pb geochronometry.

These mutually independent constraints convergently indicate a most probably early Late to middle Late Campanian age for the marine Bozeș Formation at Petrești, as well as start of continental deposition represented by the overlying Sebeș Formation by late middle to late Late Campanian. These deposits thus host the oldest reliably dated continental vertebrate occurrences from Hațeg Island, predating classical dinosaur-bearing successions such as those from the nearby Hațeg Basin.

The abundance patterns of the calcareous nannofossil *Watznaueria barnesiae* and of the planktonic foraminifera point to oligotrophic warm surface/subsurface open sea conditions during the early and middle Late Campanian in the Petrești area, alternating with very short mesoeutrophic episodes with cold water influxes. Palaeoenvironment-informative parameters of the calcareous nannofossil assemblages reflect stable environmental conditions within the water column, whereas similar parameters derived from foraminifera assemblages indicate fluctuations in the nutrient supply to the seafloor and generally suboxic conditions. The local palaeontological record shows that the Bozeș Formation at Petrești was deposited in relatively shallow marine waters characteristic of the continental shelf, despite the flyschoid aspect of the deposits, and indicates proximity of emergent land throughout the Late Campanian.

The newly acquired age constraints reveal that emergence of the Hațeg Island vertebrate faunas was already underway during the middle to early late Late Campanian, although certain iconic dinosaur taxa such as titanosaurs and hadrosauroids were apparently added slightly later, most probably during the early part of the early Maastrichtian. They further support the presence of endemic kogaionid multituberculates on Hațeg Island by the middle Late Campanian, extending their fossil record that was previously considered to start in the Maastrichtian.

Our study shows that integrated high-resolution investigations of micropaleontological assemblages represent an extremely useful tool for providing precise age constraints and detailed palaeoenvironmental-palaeoecological condition reconstructions in key lithostratigraphic sections. Such sections, on their turn, are extremely important for local and regional correlations, and hold promises of documenting and tracking in great details important events of palaeogeographic and faunal evolution.

Supplementary data to this article can be found online at <https://doi.org/10.1016/j.marmicro.2023.102328>

#### CRedit authorship contribution statement

**R. Bălc:** Data curation, Investigation, Methodology, Validation,

Writing – review & editing. **R. Bindu-Haitonic:** Conceptualization, Data curation, Formal analysis, Investigation, Methodology, Supervision, Validation, Visualization, Writing – original draft, Writing – review & editing. **S.-A. Kövecsi:** Data curation, Methodology, Software, Writing – review & editing. **M. Vremir:** Data curation, Investigation, Methodology. **M. Ducea:** Data curation, Formal analysis, Investigation, Methodology, Validation, Writing – original draft, Writing – review & editing. **Z. Csiki-Sava:** Conceptualization, Funding acquisition, Project administration, Resources, Supervision, Validation, Visualization, Writing – original draft, Writing – review & editing. **D. Țabără:** Formal analysis, Investigation, Methodology, Writing-original draft, Writing - review & editing. **Ș. Vasile:** Visualization, Writing - review & editing.

#### Declaration of competing interest

The authors declare that they have no known competing financial interests or personal relationships that could have appeared to influence the work reported in this paper.

#### Data availability

Data will be made available on request.

#### Acknowledgments

This study represents a contribution to the project PN-III-P4-ID-PCE-2020-2570 funded by a grant of the Ministry of Research, Innovation and Digitization, CNCS/CCDI, through the Executive Agency for Higher Education, Research, Development and Innovation Funding (UEFISCDI). Szabolcs-Attila Kövecsi thanks the POCU/993/5/13, project “Development of advanced and applied research skills in STEAM+ Health logic” for financial support. Mihai Nicolae Ducea acknowledges grant C1.2.PFE-CDI.2021-587/Contract no. 41PFE/30.12.2021 from the Romanian MCID (Ministry of Research). For their important contribution to the extensive June 2017 sampling at the Petrești section, sampling that represents the foundation for our study, we thank our colleagues Jingmai K. O’Connor, Alexandra J. Buczek, and, most importantly, Jocelyn Sessa and Mark A. Norell. Prof. Dr. Sorin Filipescu is thanked for his help in acquiring the scanning electron microscopy images of the foraminifera. We thank lecturer Eugen Wohl for reviewing the language and grammar of the manuscript. The Journal Associate Editor Shijun Jiang and the anonymous reviewers are kindly thanked for their comments and suggestions that helped improve the previous version of our manuscript considerably.

#### References

- Abbinck, O.A., Van Konijnenburg-Van Cittert, J.H.A., Visscher, H., 2004. A sporomorph ecogroup model for the Northwest European Jurassic – Lower Cretaceous: concepts and framework. *Netherlands J. Geosci./Geol. en Mijnbouw* 83 (1), 17–38. <https://doi.org/10.1017/S0016774600020436>.
- Abramovich, S., Keller, G., Stüben, D., Berner, Z., 2003. Characterization of late Campanian and Maastrichtian planktonic foraminiferal depth habitats and vital activities based on stable isotopes. *Palaeogeogr. Palaeoclimatol. Palaeoecol.* 202, 1–29. [https://doi.org/10.1016/S0031-0182\(03\)00572-8](https://doi.org/10.1016/S0031-0182(03)00572-8).
- Abramovich, S., Yovel-Corem, S., Almogi-Labin, A., Benjamini, C., 2010. Global climate change and planktic foraminiferal response in the Maastrichtian. *Paleoceanography* 25, 1–15. <https://doi.org/10.1029/2009PA001843>.
- Alegret, L., Molina, E., Thomas, E., 2003. Benthic foraminiferal turnover across the Cretaceous/Paleogene boundary at Agost (southeastern Spain): paleoenvironmental inferences. *Mar. Micropaleontol.* 48, 251–279. [https://doi.org/10.1016/S0377-8398\(03\)00022-7](https://doi.org/10.1016/S0377-8398(03)00022-7).
- Alekseev, A.S., Kopaevich, L.F., 1997. Foraminiferal biostratigraphy of the uppermost Campanian-Maastrichtian in SW Crimea (Bakhchisaray and Chakhmakhly sections). *Bulletin de l’Institut Royal des Sciences Naturelles de Belgique. Sci. Terre* 67, 103–118.
- Alves, A.N., Bruno, M.D.R., Do Monte Guerra, R., Fauth, G., 2018. Biostratigraphy and paleoecological inferences during the late Campanian-Maastrichtian interval: evidence based on calcareous nannofossils from Goba Spur. *Mar. Micropaleontol.* 142, 40–47. <https://doi.org/10.1016/j.marmicro.2018.06.002>.
- Antonescu, E., 1973. Asociații palinologice caracteristice unor formațiuni cretacee din Munții Metaliferi. *Dări de Seamă ale Ședințelor (Paleontologie)* 59, 115–169.

- Antonescu, E., Odin, G.S., 2001. Répartition stratigraphique du pollen et des spores dans le Campanien et le Maastrichtien du site géologique de Tercis les Bains (SW France). In: Odin, G.S. (Ed.), *The Campanian–Maastrichtian Stage Boundary, Characterisation at Tercis les Bains (France) and Correlation with Europe and Other Continents*. IUGS Special Publication (Monograph) Series, 36. Developments in Palaeontology and Stratigraphy, vol. 19, pp. 192–199.
- Antonescu, E., Lupu, D., Lupu, M., 1983. Corrélation palynologique du Crétacé terminal du sud-est des Monts Metaliferi et des Dépressions de Hațeg et de Rusca Montană. *Anuarul Institutului de Geologie și Geofizică* 59, 71–77.
- Armstrong, H.A., Brasier, M.D., 2005. *Microfossils*, Second edition., Blackwell Publishing Ltd., pp. 1–304.
- Arreguín-Rodríguez, G.J., Alegret, L., Thomas, E., 2016. Late Paleocene-middle Eocene benthic foraminifera on a Pacific seamount (Allison Guyot, ODP Site 865): Greenhouse climate and superimposed hyperthermal events. *Paleoceanography* 31, 346–364. <https://doi.org/10.1002/2015PA002837>.
- Bălc, R., Suciuc-Krausz, E., Borbei, F., 2007. Biostratigraphy of the Cretaceous deposits in the Western Transylvanides from Ampoi Valley (Southern Apuseni Mountains, Romania). *Studia UBB Geo.* 52, 37–43.
- Bălc, R., Silye, L., Zaharia, L., 2012. Calcareous nannofossils and sedimentary facies in the Upper Cretaceous Bozeș Formation (Southern Apuseni Mountains, Romania). *Studia UBB Geo.* 57, 23–32.
- Balintoni, I., Balica, C., Ducea, M.N., Hann, H.-P., 2014. Peri-Gondwanan terranes in the Romanian Carpathians: A review of their spatial distribution, origin, provenance, and evolution. *Geosci. Front.* 5, 395–411. <https://doi.org/10.1016/j.gsf.2013.09.002>.
- Batten, D.J., 1999. Small palynomorphs. In: Jones, T.P., Rowe, N.P. (Eds.), *Fossil Plants and Spores: Modern Techniques*. Geological Society, London, pp. 15–19.
- Benton, M.J., Csiki, Z., Grigorescu, D., Redelstorff, R., Sander, P.M., Stein, K., Weishampel, D.B., 2010. Dinosaurs and the island rule: the dwarfed dinosaurs from Hațeg Island. *Palaeogeogr. Palaeoclimatol. Palaeoecol.* 293, 438–454. <https://doi.org/10.1016/j.palaeo.2010.01.026>.
- Bergen, J.A., Sikora, P.J., 1999. Microfossil diachronism in southern Norwegian North Sea Chalks: Valhall and Hod fields. In: Jones, R.W., Simmons, M.D. (Eds.), *Biostratigraphy in Production and Development Geology*, Geological Society, London, Special Publications, vol. 152, pp. 85–111. <https://doi.org/10.1144/GSL.SP.1999.152.01.06>.
- Bernhard, J.M., Bowser, S.S., 1999. Benthic foraminifera of dysoxic sediments: Chloroplast sequestration and functional morphology. *Earth Sci. Rev.* 46 (1–4), 149–165. [https://doi.org/10.1016/S0012-8252\(99\)00017-3](https://doi.org/10.1016/S0012-8252(99)00017-3).
- Berza, T., Constantinescu, E., Vlad, S.N., 1998. Upper Cretaceous magmatic series and associated mineralisation in the Carpathian-Balkan Orogen. *Resour. Geol.* 48 (4), 281–306.
- Bindiu, R., Filipescu, S., Bălc, R., 2013. Biostratigraphy and paleoenvironment of the Upper Cretaceous deposits in the northern Tarcău Nappe (Eastern Carpathians) based on foraminifera and calcareous nannoplankton. *Geol. Carpath.* 64 (2), 117–132. <https://doi.org/10.2478/geoca-2013-0008>.
- Bindiu, R., Filipescu, S., Bălc, R., Cociș, L., Gligor, D., 2016. The middle/late Eocene transition in the Eastern Carpathians (Romania) based on foraminifera and calcareous nannofossil assemblages. *Geo. Qua.* 60 (1), 38–55. <https://doi.org/10.7306/gq.1237>.
- Bindiu-Haitonic, R., Niculici, S., Filipescu, S., Bălc, R., Aroldi, C., 2017. Biostratigraphy and paleoenvironments of the Eocene deep-water deposits of the Tarcău Nappe (Eastern Carpathians, Romania) based on agglutinated foraminifera and calcareous nannofossil assemblages. In: Kaminski, M.A., Alegret, L. (Eds.), *Proceedings of the Ninth International Workshop on Agglutinated Foraminifera*. Grzybowski Foundation Special Publication, 22, pp. 15–35.
- Bindiu-Haitonic, R., Filipescu, S., Aroldi, C., Oltean, G., Chira, C.M., 2019. Eocene Deep Water foraminifera from the Eastern Carpathians (Romania). *Paleoenvironments and biostratigraphical remarks*. *Micropaleontology* 65 (1), 47–61. <https://doi.org/10.47894/mpal.65.1.03>.
- Bindiu Haitonic, R., 2018. *Relația dintre asociațiile de foraminifere fosile și mediile depozitionale din Nordul Pânzei de Tarcău (Carpații Orientali, România)*. Presa Universitară Clujeană, p. 237.
- Bindiu-Haitonic, R., Bălc, R., Kövecsi, S.A., Pleș, G., Silye, L., 2021. In the shadow of giants: Calcareous nannoplankton and smaller benthic foraminifera from an Eocene nummulitic accumulation (Transylvanian Basin, Romania). *Mar. Micropaleontol.* 165 (101988), 1–18. <https://doi.org/10.1016/j.marmicro.2021.101988>.
- Botfalvai, G., Csiki-Sava, Z., Kocsis, L., Albert, G., Magyar, J., Bodor, E.R., Țabără, D., Ulyanov, A., Makádi, L., 2021. 'X' marks the spot! Sedimentological, geochemical and palaeontological investigations of Upper Cretaceous (Maastrichtian) vertebrate fossil localities from the Vălioara valley (Densuș-Ciula Formation, Hațeg Basin, Romania). *Cretac. Res.* 123, 104781 <https://doi.org/10.1016/j.cretres.2021.104781>.
- Bottini, C., Erba, E., Tiraboschi, D., Jenkyns, H.C., Schouten, S., Sinninghe Damsté, J.S., 2015. Climate variability and ocean fertility during the Aptian Stage. *Clim. Past* 11, 383–402. <https://doi.org/10.5194/cp-11-383-2015>.
- Bowman, V.C., Francis, J.E., Askin, R.A., Riding, J.B., Swindles, G.T., 2014. Latest Cretaceous–earliest Paleogene vegetation and climate change at the high southern latitudes: palynological evidence from Seymour Island, Antarctic Peninsula. *Palaeogeogr. Palaeoclimatol. Palaeoecol.* 408, 26–47.
- Bown, P.R., Young, J.R., 1998. *Techniques*. In: Bown, P.R. (Ed.), *Calcareous Nannofossil Biostratigraphy*. British Micropaleont. Soc. Ser. Chapman and Hall, London, pp. 16–28.
- Bralower, T.J., Leckie, R.M., Sliter, W.V., Thierstein, H.R., 1995. An integrated Cretaceous microfossil biostratigraphy. In: Berggren, W.A., Kent, D.V., Aubry, M.-P., Hardenbol, J. (Eds.), *Geochronology, Time Scales, and Global Stratigraphic Correlation*. Spec. Publ. – SEPM (Soc. Sediment. Geol.), 54, pp. 65–79.
- Brusatte, S.L., Vremir, M., Watanabe, A., Csiki-Sava, Z., Naish, D., Dyke, G., Erickson, G.M., Norell, M.A., 2013. An infant ornithomimid dinosaur tibia from the Late Cretaceous of Sebeș, Romania. *Terra Sebus. Acta Musei Sabesiensis* 5, 627–644.
- Burnett, J.A., 1991. A new nannofossil zonation scheme for the Boreal Campanian. *Intern. Nannoplankton Associa. News.* 12, 67–70.
- Burnett, J.A., 1998. Upper Cretaceous. In: Bown, P.R. (Ed.), *Calcareous Nannofossil Biostratigraphy*. British Micropaleont. Soc. Ser. Chapman and Hall, London, pp. 132–199.
- Buzas, M.A., Gibson, T.G., 1969. Species diversity: benthic foraminifera in Western North Atlantic. *Science* 163, 72–75. <https://doi.org/10.1126/science.163.3862.7>.
- Caron, M., 1985. Calcareous planktic foraminifera. In: Bolli, H.M., Saunders, J.B., Perch-Nielsen, K. (Eds.), *Plankton Stratigraphy*. Cambridge University Press, Cambridge, UK, pp. 17–86.
- Cetean, C.G., Bălc, R., Kaminski, M.A., Filipescu, S., 2011. Integrated biostratigraphy and paleoenvironments of an upper Santonian–upper Campanian succession from the southern part of the Eastern Carpathians, Romania. *Cretac. Res.* 32 (5), 575–590. <https://doi.org/10.1016/j.cretres.2010.11.001>.
- Chan, S.A., Bălc, R., Humphrey, J.D., Amao, A.O., Kaminski, M.A., Alzayer, Y., Duque, F., 2022. Changes in paleoenvironmental conditions during the Late Jurassic of the western Neo-Tethys: Calcareous nannofossils and Geochemistry. *Mar. Micropaleontol.* 73, 102116 <https://doi.org/10.1016/j.marmicro.2022.102116>.
- Ciulavu, D., Bertotti, G., 1994. The Transylvanian Basin and its Upper Cretaceous substratum: ALCAPA II Field Guidebook Romanian Journal of Tectonics and Regional. *Geology* 75, 59–65.
- Coccioni, R., Premoli Silva, I., 2015. Revised Upper Albian-Maastrichtian planktonic foraminiferal biostratigraphy of the classical Tethyan Gubbio section (Italy). *Newsl. Stratigr.* 48 (1), 47–90. <https://doi.org/10.1127/nos/2015/0055>.
- Codrea, V.A., Vremir, M., Jipa, C., Godefroit, P., Csiki, Z., Smith, T., Fărcaș, C., 2010. More than just Nopcsa's Transylvanian dinosaurs: A look outside the Hațeg Basin. *Palaeogeogr. Palaeoclimatol. Palaeoecol.* 293, 391–405. <https://doi.org/10.1016/j.palaeo.2009.10.027>.
- Crux, J.A., 1982. Upper Cretaceous (Cenomanian to Campanian) calcareous nannofossils. In: Lord, A.R. (Ed.), *A Stratigraphical Index of Calcareous Nannofossils*. British Micropaleontological Society Series, Chapman and Hall, pp. 81–135.
- Csiki-Sava, Z., Bălc, R., Brusatte, S.L., Dyke, G.L., Naish, D., Norell, M.A., Vremir, M.M., 2012. Petrești-Arini (Transylvanian Basin, Romania) – A very important but ephemeral Late Cretaceous (early Maastrichtian) vertebrate site. In: Royo-Tores, R., Gascó, F., Alcalá, L. (Eds.), 10<sup>th</sup> Annual Meeting of the European Association of Vertebrate Palaeontologists. *Fundamenta!* 20, pp. 53–55. Teruel, Spain.
- Csiki-Sava, Z., Buffetaut, E., Ősi, A., Pereda-Suberbiola, X., Brusatte, S.L., 2015. Island life in the Cretaceous – faunal composition, biogeography, evolution, and extinction of land-living vertebrates on the Late Cretaceous European archipelago. *ZooKeys* 469, 1–161. <https://doi.org/10.3897/zookeys.469.8439>.
- Csiki-Sava, Z., Vremir, M., Vasile, Ș., Brusatte, S.L., Dyke, G., Naish, D., Norell, M.A., Totoianu, R., 2016. The East Side Story – the Transylvanian latest Cretaceous continental vertebrate record and its implications for understanding Cretaceous–Paleogene boundary events. *Cretac. Res.* 57, 662–698. <https://doi.org/10.1016/j.cretres.2015.09.003>.
- Csiki-Sava, Z., Meng, J., Vremir, M., Vasile, Ș., Brusatte, S.L., Norell, M.A., 2021. Multities of the Dawn – the oldest multituberculate occurrences in the uppermost Cretaceous of Transylvania, and mosaic evolution within the Kogaionidae. In: Belvedere, M., Díez Díaz, V., Mecozzi, B., Sardella, R. (Eds.), *Abstract book of the 18th annual conference of the European Association of Vertebrate Palaeontologists*, online. *Palaeovertebrata*, 44, p. 62.
- Csiki-Sava, Z., Vremir, M., Meng, J., Vasile, Ș., Brusatte, S.L., Norell, M.A., 2022. Spatial and temporal distribution of the island-dwelling Kogaionidae (Mammalia, Multituberculata) in the uppermost Cretaceous of Transylvania (western Romania). *Bull. Am. Mus. Nat. Hist.* 456, 1–109. <http://hdl.handle.net/2246/7297>.
- Daly, R.J., Jolley, D.W., 2015. What was the nature and role of Normapolles angiosperms? A case study from the earliest Cenozoic of Eastern Europe. *Palaeogeogr. Palaeoclimatol. Palaeoecol.* 418, 141–149. <https://doi.org/10.1016/j.palaeo.2014.10.014>.
- de Broucker, G., Mellin, A., Duindam, P., 1998. Tectono-Stratigraphic evolution of the Transylvanian Basin, pre-salt sequence, Romania. In: Dinu, C., Mocanu, V. (Eds.), *Geological and Hydrocarbon Potential of the Romanian Areas*, Bucharest Geosciences Forum Special Volume, vol. 1, pp. 36–70.
- Doeven, P.H., 1983. Cretaceous nannofossil stratigraphy and paleoecology of the Canadian Atlantic margin. *Bull./Geo. Sur. Canada* 356, 1–70.
- Dubicka, Z., Peryt, D., 2016. *Bolivinioides* (benthic foraminifera) from the Upper Cretaceous of Poland and western Ukraine: taxonomy, evolutionary changes and stratigraphic significance. *J. Foram. Res.* 46, 75–94. <https://doi.org/10.2113/gsfjr.46.1.75>.
- Ducea, M.N., Saleeby, J.B., Bergantz, G., 2015. The architecture, chemistry, and evolution of continental magmatic arcs. *Annu. Rev. Earth Planet. Sci.* 43, 299–331. <https://doi.org/10.1146/annurev-earth-060614-105049>.
- Eicher, D.L., 1969. Cenomanian and Turonian planktonic foraminifera from the Western Interior of the United States. In: Bronnimann, P., Renz, H.H. (Eds.), *Proceedings of the First International Conference on Planktonic Microfossils*, Volume 2. E. J. Brill, Leiden, pp. 163–174.
- Eicher, D.L., Worstell, P., 1970. Cenomanian and Turonian foraminifera from the Great Plains, United States. *Micropaleontology* 16 (3), 269–324. <https://doi.org/10.2307/1485079>.
- Erba, E., 1992. Middle Cretaceous calcareous nannofossils from the Western Pacific (Leg 129): Evidence for paleoequatorial crossing. In: Larson, R.L., Lancelot, Y. (Eds.),

- Proceedings of the Ocean Drilling Program, Scientific Results, vol. 129, pp. 189–201. <https://doi.org/10.2973/odp.proc.sr.129.119.1992>.
- Erba, E., Castradori, D., Guasti, G., Ripepe, M., 1992. Calcareous nannofossils and Milankovitch cycles: the example of the Albanian Gault Clay Formation (southern England). *Palaeogeogr. Palaeoclimatol. Palaeoecol.* 93, 47–69. [https://doi.org/10.1016/0031-0182\(92\)90183-6](https://doi.org/10.1016/0031-0182(92)90183-6).
- Erbachen, J., Gerth, W., Schmiedl, G., Hemleben, C., 1998. Benthic foraminiferal assemblages of late Aptian–early Albian black shale intervals in the Vocotian Basin, SE France. *Cretac. Res.* 19 (6), 805–826. <https://doi.org/10.1006/cres.1998.0134>.
- Falzone, F., Petrizzo, M.R., Huber, B.T., MacLeod, K.G., 2014. Insights into the meridional ornamentation of the planktonic foraminiferal genus *Rugoglobigerina* (Late Cretaceous) and implications for taxonomy. *Cretac. Res.* 47, 87–104. <https://doi.org/10.1016/j.cretres.2013.11.001>.
- Friedrich, O., Nishi, H., Pross, J., Schmiedl, G., Hemleben, C., 2005. Millennial- to Centennial-Scale Interruptions of the Oceanic Anoxic Event 1b (early Albian, mid-Cretaceous) Inferred from Benthic Foraminiferal Repopulation events. *Palaios* 20, 64–77. <https://doi.org/10.2110/palo.2003.p03-75>.
- Friedrich, O., Norris, R.D., Erbachen, J., 2012. Evolution of middle to Late Cretaceous oceans – A 55 my record of Earth's temperature and carbon cycle. *Geology* 40, 107–110. <https://doi.org/10.1130/G32701.1>.
- Friis, E.M., Crane, P.R., Pedersen, K.R., 2011. *Early Flowers and Angiosperm Evolution*. Cambridge University Press, p. 585.
- Gallhofer, D., von Quadt, A., Peytcheva, I., Schmid, S.M., Heinrich, C.A., 2015. Tectonic, magmatic, and metallogenic evolution of the Late Cretaceous arc in the Carpathian-Balkan orogen. *Tectonics* 34 (9), 1813–1836. <https://doi.org/10.1002/2015TC003834>.
- Gardin, S., 2002. Late Maastrichtian to early Danian calcareous nannofossils at Elles (Northwest Tunisia). A tale of one million years across the K-T boundary. *Palaeogeogr. Palaeoclimatol. Palaeoecol.* 178, 211–231. [https://doi.org/10.1016/S0031-0182\(01\)00397-2](https://doi.org/10.1016/S0031-0182(01)00397-2).
- Gawor-Biedowa, E., 1992. Campanian and Maastrichtian foraminifera from the Lublin Upland, Eastern Poland. *Palaeontol. Pol.* 52, 1–187.
- Gebhardt, H., Ćorić, S., Darga, R., Briguglio, A., Schenk, B., Werner, W., Andersen, N., Sames, B., 2013. Middle to late Eocene paleoenvironmental changes in a marine transgressive sequence from the northern Tethyan margin (Adelholzen, Germany). *Austrian J. Earth Sci.* 106 (2), 45–72.
- Gehrels, G., 2014. Detrital zircon U-Pb geochronology applied to tectonics. *Annu. Rev. Earth Planet. Sci.* 42, 127–149. <https://doi.org/10.1146/annurev-earth-050212-124012>.
- Gehrels, G.E., Valencia, V., Ruiz, J., 2008. Enhanced precision, accuracy, efficiency, and spatial resolution of U-Pb ages by laser ablation-multicollector-inductively coupled plasma-mass spectrometry. *Geochim. Geophys. Geosyst.* 9, Q03017. <https://doi.org/10.1029/2007GC001805>.
- Georgescu, M.D., 2018. Monographic study of the Late Cretaceous representatives of the bolivinoïd benthic foraminifera. *Studia UBB Geol.* 62 (1), 5–57.
- Ghițulescu, T.P., Socolescu, M., 1941. Etude géologique et minière des Monts Métallifères. *Analele Institutului Geologic* 21, 181–463.
- Gibson, T.G., 1989. Planktonic benthic foraminiferal ratios: modern patterns and Tertiary applicability. *Mar. Micropaleontol.* 15 (1–2), 29–52. [https://doi.org/10.1016/0377-8398\(89\)90003-0](https://doi.org/10.1016/0377-8398(89)90003-0).
- Góczán, F., 1964. Stratigraphic palynology of the Hungarian Upper Cretaceous. *Acta Geol. Acad. Sci. Hung.* 8 (1–4), 229–264.
- Góczán, F., Siegl-Farkas, Á., 1989. Palynostratigraphy of the Rendek Member of the Polány Marl Formation. *MÁFI Évi Jelentései az 1988. Évről* 2, 47–85.
- Góczán, F., Siegl-Farkas, Á., 1990. Palynostratigraphical zonation of Senonian sediments in Hungary. *Rev. Palaeobot. Palynol.* 66, 361–377. [https://doi.org/10.1016/0034-6667\(90\)90047-M](https://doi.org/10.1016/0034-6667(90)90047-M).
- Gradstein, F.M., Ogg, J.G., Schmitz, M.D., Ogg, G.M., 2020. *The Geological Time Scale 2020*. Elsevier, Amsterdam, p. 1357.
- Grigorescu, D., 2010. The latest Cretaceous fauna with dinosaurs and mammals from the Hateg Basin — A historical overview. *Palaeogeogr. Palaeoclimatol. Palaeoecol.* 293, 271–282. <https://doi.org/10.1016/j.palaeo.2010.01.030>.
- Grigorescu, D., Melinte, M.C., 2001. The stratigraphy of the Upper Cretaceous marine sediments from the NW Hațeg area (South Carpathians, Romania). *Acta Paleont. Rom.* 3, 153–160.
- Guerrera, F., Martin, M.M., Martin-Perez, J.A., Martin-Rojas, I., Mićlăuș, C., Serrano, F., 2012. Tectonic control on the sedimentary record of the central Moldavian Basin (Eastern Carpathians, Romania). *Geol. Carpath.* 63 (6), 463–479. <https://doi.org/10.2478/v10096-012-0036-0>.
- Hammer, Ø., Harper, D.A.T., 2006. *Paleontological Data Analysis*. Blackwell Publishing, p. 351.
- Hammer, Ø., Harper, D.A.T., Ryan, P.D., 2001. PAST: Paleontological Statistics Software Package for Education and Data Analysis. *Palaeontol. Electron.* 4 (1), 9.
- Hayward, B.W., 1986. A guide to paleoenvironmental assessment using New Zealand Cenozoic foraminiferal faunas. *New Zealand Geol. Sur. Report Pal.* 109, 73.
- Hayward, B.W., 2004. Foraminifera-based estimates of paleobathymetry using Modern Analogue Technique, and the subsidence history of the early Miocene Waitemata Basin. *N. Z. J. Geol. Geophys.* 47 (4), 749–767. <https://doi.org/10.1080/00288306.2004.9515087>.
- Hayward, B.W., Buzas, M.A., 1979. Taxonomy and paleoecology of early Miocene benthic foraminifera of northern New Zealand and the North Tasman Sea. *Smithson. Contrib. Paleobiol.* 36, 154.
- Hayward, B.W., Grenfell, H.R., Reid, C.M., Hayward, K.A., 1999. Recent New Zealand shallow-water benthic foraminifera: taxonomy, ecologic distribution, biogeography, and use in paleoenvironmental assessment. *Ins. Geo. & Nuclear Sci. Mono.* 21, 258.
- Herlle, J.O., Pross, J., Friedrich, O., Hemleben, C., 2003. Short-term environmental changes in the Cretaceous Tethyan Ocean: micropaleontological evidence from the early Albian Oceanic Anoxic Event 1b. *Terra Nova* 15, 14–19. <https://doi.org/10.1046/j.1365-3121.2003.00448.x>.
- Hoogakker, B.A., Elderfield, H., Schmiedl, G., McCave, I.N., Rickaby, R.E., 2015. Glacial–interglacial changes in bottom-water oxygen content on the Portuguese margin. *Nat. Geosci.* 8, 40–43. <https://doi.org/10.1038/ngeo2317>.
- Hradecká, L., 2002. Foraminifers as an indicator of paleobathymetry in the Gosau group of eastern Austria. *Geol. Carpath.* 53 (3), 191–195.
- Huber, B.T., Watkins, D.K., 1992. Biogeography of Campanian-Maastrichtian calcareous plankton in the region of the Southern Ocean: Paleogeographic and paleoclimatic implications. In: Kennett, J.P., Warnke, D.A. (Eds.), *The Antarctic Paleoenvironment: A Perspective on Global Change*, American Geophysical Union Antarctic Research Series, vol. 56, pp. 31–60. <https://doi.org/10.1029/AR056p0031>.
- Huber, B.T., Hodell, D.A., Hamilton, C.P., 1995. Middle-Late Cretaceous climate of the southern high latitudes: Stable isotopic evidence for minimal equator-to-pole thermal gradients. *GSA Bull.* 107, 1164–1191. <https://doi.org/10.1130/0016-7606.1995.1130-0016-7606>.
- Huismans, R.S., Bertotti, G., Ciulavu, D., Sanders, C.A.E., Cloetingh, S., Dinu, C., 1997. Structural evolution of the Transylvanian Basin (Romania): a sedimentary basin in the bend zone of the Carpathians. *Tectonophysics* 272, 249–268. [https://doi.org/10.1016/S0040-1951\(96\)00261-2](https://doi.org/10.1016/S0040-1951(96)00261-2).
- Hurlbert, S.H., 1971. The nonconcept of species diversity: a critique and alternative parameters. *Ecology* 52 (4), 577–586. <https://doi.org/10.2307/1934145>.
- Ilieș, I.A., Oltean, G., Bîndiu-Haitonic, R., Filipescu, S., Miclea, A., Jipa, C., 2020. Early middle Miocene paleoenvironmental evolution in Southwest Transylvania (Romania): Interpretation based on foraminifera. *Geol. Carpath.* 71 (5), 444–461. <https://doi.org/10.31577/GeolCarp.71.5.5>.
- Ion, J., Antonescu, E., Melinte, M.C., Szasz, L., 1998. Tentative for an integrated standard biostratigraphy - on the basis of macrofauna, planktonic foraminifera, calcareous nannoplankton, dinoflagellates, pollen - for the Upper Cretaceous deposits from Romania. *Roman. J. Stratigr.* 77, 65–83.
- Jaff, R.B.N., 2021. Biostratigraphy of *Bolivinoïdes* and *Neoflabellina* benthic foraminifera in the Upper Cretaceous Shiranish Formation, Kurdistan region, NE Iraq. *Iraqi Bulletin of Geology and Mining* 17 (1), 1–13.
- Jaff, R.B.N., Lawa, F.A., 2019. Paleoenvironmental signature of the Late Campanian–Early Maastrichtian benthic foraminiferal assemblages of Kurdistan, Northeast Iraq. *J. Afr. Earth Sci.* 151, 255–273. <https://doi.org/10.1016/j.jafrearsci.2022.104474>.
- Jaff, R.B.N., Williams, M., Wilkinson, I.P., Lawa, F., Lee, S., Zalasiewicz, J., 2014. A refined foraminiferal biostratigraphy for the Late Campanian–Early Maastrichtian succession of northeast Iraq. *GeoArabia*. 19 (1), 161–180. <https://doi.org/10.2113/geoarabia1901161>.
- Jain, S., Farouk, S., 2017. Shallow water agglutinated foraminiferal response to Late Cretaceous–Early Paleocene sea-level changes in the Dakhla Oasis, Western Desert, Egypt. *Cretac. Res.* 78, 240–257.
- Józsa, S., Setoyama, E., Hálasová, E., Nagy, Š., 2023. Latest Hauterivian foraminiferal and calcareous nannofossil assemblages and bioevents from the *Pseudothurmannia* beds (Central Western Carpathians, Slovakia): A prelude to the Foraoeni event. *Cretac. Res.* 144, 1–17. <https://doi.org/10.1016/j.cretres.2022.105457>.
- Kaiho, K., 1991. Global changes of Paleogene aerobic/anaerobic Benthic foraminifera and deep-sea circulation. *Palaeogeogr. Palaeoclimatol. Palaeoecol.* 83 (1–3), 65–85. [https://doi.org/10.1016/0031-0182\(91\)90076-4](https://doi.org/10.1016/0031-0182(91)90076-4).
- Kaiho, K., 1994. Benthic foraminiferal dissolved-oxygen index and dissolved-oxygen levels in the modern ocean. *Geology* 22 (8), 719–722. <https://doi.org/10.1130/0091-7613.1994.0220801>.
- Kallanxhi, M.E., Bălc, R., Ćorić, S., Székely, S.F., Filipescu, S., 2018. The Rupelian–Chattian transition in the north-western Transylvanian Basin (Romania) revealed by calcareous nannofossils: implications for biostratigraphy and paleoenvironmental reconstruction. *Geol. Carpath.* 69 (3), 264–282.
- Kaminski, M.A., 2012. Calibration of the benthic foraminiferal oxygen index in the Marmara Sea. *Geo. Qua.* 56 (4), 757–764. <https://doi.org/10.7306/gq.1061>.
- Kaminski, M.A., Kuhnt, W., Mollade, M., 1999. The evolution and paleobiogeography of abyssal agglutinated foraminifera since the Early Cretaceous: A tale of four faunas. *Neues Jahrb. Geol. Palaontol. Abh.* 212 (1–3), 401–439. <https://doi.org/10.1127/njgpa/212/1999/401>.
- Kaminski, M.A., Gradstein, F.M., collaborators, 2005. *Atlas of Paleogene Cosmopolitan Deep-water Agglutinated Foraminifera*, 10. Grzybowski Foundation special Publication, p. 546.
- Keller, G., Han, Q., Adatte, T., Burns, S.J., 2001. Paleoenvironment of the Cenomanian Turonian transition at Eastbourne, England. *Cretac. Res.* 22 (4), 391–422. <https://doi.org/10.1006/cres.2001.0264>.
- Kender, S., Kaminski, M.A., Jones, R.W., 2008. Early to middle Miocene foraminifera from the deep-sea Congo Fan, offshore Angola. *Micropaleontology* 54 (6), 477–568.
- Kielan-Jaworowska, Z., Cifelli, R.L., Luo, Z.-X., 2004. *Mammals from the Age of Dinosaurs: Origins, Evolution and Structure*. Columbia University Press, p. 630.
- Koutsoukos, E., Hart, B., 1990. Cretaceous foraminiferal morphogroup distribution patterns, paleoecologies and trophic structures: A case study from the Sergipe Basin, Brazil. *Trans. R. Soc. Edinb. Earth Sci.* 81 (3), 221–246. <https://doi.org/10.1017/S0263593300005253>.
- Kranner, M., Harzhauser, M., Beer, C., Auer, G., Piller, E., 2022. Calculating dissolved marine oxygen values based on an enhanced Benthic Foraminifera Oxygen Index. *Sci. Rep.* 12, 1376. <https://doi.org/10.1038/s41598-022-05295-8>.
- Krézsek, C., Bally, A.W., 2006. The Transylvanian Basin (Romania) and its relation to the Carpathian Fold and Thrust Belt: insights in gravitational salt tectonics. *Mar. Pet. Geol.* 23, 405–446. <https://doi.org/10.1016/j.marpetgeo.2006.03.003>.

- Kuhnt, W., Moullade, M., Kaminski, M.A., 1996. Ecological structuring and evolution of deep sea agglutinated foraminifera - a review. *Rev. Micropaleontol.* 39 (4), 271–281. [https://doi.org/10.1016/S0035-1598\(96\)90119-1](https://doi.org/10.1016/S0035-1598(96)90119-1).
- Leckie, R.M., 1987. Paleogeology of mid-Cretaceous planktonic foraminifera: A comparison of open ocean and Epicontinental Sea assemblages. *Micropaleontology* 33 (2), 164–176.
- Lees, J.A., 2002. Calcareous nannofossil biogeography illustrates paleoclimate change in the Late Cretaceous Indian Ocean. *Cretac. Res.* 23, 537–634. <https://doi.org/10.1006/cres.2003.1021>.
- Li, L., Keller, G., 1998. Diversification and extinction in Campanian-Maastrichtian planktic foraminifera of Northwestern Tunisia. *Eclogae Geol. Helv.* 91 (1), 75–102.
- Linnert, C., Mutterlose, J., Herrle, J.O., 2011. Late Cretaceous (Cenomanian-Maastrichtian) calcareous nannofossils from Goban Spur (DSDP Sites 549, 551): Implications for the palaeoceanography of the proto-North Atlantic. *Palaeogeogr. Palaeoclimatol. Palaeoecol.* 299, 507–528. <https://doi.org/10.1016/j.palaeo.2010.12.001>.
- Linnert, C., Robinson, S.A., Lees, J.A., Bown, P.R., Pérez-Rodríguez, I., Petrizzo, M.R., Falzoni, F., Littler, K., Arz, J.A., Russell, E.E., 2014. Evidence for global cooling in the Late Cretaceous. *Nat. Commun.* 5, 4194. <https://doi.org/10.1038/ncomms5194>.
- Lommerzhelm, A., 1991. Micropaleontological indicators of paleoclimate and paleobathymetry in the boreal Upper Cretaceous; Metelen 1001 well (Münsterland, NW Germany; Upper Santonian-Upper Campanian). *Facies* 24, 183–254. <https://doi.org/10.1007/BF02536847>.
- Melinte-Dobrincescu, M.C., 2010. Lithology and biostratigraphy of Upper Cretaceous marine deposits from the Hațeg region (Romania): paleoenvironmental implications. *Palaeogeogr. Palaeoclimatol. Palaeoecol.* 293, 283–294. <https://doi.org/10.1016/j.palaeo.2009.04.001>.
- Michels, F.H., Alves de Souza, P., Premaor, E., 2018. Aptian-Albian palynologic assemblages interbedded within salt deposits in the Espírito Santo Basin, eastern Brazil: Biostratigraphical and paleoenvironmental analysis. *Mar. Pet. Geol.* 91, 785–799. <https://doi.org/10.1016/j.marpetgeo.2018.01.023>.
- Mortimer, C.P., 1987. Upper Cretaceous Calcareous Nannofossil Biostratigraphy of the Southern Norwegian and Danish North Sea Area. *Abhandlungen der Geologisches Bundesanstalt* 39, 143–175.
- Murray, J.W., 1973. *Distribution and Ecology of Living Benthic Foraminiferids*. Heinemann Educational Books, London, p. 274.
- Murray, J.W., 1976. A method of determining proximity of marginal seas to an ocean. *Mar. Geol.* 22, 103–119. [https://doi.org/10.1016/0025-3227\(76\)90033-5](https://doi.org/10.1016/0025-3227(76)90033-5).
- Murray, J.W., 1991. *Ecology and Palaeoecology of Benthic Foraminifera*. Longman Group, p. 397.
- Murray, J., 2006. *Ecology and Applications of Benthic Foraminifera*. Cambridge University Press, Cambridge, New York, Melbourne, p. 426.
- Nagy, J., Basov, V.A., 1998. Revised foraminiferal taxa and biostratigraphy of Bathonian to Ryazanian deposits in Spitsbergen. *Micropaleontology* 44 (3), 217–255.
- Nagy, J., Løfaldli, M., Bäckström, S.A., 1988. Aspects of foraminiferal distribution and depositional conditions in Middle Jurassic to Early Cretaceous shales in eastern Spitsbergen. *Abhandlungen der Geologischen Bundesanstalt* 41, 287–300.
- Nagy, J., Kaminski, M.A., Kuhnt, W., Bremer, M.A., 2000. Agglutinated Foraminifera from neritic to bathyal facies in the Paleogene of Spitsbergen and the Barents Sea. In: Hart, M.B., Kaminski, M.A., Smart, C.W. (Eds.), 2000. *Proceedings of the Fifth International Workshop on Agglutinated Foraminifera*. Grzybowski Foundation special Publication, 7, pp. 333–361.
- Neagu, T., 1992. White chalk foraminiferal fauna from southern Dobrogea, Romania. III. Calcareous benthic foraminifera. *Rev. Esp. Micropaleontol.* 24, 59–115.
- Niechwedowicz, M., Walaszczyk, I., 2022. Dinoflagellate cysts of the upper Campanian-basal Maastrichtian (Upper Cretaceous) of the Middle Vistula River section (Central Poland): stratigraphic succession, correlation potential and taxonomy. *Newsl. Stratigr.* 55 (1), 21–67. <https://doi.org/10.1127/nos/2021/0639>.
- Nopcsa, F., 1923. On the geological importance of the primitive reptilian fauna of the uppermost Cretaceous of Hungary; with a description of a new tortoise (*Kalkokibotium*). *Q. J. Geol. Soc. Lond.* 79, 100–116.
- Ortiz, N., 1995. Differential patterns of benthic foraminiferal extinctions near the Paleocene/Eocene boundary in the North Atlantic and the western Tethys. *Mar. Micropaleontol.* 26 (1–4), 341–359. [https://doi.org/10.1016/0377-8398\(95\)00039-9](https://doi.org/10.1016/0377-8398(95)00039-9).
- Paraschiv, D., 1979. Romanian oil and gas fields. *Tech. and Eco. Stu.* 13, 382.
- Pardo, A., Keller, G., 2008. Biotic effects of environmental catastrophes at the end of the Cretaceous and early Tertiary: *Guembelitra* and *Heterohelix* blooms. *Cretac. Res.* 29 (5–6), 1058–1073. <https://doi.org/10.1016/j.cretres.2008.05.031>.
- Pavlishina, P., Dochev, D., Nikolov, V., Yaneva, M., Konyovska, R., 2019. Palynostratigraphy of dinosaur bone-bearing deposits from the Upper Cretaceous of Western Bulgaria. *Acta Geol. Pol.* 69 (4), 617–626.
- Perch-Nielsen, K., 1985. Cenozoic calcareous nannoplankton. In: Bolli, H.M., Saunders, J. B., Perch-Nielsen, K. (Eds.), *Plankton Stratigraphy*. Cambridge University Press, pp. 427–554.
- Peryt, D., Dubicka, Z., 2015. Foraminiferal bioevents in the Upper Campanian to lowest Maastrichtian of the Middle Vistula River section. *Poland. Geo. Qua.* 59 (4), 814–830. <https://doi.org/10.7306/gq.1252>.
- Peryt, D., Dubicka, Z., Wierny, W., 2022. Planktonic Foraminiferal Biostratigraphy of the Upper Cretaceous of the central European Basin. *Geosciences* 12, 22. <https://doi.org/10.3390/geosciences12010022>.
- Petrizzo, M.R., 2002. Palaeoceanographic and palaeoclimatic inferences from Late Cretaceous planktonic foraminiferal assemblages from the Exmouth Plateau (ODP Sites 762 and 763, eastern Indian Ocean). *Mar. Micropaleontol.* 45 (2), 117–150. [https://doi.org/10.1016/S0377-8398\(02\)00020-8](https://doi.org/10.1016/S0377-8398(02)00020-8).
- Petrizzo, M.R., Falzoni, F., Premoli Silva, I., 2011. Identification of the base of the lower-to-middle Campanian *Globotruncana ventricosa* Zone: comments on reliability and global correlations. *Cretac. Res.* 32, 387–405. <https://doi.org/10.1016/j.cretres.2011.01.010>.
- Phleger, F.B., Parker, F.L., 1951. *Ecology of foraminifera, Northwest Gulf of Mexico*. GSA Memoir 46 (2), 1–64.
- Podobina, V.M., 1995. Zonal Stratigraphy of Upper Cretaceous Deposits in Western Siberia, on Foraminifera. Second International Symposium on Cretaceous Stage Boundaries. Brussels, Abstract Volume, p. 93.
- Pojar, I., Zaharia, L., Benea, M., 2014. Heavy mineral distributions in Upper Cretaceous Bozeș Formation (Apuseni Mountains, Romania) – implications for sediment provenance. *Carpathian J. Earth and Environ. Sci.* 9, 125–132.
- Polette, F., Batten, D.J., 2017. Fundamental reassessment of the taxonomy of five Normapolles pollen genera. *Rev. Palaeobot. Palynol.* 243, 47–91. <https://doi.org/10.1016/j.revpalbo.2017.04.001>.
- Premoli Silva, I., Erba, E., Tornaghi, M.E., 1989. Paleoenvironmental signals and changes in surface fertility in mid-Cretaceous Corg-Rich pelagic facies on the Fucoid Marls (Central Italy). *Geobios* 11, 225–236. [https://doi.org/10.1016/S0016-6995\(89\)80059-2](https://doi.org/10.1016/S0016-6995(89)80059-2).
- Rathburn, A.E., Willingham, J., Ziebis, W., Burkett, A.M., Corliss, B.H., 2018. A new biological proxy for deep-sea paleo-oxygen: Pores of epifaunal benthic foraminifera. *Sci. Rep.* 8 (1), 1–8. <https://doi.org/10.1038/s41598-018-27793-4>.
- Reolid, M., Sebane, A., Rodríguez-Tovar, F.J., Marok, A., 2012. Foraminiferal morphogroups as a tool to approach the Toarcian Anoxic Event in the Western Saharan Atlas (Algeria). *Palaeogeogr. Palaeoclimatol. Palaeoecol.* 323–325, 87–99. <https://doi.org/10.1016/j.palaeo.2012.01.034>.
- Robaszynski, F., Pomerol, B., Masure, E., Bellier, J.P., Deconinck, J.F., 2005. Stratigraphy and stage boundaries in reference sections of the Upper Cretaceous Chalk in the east of the Paris Basin: the “Craie 700” Provinces boreholes. *Cretac. Res.* 26, 157–169.
- Rostami, M.A., Balmaki, B., 2018. Biostratigraphy and paleoecology of Maastrichtian and Paleocene sediments in the northern Alborz, Iran, using foraminifera. *Intern. J. Geogra. and Geo.* 7 (3), 56–72. <https://doi.org/10.18488/journal.10.2018.73.56.72>.
- Roth, P.H., 1989. Ocean circulation and calcareous nannoplankton evolution during the Jurassic and Cretaceous. *Palaeogeogr. Palaeoclimatol. Palaeoecol.* 74, 111–126.
- Roth, P.H., Bowdler, J.L., 1981. Middle Cretaceous calcareous nannoplankton biogeography and oceanography of the Atlantic Ocean. *SEPM Spec. Publ.* 32, 517–546.
- Roth, P.H., Krumbach, K.R., 1986. Middle Cretaceous calcareous nannofossil biogeography and preservation in the Atlantic and Indian oceans: Implications for paleoceanography. *Mar. Micropaleontol.* 10, 235–266. [https://doi.org/10.1016/0377-8398\(86\)90031-9](https://doi.org/10.1016/0377-8398(86)90031-9).
- Russo, B., Ferraro, L., Correggia, C., Alberico, I., Foresi, L.M., Vallefucio, M., Lirer, F., 2022. Deep-water paleoenvironmental changes based on early-middle Miocene benthic foraminifera from Malta Island (Central Mediterranean). *Palaeogeogr. Palaeoclimatol. Palaeoecol.* 586, 110722. <https://doi.org/10.1016/j.palaeo.2021.110722>.
- Sândulescu, M., 1984. *Geotectonica, României*. Ed. Tehnică, Bucharest, p. 329 (in Romanian).
- Săsăran, E., Săsăran, L., 2003. Facies Analysis of the Late Cretaceous deposits from Corni Quarry (North-Eastern border of Gilău Mountains). *Studia Universitatis Babeş-Bolyai, Geologia* 48, pp. 81–94.
- Saïdi, E., Zaghbib-Turki, D., 2016. Planktonic foraminiferal biostratigraphy and quantitative analysis during the Campanian-Maastrichtian transition at the Oued Necham section (Kalâat Senan, Central Tunisia). *Turk. J. Earth Sci.* 25, 538–572. <https://doi.org/10.3906/yer-1602-13>.
- Schweizer, M., 2006. *Evolution and Molecular Phylogeny of Cibicides and Uvigerina (Rotulida, Foraminifera)*. PhD Thesis. Geologica Ultraiecia, p. 261.
- Setoyama, E., Kanungo, S., 2020. Mesozoic biostratigraphy and paleoenvironment of the South Atlantic: A revised framework based on 20 DSDP and ODP deep-water sites. *J. S. Am. Earth Sci.* 99, 1–24. <https://doi.org/10.1016/j.jsames.2020.102511>.
- Setoyama, E., Kaminski, M., Tyszka, J., 2011a. Campanian agglutinated foraminifera from the Lomonosov Ridge, IODP Expedition 302, ACEX, in the paleogeographic context of the Arctic Ocean. *Micropaleontology* 57 (6), 507–530.
- Setoyama, E., Kaminski, M., Tyszka, J., 2011b. The Late Cretaceous–Early Paleocene palaeobathymetric trends in the southwestern Barents Sea — Palaeoenvironmental implications of benthic foraminiferal assemblage analysis. *Palaeogeogr. Palaeoclimatol. Palaeoecol.* 307, 44–58.
- Setoyama, E., Radmacher, W., Kaminski, M.A., Tyszka, J., 2013. Foraminiferal and palynological biostratigraphy and biofacies from a Santonian-Campanian submarine fan system in the Vøring Basin (offshore Norway). *Mar. Pet. Geol.* 43, 396–408. <https://doi.org/10.1016/j.marpetgeo.2012.12.007>.
- Setoyama, E., Kaminski, M.A., Tyszka, J., 2017. Late Cretaceous–Paleogene foraminiferal morphogroups as palaeoenvironmental tracers of the rifted Labrador margin, northern proto-Atlantic. In: Kaminski, M.A., Alegret, L. (Eds.), *Proceedings of the Ninth International Workshop on Agglutinated Foraminifera*. Grzybowski Foundation special Publication, 22, pp. 179–220.
- Sgarrella, F., Di Donato, V., Sprovieri, R., 2012. Benthic foraminiferal assemblage turnover during intensification of the Northern Hemisphere glaciation in the Piacenzian Punta Piccola section (Southern Italy). *Palaeogeogr. Palaeoclimatol. Palaeoecol.* 333–334, 59–74. <https://doi.org/10.1016/j.palaeo.2012.03.009>.
- Sheldon, E., Ineson, J., Bown, P., 2010. Late Maastrichtian warming in Boreal Realm: Calcareous nannofossil evidence from Denmark. *Palaeogeogr. Palaeoclimatol. Palaeoecol.* 295, 55–75. <https://doi.org/10.1016/j.palaeo.2010.05.016>.
- Siegl-Farkas, A., Haas, J., 2002. Stratigraphic and sedimentological analysis of the Upper Cretaceous sequence of the Zala Basin on the basis of the investigation of the

- Szilvagy-33 well. *Acta Geol. Hung.* 45 (2), 153–174. <https://doi.org/10.1556/ageol.45.2002.2.2>.
- Silye, L., Bălc, R., 2011. Sedimentary facies and depositional environment of the Bozeş Formation (Southeastern Apuseni Mts.). In: Csiki, Z. (Ed.), Eighth Romanian Symposium on Paleontology. Bucharest, Romania, p. 110.
- Singh, A.D., Rai, A.K., Verma, K., Das, S., Bharti, S.K., 2015. Benthic foraminiferal diversity response to the climate induced changes in the eastern Arabian Sea oxygen minimum zone during the last 30 ka BP. *Quat. Int.* 374, 118–125. <https://doi.org/10.1016/j.quaint.2014.11.052>.
- Sissing, W., 1977. Biostratigraphy of Cretaceous calcareous nannoplankton. *Geol. En. Mijnb* 56, 37–65. Den Haag.
- Slimani, H., 2001. Les kystes de dinoflagellés du Campanien au Danien dans la région de Maastricht (Belgique et Pays-Bas) et de Turnhout (Belgique): biozonation et corrélation avec d'autres régions en Europe occidentale. *Geol. Palaeontol.* 35, 161–201.
- Slimani, H., M'Hamdi, A., Uchman, A., Gasiński, M.A., Guédé, K.É., Mahboub, I., 2021. Dinoflagellate cyst biostratigraphy of Upper Cretaceous turbiditic deposits from a part of the Băkowiec section in the Skole Nappe (Outer Carpathians, southern Poland). *Cretac. Res.* 123, 104780 <https://doi.org/10.1016/j.cretres.2021.104780>.
- Sliter, W.V., 1972. Upper Cretaceous planktonic foraminiferal zoogeography and ecology-eastern Pacific margin. *Palaeogeogr. Palaeoclimatol. Palaeoecol.* 12 (1–2), 15–31. [https://doi.org/10.1016/0031-0182\(72\)90004-1](https://doi.org/10.1016/0031-0182(72)90004-1).
- Stoica, A.M., Ducea, M.N., Roban, R.D., Jianu, D., 2016. Origin and evolution of the South Carpathians basement (Romania): a zircon and monazite geochronologic study of its Alpine sedimentary cover. *Int. Geol. Rev.* 58 (4), 510–524. <https://doi.org/10.1080/00206814.2015.1092097>.
- Švábenická, L., 2001. Late Campanian/late Maastrichtian penetration of high-latitude calcareous nannoflora to the Outer Western Carpathian depositional area. *Geol. Carpath.* 52, 23–40.
- Székely, S.-F., Beldean, C., Bindiu, R., Filipescu, S., Săsăran, E., 2016. Palaeoenvironmental changes in the Transylvanian Basin during the early Miocene revealed by the foraminifera assemblages. *Geo. Qua.* 60 (1), 165–178. <https://doi.org/10.7306/gq.1245>.
- Țabără, D., Slimani, H., 2019. Palynological and palynofacies analyses of Upper Cretaceous deposits in the Hațeg Basin, southern Carpathians, Romania. *Creta. Res.* 104, 104185 <https://doi.org/10.1016/j.cretres.2019.07.015>.
- Țabără, D., Vasile, Ș., Csiki-Sava, Z., Bălc, R., Vremir, M., Chelariu, M., 2022. Palynological and organic geochemical analyses of the Upper Cretaceous Bozeş Formation at Petrești (southwestern Transylvanian Basin) – biostratigraphic and palaeoenvironmental implications. *Cretac. Res.* 134, 105148 <https://doi.org/10.1016/j.cretres.2022.105148>.
- Tantawy, A.A.A.M., 2003. Calcareous nannofossil biostratigraphy and paleoecology of the Cretaceous-Tertiary transition in the central eastern desert of Egypt. *Mar. Micropaleontol.* 47, 323–356. [https://doi.org/10.1016/S0377-8398\(02\)00135-4](https://doi.org/10.1016/S0377-8398(02)00135-4).
- Thibault, N., Gardin, S., 2007. The late Maastrichtian nannofossil record of climate change in the South Atlantic DSDP Hole 525A. *Mar. Micropaleontol.* 65, 163–184. <https://doi.org/10.1016/j.marmicro.2007.07.004>.
- Thomas, E., Zachos, J.C., Bralower, T.J., 2000. Deep-sea environments on a warm Earth: Latest Paleocene-early Eocene. In: Huber, B.T., MacLeod, K.G., Wing, L.S. (Eds.), *Warm Climates in Earth History*, B. Cambridge Univ. Press, Cambridge, UK, pp. 132–160.
- van der Zwaan, G.J., Duijnste, I.A.P., den Dulk, M., Ernst, S.R., Jannink, N.T., Kouwenhoven, T.J., 1999. Benthic foraminifers: proxies or problems? A review of paleoecological concepts. *Earth-Sci. Rev.* 46 (1–4), 213–236. [https://doi.org/10.1016/S0012-8252\(99\)00011-2](https://doi.org/10.1016/S0012-8252(99)00011-2).
- Van Itterbeeck, J., Markevich, V.S., Codrea, V., 2005. Palynostratigraphy of the Maastrichtian dinosaur and mammal sites of the Râul Mare and Bărbat valleys (Hațeg Basin, Romania). *Geol. Carpath.* 56 (2), 137–147.
- Vasile, Ș., Csiki-Sava, Z., Vremir, M., Norell, M.A., Totoianu, R., Brusatte, S.L., Bălc, R., Țabără, D., 2021. New data on the Late Cretaceous microvertebrate assemblage from Petrești-Arini (SW Transylvanian Basin, Romania). In: Ionesi, V., Miclăuș, C., Țabără, D. (Eds.), Abstract Book, Thirteenth Romanian Symposium on Paleontology, Iași, Romania. Tehnopress, Iași, pp. 51–52.
- Vasile, Ș., Csiki-Sava, Z., Vremir, M., Țabără, D., Bălc, R., Bindiu-Haitonic, R., Kövecsi, S.-A., 2022. The Late Campanian microvertebrate assemblage from Petrești (Transylvanian Basin, Romania), a new window into the evolution of European Cretaceous insular faunas. In: Belvedere, M., Mecozzi, B., Amore, O., Sardella, R. (Eds.), Abstract book of the XIX Annual Conference of the European Association of Vertebrate Palaeontologists. PalaeoVertebrata, Benevento/Pietraroia, Italy, pp. 214–215. Special Volume 1–2022.
- Vermeesch, P., 2018. IsoplotR: A free and open toolbox for geochronology. *Geosci. Front.* 9 (5), 1479–1493. <https://doi.org/10.1016/j.gsf.2018.04.001>.
- Vermeesch, P., 2021. Maximum depositional age estimation revisited. *Geoscience Frontiers* 12, 843–850.
- Vremir, M., 2010. New faunal elements from the Late Cretaceous (Maastrichtian) continental deposits of Sebeș area (Transylvania), Terra Sebus. *Acta Musei Sabasiensis* 2, 635–684.
- Vremir, M., Kellner, A.W.A., Naish, D., Dyke, G.J., 2013. A new azhdarchid Pterosaur from the Late Cretaceous of the Transylvanian Basin, Romania: implications for azhdarchid diversity and distribution. *PLoS One* 8 (1), e54268. <https://doi.org/10.1371/journal.pone.0054268>.
- Vremir, M., Bălc, R., Csiki-Sava, Z., Brusatte, S.L., Dyke, G., Naish, D., Norell, M.A., 2014. Petrești-Arini – an important but ephemeral Upper Cretaceous continental vertebrate site in the southwestern Transylvanian Basin, Romania. *Cretac. Res.* 49, 13–38. <https://doi.org/10.1016/j.cretres.2014.02.002>.
- Vremir, M., Dyke, G., Totoianu, R., 2015a. Repertoire of the Late Cretaceous vertebrate localities from Sebeș area, Alba County (Romania), Terra Sebus. *Acta Musei Sabasiensis* 7, 695–724.
- Vremir, M., Vasile, Ș., Totoianu, R., Dyke, G., Csiki-Sava, Z., 2015b. Never say never – New additions to the composition of the oldest latest Cretaceous continental vertebrate assemblage in Transylvania, western Romania. In: Jagt, J.W.M., Hebda, G., Mitrus, S., Jagt-Yazykova, E.A., Bodzioch, A., Konietzko-Meier, D., Kardinal, K., Gruntmejer, K. (Eds.), Abstracts, 13<sup>th</sup> Annual Meeting of the European Association of Vertebrate Palaeontologists. Opole, Poland, p. 73.
- Watkins, D.K., 1989. Nannoplankton productivity fluctuations and rhythmically-bedded pelagic carbonates of the greenhorn limestone (Upper Cretaceous). *Palaeogeogr. Palaeoclimatol. Palaeoecol.* 74, 75–86. [https://doi.org/10.1016/0031-0182\(89\)90020-5](https://doi.org/10.1016/0031-0182(89)90020-5).
- Watkins, D.K., Self-Trail, J.M., 2005. Calcareous nannofossil evidence for the existence of the Gulf Stream during the late Maastrichtian. *Paleoce. and Paleoclim.* 20, PA3006. <https://doi.org/10.1029/2004PA001121>.
- Watkins, D.K., Wise, S.W., Pospichal, J.J., Crux, J., 1996. Upper Cretaceous calcareous nannofossil biostratigraphy and paleoceanography of the Southern Ocean. In: Mognilevsky, A., Whatley, R.C. (Eds.), *Microfossils and Oceanic Environments*. University of Wales, Aberystwyth Press, pp. 355–381.
- Weishampel, D.B., Grigorescu, D., Norman, D.B., 1991. The Dinosaurs of Transylvania. *National Geogr. Res. & Explora.* 7 (2), 196–215.
- Wendler, I., Huber, B.T., MacLeod, K.G., Wendler, J.E., 2013. Stable oxygen and carbon isotope systematics of exquisitely preserved Turonian foraminifera from Tanzania – Understanding isotopic signatures in fossils. *Mar. Micropaleontol.* 102, 1–33. <https://doi.org/10.1016/j.marmicro.2013.04.003>.
- Williamson, M.A., Stam, B., 1988. Jurassic/Cretaceous Epistominidae from Canada and Europe. *Micropaleontology* 34 (2), 136–158. <https://doi.org/10.2307/1485658>.
- Willingshofer, E., Andriessen, P., Cloething, S., Neubauer, F., 2001. Detrital fission track thermochronology of Upper Cretaceous syn-orogenic sediments in the South Carpathians (Romania): inferences on the tectonic evolution of a collisional hinterland. *Basin Res.* 13, 379–395. <https://doi.org/10.1046/j.0950-091x.2001.00156.x>.
- Wind, F.H., 1979. Maastrichtian-Campanian nannofloral provinces of the Southern Atlantic and Indian oceans. In: Talwani, M., Hay, W., Ryan, W.B.F. (Eds.), *Deep Sea Drilling Results in the Atlantic Ocean: Continental Margins and Paleoenvironment*. American Geophysical Union, pp. 123–127.
- Wolfgang, E., Wagreich, M., Hohenegger, J., Böhm, K., Dinăres Turell, J., Gier, S., Sames, B., Spötl, C., Jin, S., 2021. An integrated multi-proxy study of cyclic pelagic deposits from the north-western Tethys: the Campanian of the Postalm section (Gosau Group, Austria). *Cretac. Res.* 120, 104704 <https://doi.org/10.1016/j.cretres.2020.104704>.
- Zaharia, L., Bălc, R., Stremțan, C.C., Socaciu, A., 2016. Geochemistry of Upper Cretaceous of the Bozeş Formation (Apuseni Mts., Romania) – provenance implications. *Geol. Quart.* 60, 746–757. <https://doi.org/10.7306/gq.1306>.